Observation and Analysis of 1550 nm LASER Link as a Free Space Optics in Simulated Rainy, Foggy and Heating Conditions.

A THESIS SUBMITTED IN PARTIAL FULFILMENT OF THE REQUIREMENTS FOR THE DEGREE OF

MASTER OF ENGINEERING

IN

ILLUMINATION ENGINEERING

By

SAYAN MISTRY

EXAMINATION ROLL NO. M4ILN22023

REGISTRATION NO. 136115 of 2016-17

JADAVPUR UNIVERSITY

Under the Supervision of

Prof. (Dr.) SASWATI MAZUMDAR

DEPARTMENT OF ELECTRICAL ENGINEERING

FACULTY OF ENGINEERING AND TECHNOLOGY

JADAVPUR UNIVERSITY

KOLKATA-700032

August 2022

JADAVPUR UNIVERSITY

Faculty of Engineering and Technology

CERTIFICATE OF RECOMMENDATION

This is to certify that the thesis entitled **"*Observation and Analysis of 1550 nm LASER Link as a Free Space Optics in Simulated Rainy, Foggy and Heating Conditions.*"**, submitted by **SAYAN MISTRY** (Examination Roll No. **M4ILN22023** & Registration No. **136115 of 2016-17**) under our supervision be accepted in partial fulfilment of the requirement for the degree of Master of Illumination Engineering.

Prof. (Dr.) SASWATI MAZUMDAR
Professor, Illumination Engineering Section
Department of Electrical Engineering
Jadavpur University
Kolkata-700032

Prof. (Dr.) SASWATI MAZUMDAR
Head of the Department
Electrical Engineering
Jadavpur University
Kolkata-700032

Prof. (Dr.) CHANDAN MAZUMDAR
Dean
Faculty of Engineering & Technology
Jadavpur University
Kolkata-700032

JADAVPUR UNIVERSITY

Faculty of Engineering and Technology

CERTIFICATE OF APPROVAL

The foregoing thesis is hereby approved as a creditable study of an engineering subject, carried out and presented in a satisfactory manner to warrant its acceptance as a pre-requisite to the degree for which it has been submitted. It is notified to be understood that by this approval, the undersigned do not necessarily endorse or approve any statement made, opinion expressed and conclusion drawn therein but approve the thesis only for the purpose for which it has been submitted.

FINAL EXAMINATION FOR EVALUATION OF THESIS.

BOARD OF EXAMINERS

_____

_____

_____

Declaration of Originality and Compliance of Academic Ethics

I, hereby declare that this thesis contains literature survey and original thesis work by the undersigned candidate, as part of Master of Engineering in Illumination Engineering course.

All information in this document has been obtained and presented in accordance with academic rules and ethical conduct.

I also declare that, as required by the rules and regulations, I have fully cited and referenced all material and results that are not original to my work.

Name: SAYAN MISTRY

Examination Roll No. : M4ILN22023

Registration No. : 136115 of 2016-17

Thesis Title : Observation and Analysis of 1550 nm LASER Link as a Free Space Optics in Simulated Rainy, Foggy and Heating Conditions.

_____

Signature with date

Acknowledgement

I would like to express my sincere and heartfelt gratitude to my professors, classmates and senior research scholars for their guidance, cooperation and knowledge that helped me sail through this degree course.

First of all, I would like to take the opportunity to express my sincere thanks and regards to my guide Prof. (Dr.) Saswati Mazumdar, Professor and HOD, Department of Electrical Engineering, Jadavpur University, Kolkata-700032, for considering me and allowing me to work under her guidance. She has been a source of constant inspiration and support throughout the course of this thesis work and provided all the necessary infrastructure to validate the experimental results furnished in this thesis.

I would like to acknowledge the Project Free Space LASER Communication Data and Voice sponsored by DRDO in EE Department.

I would also like to acknowledge the support of my teachers Prof. (Dr.) Biswanath Roy, Dr. Suddhasatwa Chakraborty and Ms. Sangita Sahana for making me capable enough to work in this field of Illumination Engineering. I would not have been able to work upon the idea of my thesis without their guidance.

I would like to give special thanks to senior research scholar Mr. Shibabrata Mukharjee, Mr. Sujoy Paul , ME student from the School of LASER Technology for being a constant source of support and inspiration and helping me to complete my thesis work in time.

Date:

Place: Jadavpur University,
Kolkata-700032

Sayan Mistry

Content

Chapter 1

Introduction and Overview of the Thesis

Chapter 1

Introduction and Overview of the Thesis

Communication has always been necessary for people. Humanity has made incredible strides in data transfer since the days when the only method to convey a message containing crucial information was to send a runner with it. We entered the Information Age [37,38] within a few centuries, during which globalization became prevalent. In the modern era, it is impossible to picture life without the Internet, which is the most common method of exchanging information and a source of knowledge. That allows us to navigate without using physical on-paper maps, send messages across continents quickly, take part in distance learning, and shop using a smartphone, but that is not the all benefit. We may study the cosmos in this incredible electronic age without using a telescope or even consult a doctor without leaving the house. In light of the former, it has gained enormous importance, notably during the lockdowns, during the COVID-19 pandemic.

One of the most significant trends in technological history is the spread of wireless communications. More quickly than anyone could have predicted thirty years ago, wireless devices and technologies are now widely used, and they will likely continue to play a significant role in contemporary society for some time to come. Due to the widespread deployment and use of wireless RF devices and systems, the term "wireless" is now almost always used to refer to radio-frequency (RF) technologies. But because most sub-bands require a license, the RF band of the electromagnetic spectrum is fundamentally constrained in capacity and expensive. The time has come to seriously consider other viable options for wireless communication using the upper parts of the electromagnetic spectrum as RF spectrum is in short supply due to the ever-increasing popularity of data-heavy wireless communications. OWC, or optical wireless communication, is the use of optical carriers—the visible, infrared (IR), and ultraviolet (UV) bands—for transmission in unguided propagation media. The historical forms of OWC include signaling with beacon fires, smoke, ship flags, and semaphore telegraph [39]. Since very early times, sunlight has also been used for long-distance signaling. The ancient Greeks and Romans are credited with using sunlight for communication for the first time when they used their polished shields to send signals by reflecting sunlight during battles [40]. The heliograph was

created by Carl Friedrich Gauss in 1810 and uses two mirrors to focus a controlled beam of sunlight onto a distant station. Although the heliograph's original purpose was geodetic survey, it was heavily employed for military operations in the late 19th and early 20th centuries. The photophone, the first wireless telephone system in the world, was created by Alexander Graham Bell in 1880 [39]. Its foundation was the voice-induced mirror vibrations at the transmitter. Sunlight reflected and projected the vibrations, which were then converted back into voice at the receiver. The photophone was touted by Bell as "the greatest invention [he had] ever made, greater than the telephone" [41], but it was never released as a manufactured good. However, the military's interest in photophones persisted. For instance, the German Army created a photophone in 1935 that used a tungsten filament lamp as the light source and an IR transmitting filter as the display. Additionally, high pressure arc lamps for optical communication were still being developed in military laboratories in Germany and the United States up until the 1950s. Nowadays, OWC transmits data using either lasers or light-emitting diodes (LEDs). TV signals could be sent over a 30-mile distance using an experimental OWC link that MIT Lincoln Labs built in 1962 using a light-emitting GaAs diode. OWC was intended to be the primary area for laser deployment after the invention of the laser, and numerous trials 2 were carried out. In fact, Bell Labs researchers used a ruby laser to transmit signals 25 miles away just a few months after the first public announcement of the operational laser in July 1960 [42]. [43] contains a thorough list of OWC demonstrations carried out between 1960 and 1970 using various laser types and modulation schemes. However, because of the significant laser beam divergence and inability to account for atmospheric effects, the results were generally disappointing. With the advent of low-loss fiber optics in the 1970s, OWC systems lost importance as the obvious choice for long-distance optical transmission. Over the years, interest in OWC has mostly been focused on covert military applications [44, 45] and space applications, such as deep-space links and intersatellite links. 1 With the exception of IrDA, which developed into a very successful wireless short-range transmission solution, OWC's mass market penetration has been relatively limited [46]. The market has started to show signs of future promise [47, 48] with the rise of visible light communication (VLC) products and the increase in businesses offering terrestrial OWC links in recent years [49] through [50]. Future heterogeneous communication networks must be built to support a variety of service types with different traffic patterns and to meet the ever-increasing demands for higher data rates. This requires the development of novel and efficient wireless

technologies for a variety of transmission links. OWC variants may be used in a wide range of communication applications, including satellite communications, outdoor inter-building links, optical interconnects within integrated circuits, and optical interconnects.

In this literature., we focus only on various atmospheric effects on the outdoor terrestrial OWC links of 1550 nm LASER , which are also widely referred to as free space optical (FSO) communication where,

Chapter 2 discusses the brief introduction on FSO technology

Chapter 3 describes the Experimental Setup and Link Budget analysis.

Chapter 4 presents the experimental results with relevant graphs and eye diagram

Chapter 5 provides the conclusion and future scope

Chapter 2

An Introduction to FSO Technology

2.1 An overview

Free-space optical communication requires line-of-sight connection between transmitter and receiver for propagation of information from one point to another. Here, the information signal from the source is modulated on the optical carrier, and this modulated signal is then allowed to propagate through the atmospheric channel or free space, rather than guided optical fibers, toward the receiver. Ground-to-satellite (optical uplink) and satellite-to-ground (optical downlink) involve propagation of optical beam through the atmosphere as well as in free space. Therefore, these links are a combination of terrestrial and space links. Figure 2.1. illustrates the application areas of FSO links.

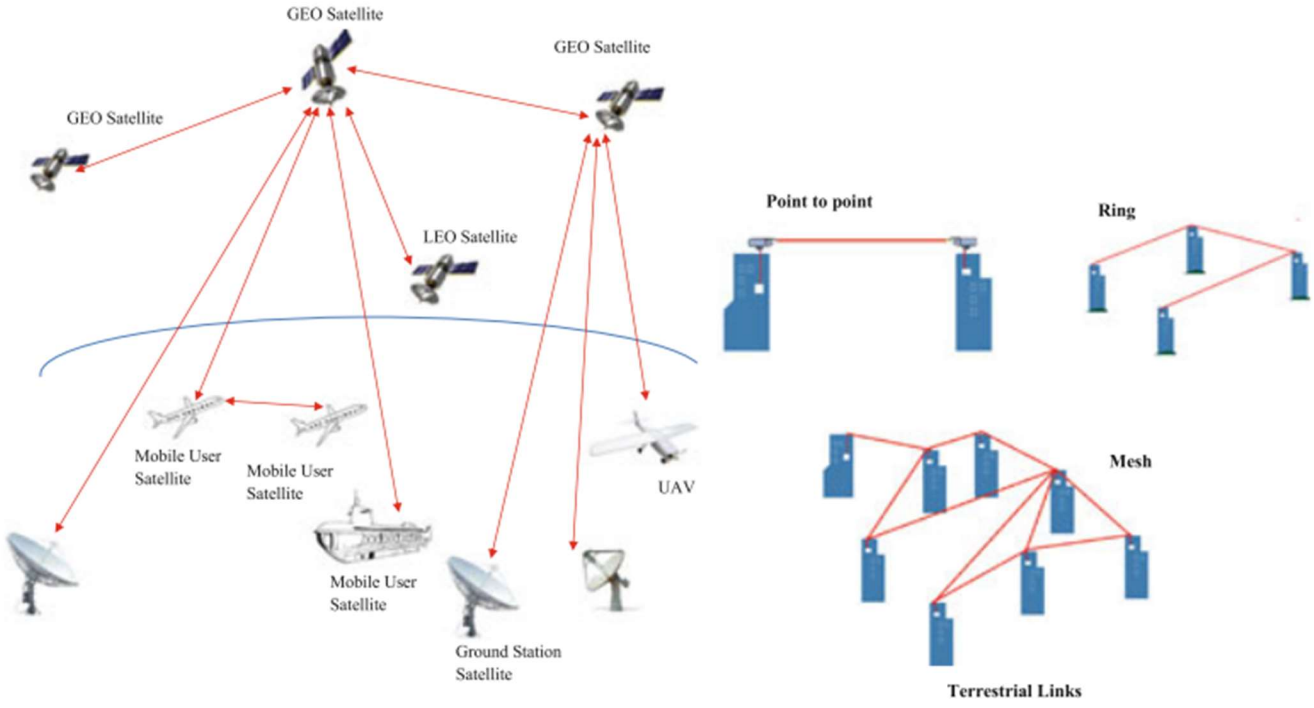

Fig 2.1. Applications of FSO technology

The basic block diagram of an FSO link is shown in Fig. 2.2. Like any other communication technologies, FSO communication link comprises of three basic subsystems, viz., transmitter, channel, and receiver [1].

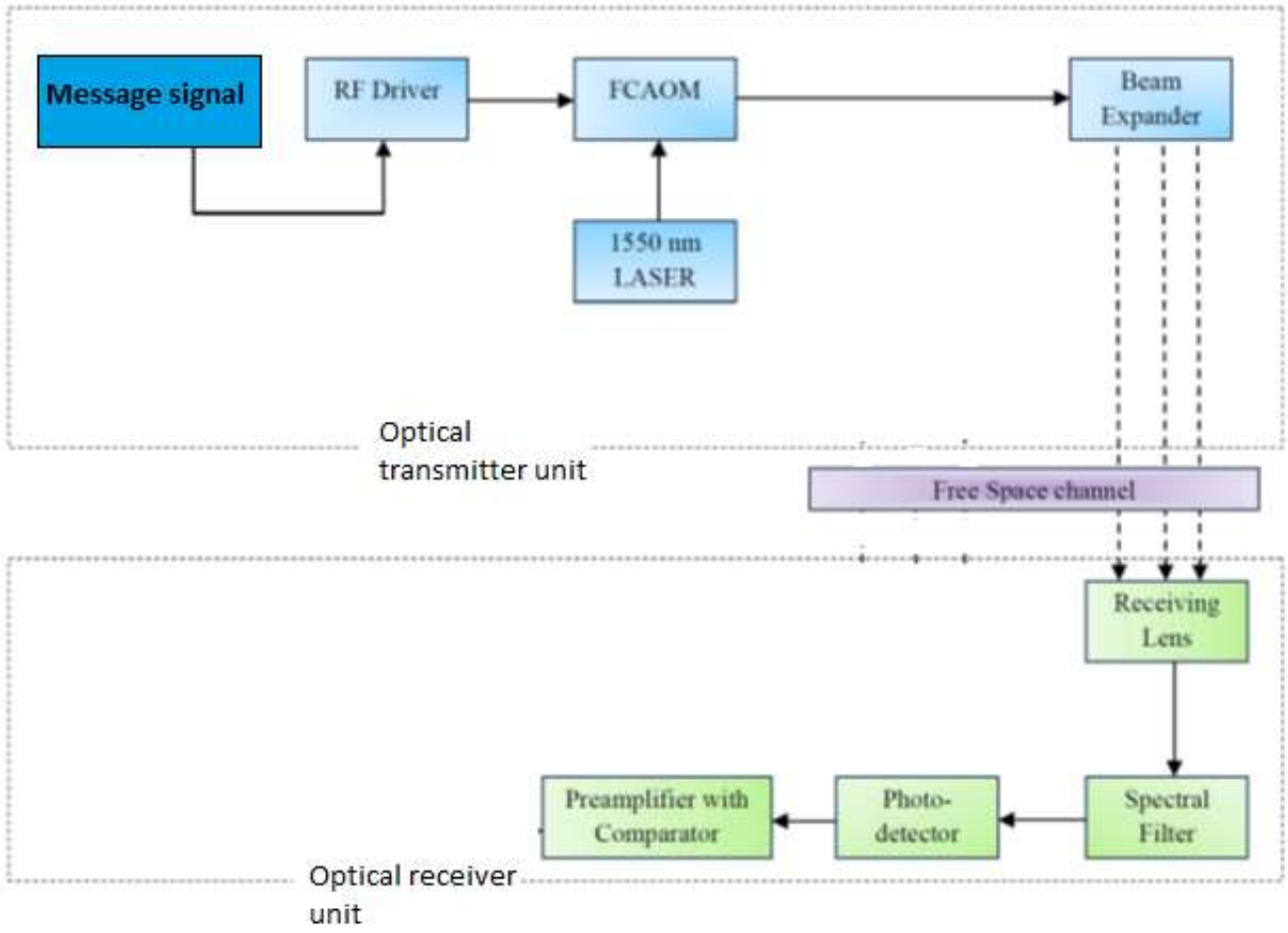

Fig 2.2: Block diagram of FSO communication link

(i) Transmitter: Its primary function is to modulate the message signal onto the optical carrier which is then propagated through the atmosphere to the receiver. The essential components of the transmitter are (a) the modulator, (b) the driver circuit for the optical source to stabilize the optical radiations against temperature fluctuations, and (c) the collimator or the telescope that modulation is the intensity modulation (IM) in which the source data is modulated on the irradiance/intensity of the optical carrier. This can beachieved by varying the driving current of

the optical source directly with the message signal to be transmitted or by using an external modulator.

(ii) Channel: Since the FSO communication channel has the atmosphere as its propagating medium, it is influenced by unpredictable environmental factors like cloud, snow, fog, rain, etc. These factors do not have fixed characteristics and cause attenuation and deterioration of the received signal. The channel is one of the limiting factors in the performance of FSO system.

(iii) Receiver: Its primary function is to recover the transmitted data from the incident optical radiation. It consists of a receiver telescope, optical filter, photodetector, and demodulator. The receiver telescope collects and focuses the incoming optical radiation onto the photodetector. The optical filter reduces the level of background radiation and directs the signal on the photodetector that converts the incident optical signal into an electrical signal.

2.2 Advantages of FSO Over Radio-Frequency and Wired (Optical Fiber) Communication Systems

FSO communication system offers several advantages over the RF system. The major difference between FSO and RF communications arises from the large difference in the wavelength. Under clear weather conditions (visibility >10 miles), the atmospheric transmission window is in the near IR region and lies between 700 and 1600 nm. The transmission window for RF lies between 30 mm and 3 m. Therefore, RF wavelength is a thousand of times larger than the optical wavelength. This high ratio of wavelengths leads to some interesting differences between the two systems as given below:

(i) Huge modulation bandwidth: It is a well-known fact that an increase in carrier frequency increases the information-carrying capacity of a communication system. In RF and microwave communication systems, the allowable bandwidth can be up to 20 % of the carrier frequency. In optical communication, even if the bandwidth is taken to be 1 % of carrier frequency. ($\approx 10^{16}$ Hz), the allowable bandwidth will be 100 THz. This makes the usable bandwidth at an optical frequency in the order of THz which is almost 10^5 times that of a typical RF carrier.

(ii) Narrow beam divergence: The beam divergence is ~λ/D_R, where λ is the carrier wavelength and D_R the aperture diameter. Thus, the beam spread offered by the optical carrier is narrower than that of RF carrier. For example, the laser beam divergence at λ = 1550 nm and aperture diameter D_R = 10 cm come out to be 0:34μ rad. On the other hand, radio-frequency signal say at X band will produce a very large beam divergence, e.g., at 10 GHz i.e., λ = 3 cm, and aperture diameter D_R = 1 m yields beam divergence to be 67.2mrad. Much smaller beam divergence at optical frequency leads to increase in the intensity of signal at the receiver for a given transmitted power. [2].

(iii) Less power and mass requirement: For a given transmitter power level, the optical intensity is more at the receiver due to its narrow beam divergence. Thus, a smaller wavelength of optical carrier permits the FSO designer to come up with a system that has smaller antenna than RF system to achieve the same gain (as antenna gain is inversely proportional to the square of operating wavelength). The typical size for the optical system is 0.3 vs. 1.5 m for the spacecraft antenna [3].

(iv) High directivity: Since the optical wavelength is very small, a very high directivity is obtained with small-sized antenna. Antenna directivity is closely related to its gain. The advantage of optical carrier over RF carrier can be seen from the ratio of antenna directivity as given below

$$\frac{Gain_{optic}}{Gain_{RF}} = \frac{4\pi/\Theta^2{}_{div(optical)}}{4\pi/\Theta^2{}_{div(RF)}} \ldots\ldots\ldots\ldots\ldots\ldots\ldots\ldots\ldots\ldots\ldots\ldots (1)$$

where $\Theta_{div(optical)}$ and $\Theta_{div(RF)}$ are the optical and RF beam divergence, respectively, and are proportional to λ/D_R. For system using optical carrier with aperture diameter D_R = 10 cm and λ = 1550 nm gives$\Theta_{div(optical)}$≈ 40μ rad. At beam divergence of 40 μ rad, the antenna gain, $Gain_{optical}$, is approximately 100db. In order to achieve the same gain in RF system using X band at λ = 3 cm, the size of aperture diameter DR becomes extremely large and unpractical to implement.

(v) Unlicensed spectrum: In RF system, interference from adjacent carrier is the major problem due to spectrum congestion. This requires the need of spectrum licensing by regulatory

authorities. But optical system is free from spectrum licensing till now. This reduces the initial setup cost and development time.

(vi) Security: It is difficult to detect the transmuted optical beam as compared to RF signal because of its narrow beam divergence. In order to detect the transmitted optical signal, one has to be physically very close (≤ 0.1 miles) to the beam spot diameter. Studies have shown that the optical signal would drop to 140 dB from its peak transmission power at a distance of 10 miles. However, RF signal has much wider region of listening. In this case, signal can easily be picked up roughly at a distance of 40 miles and is down about 40 dB at approximately 100 miles.In addition to the above advantages, the secondary advantages of FSO communication system are:

(a) it is beneficial in the cases where fiber optic cables cannot be used

(b) easily expandable and reduces the size of network segments, and

(c) light weight and compact.

2.3 Limitations of Free Space Optical(FSO) Technology

In Spite of Number of Advantages and Applications of FSO, It Has Some Limitations that May Lead to Challenges:

• **Atmospheric Disturbances:** A major impairment on FSO links is caused due to the atmospheric turbulence. It is the result of random variations in the refractive index caused due to inhomogeneities in temperature and pressure. In clear weather conditions, the atmospheric turbulence causes the intensity fluctuation of the received signal called fading which is also known as scintillation in optical communication terminology [7, 8]. Turbulence is caused by the inhomogeneities of temperature as well as pressure in the atmosphere and can, thereby, severely degrade the link performance, particularly for link distances of 1 km or longer. The performance of this technology depends strongly on certain parameters like atmospheric conditions between transmitter and receiver, parameters of the link such as length, operating wavelength. Moreover, other factors such as fog, rain, atmospheric gases, and aerosols also result in beam attenuation due to photon absorption and scattering [9]

• **Pointing Error:** Apart from scintillation effects, the performance of the FSO link degrades because of the building sway, which introduces a pointing error (PE) between transmitter

andreceiver, representing a particular problem in urban areas, where FSO equipment is placed on high-rise structures [10, 11].

• **Physical Obstructions:** Since FSO is a line-of-sight communication, any obstruction in the path can interrupt or affect the communication. These obstructions may be in the form of birds, tall trees and buildings, etc. [12]. However, interruption of this kind is temporary, and transmissions are easily and automatically resumed.

• **Geometric Losses:** These losses are the form of optical beam attenuation that is caused due to the spreading of beam and results in the reduction of power level of signal as it travels from transmitter to receiver [13]

• **Background Radiation:** Last but not least, background radiation, also called background noise or ambient noise, can degrade the performance of FSO links. In fact, in addition to the useful signal, the receiver lens also collects some undesirable background radiations that may consist of direct sunlight, reflected sunlight, or scattered sunlight from hydrometeor or other objects.

2.4 Choice of Wavelength in FSO Communication System

Wavelength selection in FSO communication system is a very important design parameter as it affects link performance and detector sensitivity of the system. Since antenna gain is inversely proportional to operating wavelength, it is more beneficial to operate at lower wavelengths. However, higher wavelengths provide better link quality and lower pointing-induced signal fade [4]. A careful optimization of operating wavelength in the design of FSO link will help in achieving better performance. The choice of wavelength strongly depends on atmospheric effects, attenuation, and background noise power. Further, the availability of transmitter and receiver components, eye safety regulations, and cost deeply impact the selection of wavelength in FSO design process. The International Commission on Illumination [5] has classified optical radiations into three categories: IR-A (700–1400 nm), IR-B (1400–3000 nm), and IR-C (3000 nm–1 mm). It can be subclassified into:

(i) near-infrared (NIR) ranging from 750 to 1450 nm which is a low attenuation window and mainly used for fiber optics

(ii) short-infrared (SIR) ranging from 1400 to 3000 nm out of which 1530– 1560 nm is a dominant spectral range for long-distance communication

(iii) mid-infrared (MIR) ranging from 3000 to 8000 nm which is used in military applications for guiding missiles

(iv) long-infrared (LIR) ranging from 8000 nm to 15μm which is used in thermal imaging, and

(v) far-infrared (FIR) which is ranging from 15μm to 1mm.

Almost all commercially available FSO systems are using NIR and SIR wavelength range since these wavelengths are also used in fiber-optic communication, andtheir components arereadily available in the market. The wavelength selection for FSO communication has to be eye and skin safe as certain wavelengths between 400 and 1500 nm can cause potential eye hazards or damage to the retina [6].

2.5 Disturbances in FSO Channel Due to Different Weather Conditions

The concentric layers around the surface of the Earth are broadly classified into two regions: homosphere and heterosphere. The homosphere covers the lower layers ranging from 0–90 km. Heterosphere lies above homosphere above 90 km. The homospheric region of atmosphere is composed of various gases, water vapors, pollutants, and other chemicals. Maximum concentrations of these particles are near the Earth surface in the troposphere that extends up to 20 km.

The density of particles decreases with the altitude up through the ionosphere (region of upper atmosphere that extends from about 90 to 600 km and contains ionized electrons due to solar radiations). These ionized electrons form a radiation belt around the surface of the Earth. These atmospheric particles interact with all signals that propagate through the radiation belt and lead to deterioration of the received signal due to absorption and scattering. Absorption is the phenomenon where the signal energy is absorbed by the particles present in the atmosphere resulting in the loss of signal energy and gain of internal energy of the absorbing particle. In scattering, there is no loss of signal energy like in absorption, but the signal energy is redistributed (or scattered) in arbitrary directions. Both absorption and scattering are strongly

dependent upon operating wavelength and will lead to decrease in received power level. These effects become more pronounced when the operating wavelength of the transmitted signal is comparable with the cross-sectional dimensions of the atmospheric particles. Peaks in attenuation at specific wavelengths is due to absorption by atmospheric particles and therefore the choice of wavelength has to be done very wisely in the high transmissive band for FSO communication links.

The atmospheric condition in FSO channel can be broadly classified into three categories, namely, clear weather, clouds, and rain. Clear weather conditions are characterized by long visibility and relatively low attenuation. Cloudy weather conditions range from mist or fog to heavy clouds and are characterized by low visibility, high humidity, and large attenuation. Rain is characterized by the presence of rain droplets of variable sizes, and it can produce severe effects depending upon rainfall rate. Various atmospheric conditions can be represented by size of the particle (i.e., cross-sectional dimension relative to operating wavelength) and the particle density (i.e., volumetric concentration of the particles). It is seen that conditions may vary from high density and small particle size like in the case of mist and fog to low density and large particle size during heavy rain. It should be noted that real atmospheric conditions may undergo various temporal changes.

2.5.1 Atmospheric Losses

The atmospheric channel consists of various gases and other tiny particles like aerosols, dust, smoke, etc., suspended in the atmosphere. Besides these, large precipitation due to rain, haze, snow, and fog is also present in the atmosphere. Each of these atmospheric constituents results in the reduction of the power level, i.e., attenuation of optical signal due to several factors, including absorption of light by gas molecules, Rayleigh, or Mie scattering. Various types of losses encountered by the optical beam when propagating through the atmospheric optical channel are described in this section. In FSO communication system, when the optical signal propagates through the atmosphere, it experiences power loss due to several factors as discussed in the following sections.

2.5.1.1 Absorption and Scattering Losses

The loss in the atmospheric channel is mainly due to absorption and scattering processes. At visible and IR wavelengths, the principal atmospheric absorbers are the molecules of water, carbon dioxide, and ozone [17, 18]. The attenuation experienced by the optical signal when it passes through the atmosphere can be quantified in terms of optical depth which correlates with power at the receiver PR and the transmitted power PT [19] as

$$P_R = P_T \exp(-\tau) \quad \ldots\ldots (2)$$

The ratio of power received to the power transmitted in the optical link is called atmospheric transmittance T_a (= P_R/P_T) .

When the optical signal propagates at a zenith angle θ; the transmittance factor is then given by $T_\theta = T_a \sec\theta$ .The atmospheric transmittance T_a and the optical depth τ are related to the atmospheric attenuation coefficient γ and the transmission range R as follows:

$$T_a = exp\left(-\int_0^R \gamma(\rho)d\rho\right) \quad \ldots\ldots (3)$$

and

$$\tau = \left(\int_0^R \gamma(\rho)d\rho\right) \quad \ldots\ldots (4)$$

In both the cases, the loss in dB that the beam experiences during propagation through the atmosphere can be calculated using the following equation

$$Loss_{prop} = -10 \log_{10} T_a \quad \ldots\ldots (5)$$

In the first case, this loss in dB will be 4:34τ. Hence, an optical depth of 0.7 gives a loss of 3 dB

The attenuation coefficient is the sum of the absorption and scattering coefficients from aerosols and molecular constituents of the atmosphere and is given by [20] :

$$\gamma(\lambda) = \alpha_m(\lambda) + \alpha_a(\lambda) + \beta_m(\lambda) + \beta_a(\lambda) \quad \ldots\ldots (6)$$

where,

$\alpha_m(\lambda)$ = Molecular absorb. coeff.

$\alpha_a(\lambda)$ = Aerosol absorb. coeff.

$\beta_m(\lambda)$ = Molecular scatt. coeff.

$\beta_a(\lambda)$ = Aerosol scatt. coeff.

The first two terms in the above equation represent the molecular and aerosol absorption coefficients, respectively, while the last two terms are the molecular and aerosol scattering coefficients, respectively. The atmospheric absorption is a wavelength-dependent phenomenon. Some typical values of molecular absorption coefficients are given in Table 2.1 for clear weather conditions. The wavelength range of FSO communication system is chosen to have minimal absorption. This is referred to as atmospheric transmission windows. In this window, the attenuation due to molecular or aerosol absorption is less than 0.2 dB/km. There are several transmission windows within the range of 700–1600 nm. Majority of FSO systems are designed to operate in the windows of 780–850 and 1520–1600 nm.

The scattering process results in the angular redistribution of the optical energy with and without wavelength change. It depends upon the radius r of the particles encountered during the propagation process.

If $r < \lambda$, the scattering process is classified as Rayleigh scattering;

if $r \approx \lambda$, it is Mie scattering.

For $r > \lambda$, the scattering process can be explained using the diffraction theory (geometric optics).

The scattering process due to various scattering particles present in the atmosphere channel is summarized in Table 2.2. Out of various scattering particles like air molecules, haze particles, fog droplets, snow, rain, hail, etc., the wavelength of fog particles is comparable with the wavelength of FSO communication system. Therefore, it plays a major role in the attenuation of an optical signal.

Table 2.1: Molecular absorption at typical wavelengths [7]

S.No	Wavelength (nm)	Molecular absorption (dB/km)
1.	550	0.31
2.	690	0.01
3.	850	0.41
4	1550	0.01

Table2.2 : Size of various atmospheric particles present in the optical channel and type of scattering process

Type	Radius (μm)	Scattering process
Air molecules	0.0001	Rayleigh
Haze particle	0.01–1	Rayleigh-Mie
Fog droplet	1–20	Mie-Geometrical
Rain	100–10,000	Geometrical
Snow	1000–5000	Geometrical
Hail	5000–50,000	Geometrical

Atmospheric scattering not only attenuates the signal beam in the atmosphere, but it is also the primary cause for sky radiance which introduces noise in daytime communication [22]. Sky radiance is due to the scattering of solar photons along the atmospheric propagating path, and it gives rise to unwanted background noise which degrades the signal-to-noise ratio at the receiver. The received background noise depends upon the geometry of the receiver and relative location of the Sun and the transmitter. Figure 2.4 shows the scattering mechanism for the layered model of the atmosphere. The atmosphere is considered to be modeled as multiple layers with each layer consisting of homogeneous mixture of gases and aerosols. The scattering angle γ_s is the angle formed between the forward direction of the Sun radiation and the point of observation. It is seen that higher the concentration of the scatterers, more will be the sky radiance. As the angular distance between the observation direction and the Sun decreases, there is an increase in

sky radiance. Within 30° from the Sun, sky radiance is greatly dominated by aerosol contribution. As the angular distance from the Sun increases, the dominant source of background radiation is due to Rayleigh scattering.

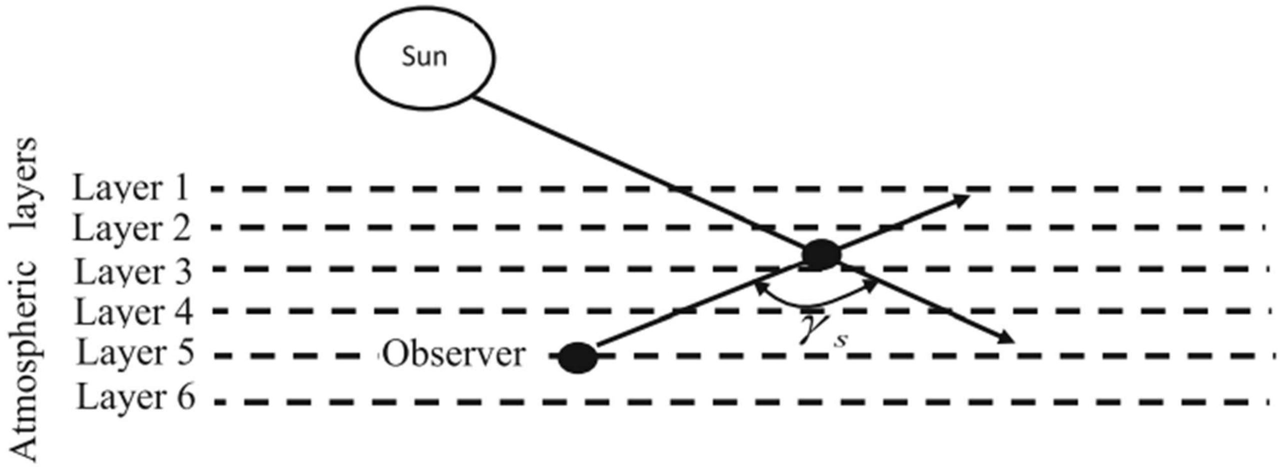

Fig 2.4: Sky radiance due to scattering mechanism

2.5.1.2 Beam Divergence Loss

As the optical beam propagates through the atmosphere, it spreads out due to diffraction. It may result in a situation in which the receiver aperture is not able to collect a fraction of the transmitted beam and resulting in beam divergence loss as depicted in Fig. 2.5. A typical FSO system transmits optical beam which is 5–8 cm in diameter at the transmitter. This beam spreads to roughly 1–5 m in diameters after propagating 1 km distance. However, FSO receiver has narrow field of view (FOV), and it is not capable of collecting all the transmitted power resulting in the loss of energy. Figure 2.5 depicts beam divergence loss where the receiver is capable of collecting only a small portion of the transmitted beam. The optical power collected by the receiver is given by

$$P_R = P_T G_T G_R L_P \quad (7)$$

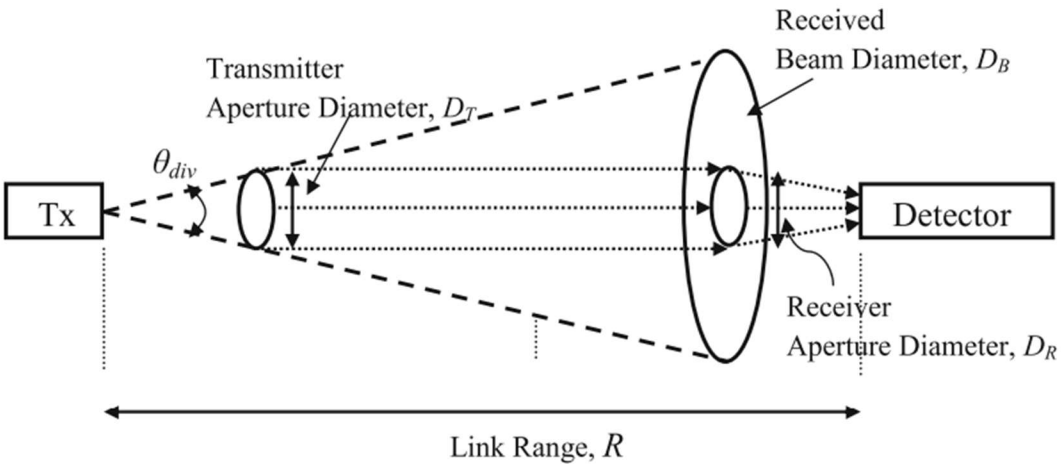

Fig 2.5: Loss due to beam divergence

where P_T is the transmitted power, L_P the free-space path loss, and G_T and G_R the effective antenna gain of transmitter and receiver, respectively. Substituting the values of $L_P = \left(\frac{\lambda}{4\pi R}\right)^2$, $G_T \approx \left(\frac{4D_T}{\lambda}\right)^2$, and $G_R = \left(\frac{\pi D_T}{\lambda}\right)^2$ gives received optical power as

$$P_R \approx P_T\left(\frac{D_T D_R}{\lambda R}\right)^2 \approx P_T\left(\frac{4}{\pi}\right)^2 \left(\frac{A_T A_R}{\lambda^2 R^2}\right)^2 \quad \text{.....(8)}$$

Therefore, diffraction-limited beam divergence loss/geometric loss expressed in dB is given as

$$L_G \text{ (Geometric Loss)} = -10\left[2\log\left(\frac{4}{\pi}\right) + log\left(\frac{A_T A_R}{\lambda^2 R^2}\right)\right] \quad \text{.....(9)}$$

In general, optical source with narrow beam divergence is preferable. But narrow beam divergence causes the link to fail if there is a slight misalignment between the transceivers. Therefore, an appropriate choice of beam divergence has to be made in order to eliminate the need for active tracking and pointing system and, at the same time, reduce the beam divergence loss. Many times, beam expander is used to reduce the loss due to diffraction-limited beam divergence as beam divergence is inversely proportional to the transmitted aperture diameter ($\theta_{div} \approx \lambda/D_T$). In this case, diffracting aperture is increased with the help of two converging lens as shown in Fig. 2.6.

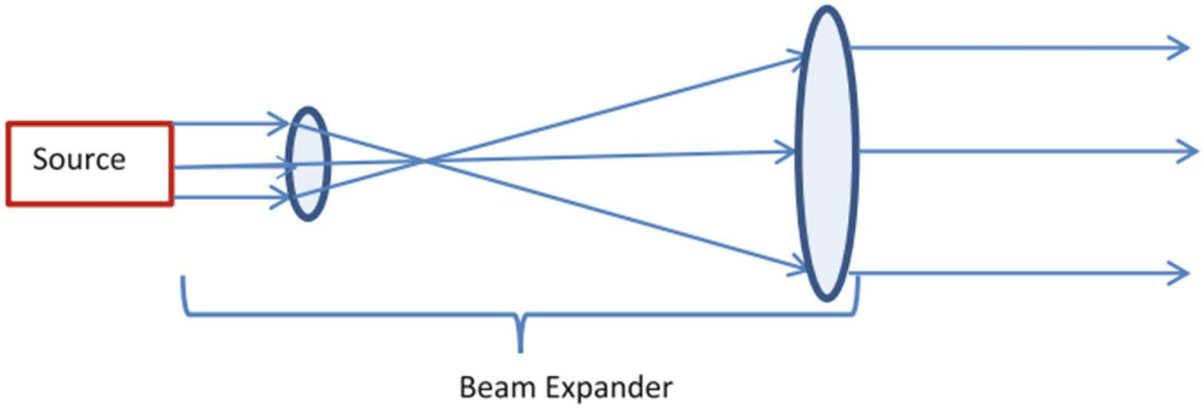

Fig 2.6: Beam expander to increase diffraction aperture

For non-diffraction-limited case, a source of divergence angle θ_{div} and diameter D_T will make the beam size of $(D_T + \theta_{div}R)$ for link distance equals to R. In this case, the fraction of received power, PR to the transmitted power, P_T is given by

$$\frac{P_R}{P_T} = \frac{D_R^2}{(D_T + \theta_{div}R)^2} \quad \ldots\ldots\ldots\ldots\ldots\ldots\ldots\ldots\ldots\ldots\ldots\ldots (10)$$

and the beam divergence or geometric loss in dB will be

$$L_G \text{ (Geometric Loss)} = -20 \log \left[\frac{D}{(D_T + \theta_{div}R)}\right] \ldots\ldots\ldots\ldots\ldots\ldots\ldots\ldots (11)$$

2.5.1.3 Loss due to Weather Conditions

The performance of FSO link is subject to various environmental factors like fog, snow, rain, etc. that leads to decrease in the received signal power. Out of these environmental factors, the atmospheric attenuation is typically dominated by fog as the particle size of fog is comparable with the wavelength of interest in FSO system. It can change the characteristics of the optical signal or can completely hinder the passage of light because of absorption, scattering, and reflection. The atmospheric visibility is the useful measure for predicting atmospheric environmental conditions. Visibility is defined as the distance that a parallel luminous beam travels through in the atmosphere until its intensity drops 2 % of its original value. In order to

predict the optical attenuation statistics from the visibility statistics for estimating the availability of FSO system, the relationship between visibility and attenuation has to be known. Several models that describe the relation between visibility and optical attenuation are given in [23,24,25]. To characterize the attenuation of optical signal propagating through a medium, a term called "specific attenuation" is used which means attenuation per unit length expressed in dB/km and is given as

$$\beta(\lambda)=\frac{1}{R}10\log(\frac{P_0}{P_R}) = \frac{1}{R}10\log(e^{\gamma(\lambda)R})\ldots\ldots\ldots\ldots\ldots\ldots\ldots\ldots\ldots\ldots \quad (12)$$

where R is the link length, P_0 the optical power emitted from the transmitter, P_R the optical power at distance R, and $\gamma(R)$ the atmospheric attenuation coefficient. The specific attenuation due to fog, snow, and rain is described below

(i) Effect of fog:

The attenuation due to fog can be predicted by applying Mie scattering theory. However, it involves complex computations and requires detailed information of fog parameters. An alternate approach is based on visibility range information, in which the attenuation due to fog is predicted using common empirical models. The wavelength of 550 nm is usually taken as the visibility range reference wavelength. Equation below defines the specific attenuation of fog given by common empirical model for Mie scattering

$$\beta_{fog}(\lambda) = \frac{17}{V}(\frac{\lambda}{550})^{-q}\ldots\ldots\ldots\ldots\ldots\ldots\ldots\ldots\ldots\ldots\ldots \quad (13)$$

where V(km) stands for visibility range, λ(nm) is the operating wavelength, and p the size distribution coefficient of scattering.

According to Kim model, p is given as:

$$p = \begin{cases} 1.6 & V>50km \\ 1.3 & 6km<V<50\ km \\ 0.16V + 0.34 & 1km<V<6km \\ V-0.5 & 0.5km<V<1km \\ 0 & V<0.5km\} \end{cases}$$

According to Kruse model, p is given as:

$$p = \begin{cases} 1.6 & V>50\ km \\ 1.3 & 6km<V<50\ km \\ 0.585V^{1/3} & V<6\ km \end{cases}$$

Different weather conditions can be specified based on their visibility range values. Table 2.3 summarizes the visibility range and maximum loss for different weather conditions.

Another two models are also very famous

Alnaboulsi Convection: $\beta_{fog}(\lambda) = 4.343\left(\frac{0.11478\lambda + 3.8367}{V}\right) dB/km$ ..... (14)

Kim model has been used in this experiment.

Ijaz Model: $\beta_{fog}(\lambda) = \frac{17}{V}\left\{\frac{\lambda}{0.55}\right\}^{-q\lambda}, q(\lambda) = 0.1428\lambda - 0.0947 dB/km$ ..... (15)

Table 2.3 visibility range and maximum loss for different weather conditions according to Kim Model

Sl No.	Weather Condition	Visibility Range(KM)	loss (dB/ km) (max) for 1550 nm
1.	Extremely Clear weather	50	0.04
2.	Very Clear	25	0.1
3.	Clear	10	0.5

4.	Light Haze	5	1.5
5.	Haze	2	5
6.	Thin Fog	1	10.1
7.	Light Fog	0.500	20.2
8.	Moderate Fog	0.250	41
9.	Thick Fog	0.1	100
10.	Dense fog	.05	250

Effect of rain:

The sizable rain droplets can cause wavelength-independent scattering, and the attenuation produced by rainfall increases linearly with rainfall rate. The specific attenuation for rain rate R (mm/hr) is given by

$$\beta_{rain} = 1.076R^{0.67} \quad \text{.....(16)}$$

Loss due to Different rain rate can be specified based on above calculation and Table.2.4 summarize the loss for different rain rate.

Table. 2.4 Attenuation due to Rain

Sl. No.	Rain Rate (mm/hr)	Loss (dB/Km)
1	5	3.16
2	10	5.03
3.	15	6.6
4.	20	8.00
5.	25	9.29
6.	30	10.51
7.	35	11.65
8.	40	12.74

9.	45	13.75
10.	50	14.80
11.	55	15.77
12.	60	16.72
13.	65	17.64
14.	70	18.53
15.	75	19.41
16.	80	20.27
17.	85	21.11
18.	90	21.93
19.	95	22.74
20.	100	23.47

Effect of Snowfall:

Attenuation due to snowfall is given by the equation

$$A_{snow}\ [dB/km] = aS^b \quad \ldots\ldots\ldots\ldots\ldots\ldots\ldots\ldots\ldots\ldots\ldots\ldots \text{(17)}$$

S is the snowfall rate in mm/hour

a and b are the constant is given as for the two different condition as

(a) Wet Snow(attitude < 500m);

  $a = 0.0001023\lambda+3.78554766$

  $b = 0.72$

(b) Dry Snow ((attitude > 500m);

  $a = 0.0000542\lambda+5.4958776$

  $b = 1.38$

Calculation: for a moderate snow rate 5mm/hour and λ= 1550nm

(a) a = 3.94andb = .72 for Dry Snow

  A_{snow}= 12.55 dB

(b) a = 5.58 and b= 1.38 for Wet Snow

A_{snow} = 51.43 dB

Loss due to Different snow rate can be specified based on above calculation and Table. 2.5 summarize the loss for different snowfall rate.

The experiment for snow could not be performed due to lack of proper infrastructure.

Table 2.5: Attenuation due to snowfall

Wet Snow		
Sl No.	**Snow Rate (mm/hr)**	**Loss (dB/Km)**
1.	5	12.55
2.	10	20.68
3.	15	27.69
4.	20	34.06
Dry Snow		
1.	5	51.43
2.	10	133.85
3.	15	234.23
4.	20	348.38

2.5.1.4 Effect of Atmospheric Turbulence:

Atmospheric turbulence is induced due to the fluctuation of refractive index of air in a Sunny day. Random variations of the atmospheric refractive index along the propagation path of the optical ray caused by atmospheric turbulence. This fluctuation of refractive index is resulting from the random changes in atmospheric temperature, which is a function of the atmospheric temperature, which is a function of the atmospheric air pressure, elevation and time of the days and wind speed.[27]

$$n = 1 + 77.6 \times 10^{-6} \times (1 + 7.52 \times 10^{-3} \lambda^{-2}) \times (\frac{P}{T_e}) \quad \text{.....(18)}$$

P is the atmospheric pressure in millibars

Te is the temp in Kelvin

λ = is the wavelength in microns.

Change of refractive index with temp in given by

$$-\frac{dn}{dTe}=7.8\times10^{-5}\frac{P}{T_e^2} \quad \text{..... (19)}$$

Refractive index structure C_n^2 is the main considerable parameter that defines the turbulence. It depends on time, altitude and location of the day and so on season.

$$C_n^2(h)= 0.00594\left(\frac{V}{27}\right)^2(10-5h)10\exp\left(-\frac{h}{1000}\right)+ 2.7X10^{-16}\exp\left(-\frac{h}{1500}\right)+ A\exp\left(-\frac{h}{100}\right)$$

.....(20)

h= is altitude in meter, V= wind speed in m/s

A= turbulence strength at ground level A=10-14m-2/3

The wind and altitude are the most important variable in the model.

Depending on the size of turbulent eddy and transmitter beam size, three types of atmospheric turbulence effects are observed:

(**a)Beam Wander (or beam steering):** If the size of eddies are larger than the transmitter beam size, it will deflect the beam as a whole in random manner from its original path. This phenomenon is called beam wander, and it effectively leads to pointing error displacement of the beam that causes the beam to miss the receiver.

(b)Beam Scintillation: If the eddy size is of the order of beam size, then the eddies will act like lens that will focus and de-focus the incoming beam leading to irradiance fluctuations at the receiver and the process is called scintillation. Scintillations cause the loss of signal-to-noise ratio and result in deep random signal fades. Scintillation losses depend upon the intensity of thermal turbulences. It can be calculated as

$$\alpha_{scin}=\sqrt{23.17[\frac{2\pi}{\gamma}[10^9]^{\frac{7}{6}}C_n^2 l^{\frac{11}{6}}]} \quad \text{.....(21)}$$

λ = Wavelength of laser Source in (nm) = 1550 nm

L = length of channel in meter

C_n^2 = Refractive index structure parameter

C_n^2 = 10-16 (For Low turbulence)
10-14 (For Moderate turbulence)
10-13 (For High turbulence)

Scintillation results due to atmospheric turbulence and the attenuation due to this are unpredictable and it in maximum during midday when temperature in maximum. Loss due to Scintillation can be specified based on Turbulence and Table. 2.6 summarize the loss for different turbulence.

Table 2.6: The loss for different turbulence.

Low Turbulence		
Sl No.	Link range (m)	Scintillation Loss (dB)
1.	200	0.044
2.	500	0.103
3.	1000	0.194
4.	2000	0.366
Moderate Turbulence		
5.	200	0.443
6.	500	1.025
7.	1000	1.935
8.	2000	3.655
High Turbulence		

9.	200	1.5005
10.	500	3.244
11.	1000	6.125
12.	2000	11.56

(c)Beam Spreading: If the eddy size is smaller than the beam size, then a small portion of the beam will be diffracted and scattered independently. This will lead to reduction in the received power density and will also distort the received wave front. However, the effect of turbulence-induced beam spreading will be negligible if the transmitter beam diameter is kept smaller than the coherence length of the atmosphere or if the receiver aperture diameter is kept greater than the size of first Fresnel zone. In this case, the only effect will be due to turbulence-induced beam wander effect and scintillation effect.

By increasing transmitter power; the atmospheric turbulence effect cannot be completely mitigated. The effect of scintillation can be reduced by employing techniques like multiple transmit/receive antennae, aperture averaging, etc. The turbulence badly effect the BER value of a FSO communication receiver. The mitigation technique to improve BER and 99.9% of availably of FSO link are

(i)Diversity technique

(ii)Aperture averaging

(iii)Different modulation and coding technique

(iv)Forward error correction (FEC implementation)

2.6 Applications of FSO Communication Systems

Applications of FSO communication systems range from short range (< 1 km) to long range and space applications. It provides broadband solution (high data rates without cabling) for connecting end users to the backbone. Short-range application provides last mile access by connecting various towers, buildings, etc. in urban areas where digging of cables is a difficult

task. It includes point-to-point or point-to-multipoint links or broadband links. Various applications of FSO systems are listed below:

(i) Enterprise connectivity: FSO link can easily be deployed to connect various tower/building enabling local area connectivity. It can also be extended to connect metropolitan area fiber rings, connect new networks, and provide high speed network expansion.

(ii) Fiber backup: In case of optical fiber link failure, FSO link can be deployed as a backup link to ensure availability of the system.

(iii) Point-to-point links: It coves inter- (LEO-LEO) and intra-orbital (LEO-GEO) links and satellite-to-ground/ground-to-satellite link. This type of link requires good pointing and tracking system. Here, the output power of the transmitter, power consumption, size, mass, and deployment cost increase with the link range.

(iv) Point-to-multipoint links: Multi-platform multi-static sensing, interoperable satellite communications, and shared spaceborne processing are unique network application of FSO system.

(v) Hybrid wireless connection/network redundancy: FSO communication is prone to weather conditions like fog, heavy snow, etc. In order to obtain 100 % availability of the network, FSO links can be combined with microwave links that operate at high frequencies (in GHz range) and offer comparable data rates.

(vi) Disaster recovery: FSO communication system provides high-capacity scalable link in case of collapse of existing communication network.

(vii) Backhaul for cellular networks: With the advent of 3G/4G cellular communication, there is a growing challenge to increase the backhaul capacity between the cell towers to cope up with the increase in demand of broadband mobile customers. The viable backhaul options for 4G network are to deploy fiberoptic cables or to install FSO connection between towers. Deploying fiber cables is time-consuming and an expensive task. So FSO communication system plays an important role in providing backhaul capacity for cellular networks.

(viii) Broadcasting: In broadcasting of live events such as sports and ceremonies or television reporting from remote areas and war zones, signals from the camera (or a number of cameras)

need to be sent to the broadcasting vehicle which is connected to a central office via satellite uplink. The required high-quality transmission between the cameras and the vehicle can be provided by a FSO link. FSO links are capable of satisfying even the most demanding throughput requirements of today's high definition television (HDTV) broadcasting applications. For example, during 2010 FIFA World Cup, UK TV station BBC deployed FSO links for Ethernet-based transport of high definition video between temporary studio locations set up in Cape Town, South Africa.

Currently, there are several companies which are working on the design and manufacturing of FSO systems as outdoor wireless transmission solutions such as Canon (Japan), Cassidian

(Germany), fSONA (Canada), GeoDesy (Hungary), Laser ITC (Russia), LightPointe Communications (USA), MRV (USA), Northern Hi-Tec (UK), Novasol (USA), Omnitek (Turkey), Plaintree Systems (Canada), and Wireless Excellence (UK) among others.

2.7 Eye Safety and Regulations

While designing an FSO link, the designer has to ensure that the chosen operating wavelength has to be eye and skin safe. This means that the laser should not pose any kind of danger to the people who might encounter the communication beam. Figure 2.4 clearly shows the region where different wavelengths of light get absorbed in the human eye.

Microwaves and gamma rays are absorbed by the human eye and can cause high degree of damage to lenses and retina. Near-ultraviolet (UV) wavelengths are absorbed in the lens making them cloudy (cataract) which leads to dim vision or

blurring. In far UV and IR regions, wavelengths are absorbed in the cornea and produce an effect called photokeratitis which can lead to pain/watering in the eye or pigmentation in the cornea. Visible and near IR region (wavelengths used in FSO communication) has the highest potential to damage the retina of the eye, and it can lead to permanent loss of vision that cannot be healed by any surgery. The range of wavelengths between 400 and 1400 nm can cause potential eye hazards or even skin damage [6]. The impact of laser injury is more significant in case of eyes than the skin as the outer layer of the eye, i.e., the cornea, acts as a band-pass filter to the

wavelengths. Therefore, the cornea will be transparent to these wavelengths, and the energy emitted by the light sources will get focused on the retina and may cause damage to the eye due to increase in concentration of the optical energy. However, the light below 400 nm and above 1400 nm is absorbed by the cornea and does not reach the retina.

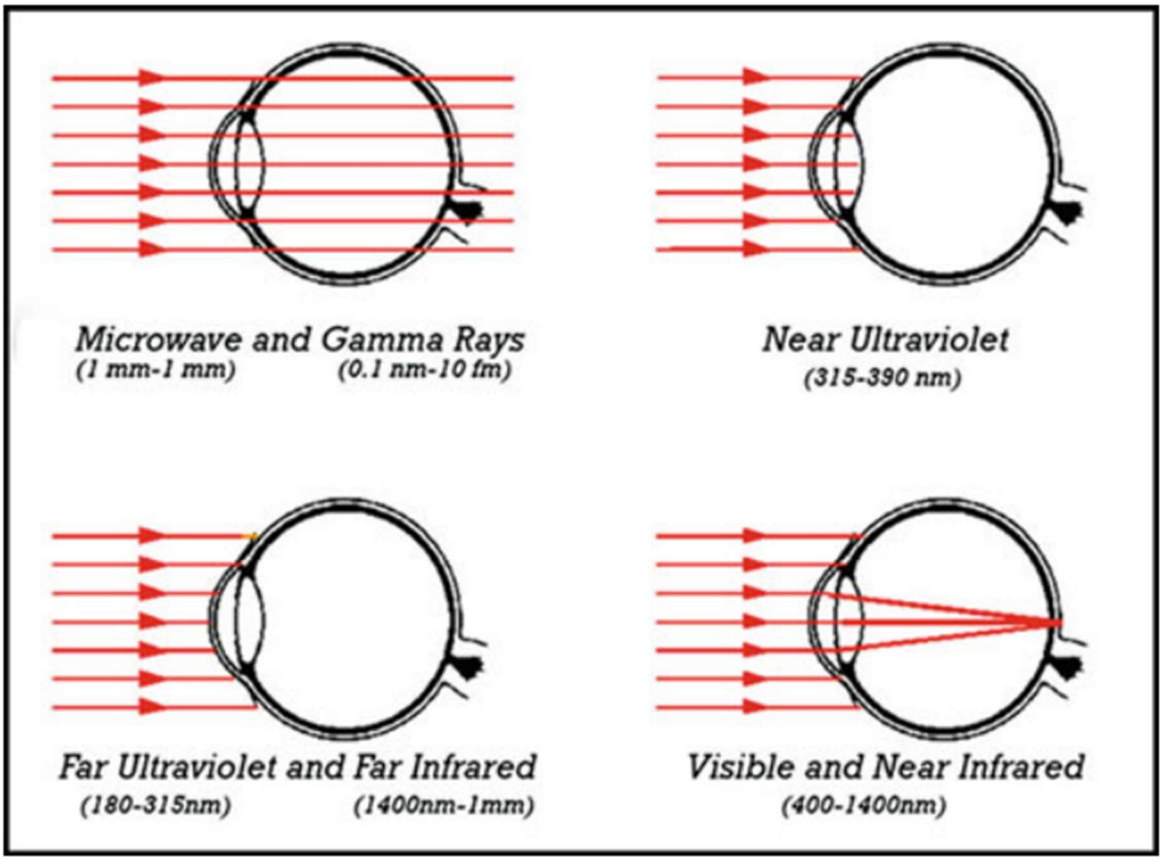

Fig 2.4: Pictorial representation of light absorption in the eye for different wavelengths [14]

The absorption coefficient of the cornea is more for higher wavelengths than (>1400 nm) than for the shorter wavelengths as can be observed from the Fig. 2.5.

Lasers can cause damage to our skin by causing thermal burns or photochemical reaction. The penetration of laser beam inside the human body depends upon the choice of operating wavelength. UV rays are absorbed by the outer layer of the skin and cause skin cancer or premature aging of the skin. Exposure of high-intensity beam for very long period can cause thermal burns or skin rashes. IR radiation can penetrate deep into skin leading to thermal burns.

Therefore, it is very essential to regulate the laser power to ensure the safety of the human eye and skin.

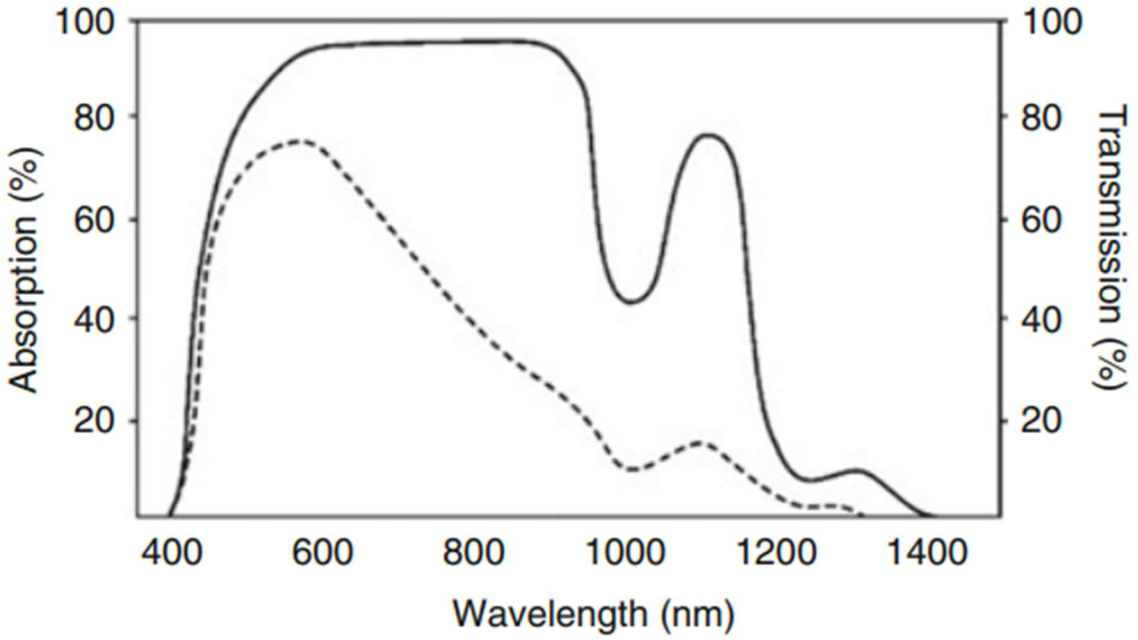

Fig 2.5: Absorption of light vs. wavelength

Various international standard bodies (such as American National Standards Institute (ANSI) Z136 in the USA, Australian/New Zealand (AS/NZ) 2211 Standard in Australia, and International Electrotechnical Commission (IEC) 60825 internationally) provide safety guidelines of laser beam depending upon their wavelength and power. Laser Institute of America (LIA) is an organization that promotes the safe use of lasers and provides laser safety information. These standards are global benchmark for laser safety, and they are used as guidelines for various manufacturers. Every organization has its own way of laser classification, and accordingly, safety precautions and administrative control measures have to be taken. The classification of the laser is based on whether or not the maximum permissible emission (MPE) is longer or shorter than the human aversion response.

MPE is a quantity that specifies a certain level up to which the unprotected human eye can be exposed to laser beam without any hazardous effect to the eye or skin. Aversion response is the autonomic response (within 0.25 s) of the blinking eye when it moves away from the bright

source of light. Another quantity that determines classification of lasers is accessible emission limit (AEL) which is the mathematical product of two terms, i.e., MPE limit and limiting area (LA) factor. Therefore, AEL = MPE × LA.

Based upon MPE and AEL calculations, lasers are broadly classified into four groups, i.e., Class 1 through Class 4. The lower classifications (Class 1 and 2) have minimum power and therefore do not require protective eye wear. This class has extended MPE measurements as the human eye will avert from the bright light long before the beam can injure the unprotected eye. The higher classification (Class 3R, 3B, and 4) has high power levels; therefore, proper eye safety precautions have to be taken during laser operations. In this class MPE is shorter than aversion response. Table 2.1 gives the comparison of laser classification according to IEC and ANSI standards.

Table 2.1: Laser classification according to IEC and ANSI standards

Classification	IEC 60825	ANSI-Z136.1
Class 1	Very low power lasers and are safe under reasonably foreseeable conditions of operation. This class is exempted from all beam-hazard control measures. It includes optical instruments for intrabeam viewing.	
Class1M	Low power lasers operating between 302.5 nm and 4000 nm wavelengths and are safe under reasonably foreseeable conditions except when used with optical instruments such as collecting lens, binoculars, telescope, etc. These lasers produce either collimated beams with large beam size or highly divergent beams.	N/A

Class 2	Low power laser operating between 400 nm to 700 nm (visible range). This laser class can be continuous wave (CW) or repetitively pulsed lasers. It is safe to use if it emits energy below Class 1 AEL for emission duration of less than 0.25 sec (i.e., the time period of the human eye aversion response). It has an average radiant power of 1mW or less.	
Class 2M	Low power laser operating between 400 nm to 700 nm (visible range). It can cause optical hazards when viewed with optical instruments such as collection lens, telescope, etc. Any emissions outside this wavelength region must be below the Class 1M AEL.	N/A
Class 3R	Average power lasers operating between 302.5 nm and 106 nm. The accessible emission limit is within 5 times the Class 2 AEL for visible range wavelengths and within 5 times the Class 1 AEL for wavelengths outside this region. It is unsafe to view the beam directly with diameter > 7mm	N/A
Class 3A	N/A	Average power lasers operating between 302.5 nm and 106 nm. The accessible emission limit is within 5 times the Class 2 AEL for visible range

		wavelengths and between 1 and 5 times the Class 1 AEL for wavelengths outside this region. It is unsafe to view the beam directly with diameter > 7mm.
Class 3B	Average power lasers that cannot emit an average radiant power greater than 0.5 Watts for an exposure time equal to or greater than 0.25 seconds. It is unsafe to view the beam directly but are normally safe when view diffused reflections	
Class 4	High power lasers and are very dangerous both under intrabeam and diffuse reflection viewing conditions. They may also cause skin injuries and are potential fire hazards.	

Table 2.2 presents the AEL for two most commonly used wavelengths in FSO communication systems. It is evident from the table that for Class 1 and 2, lasers operating at 1550 nm are almost 50 times more powerful than lasers at shorter operating wavelength, i.e., 850 nm. Also, the combination of low attenuation, high component availability, and eye safety at 1550 nm wavelength makes it a preferred choice for FSO communication. Lasers operating at 1550 nm wavelength when used with erbium-doped fiber amplifier (EDFA) technology are capable of providing high data rates (>2.5 Gbps) and high power.

Class 1 and Class 1M lasers are preferred for terrestrial FSO communication links as their radiations are safe under all circumstances. IEC60825-12 [15] covers the safety standard for free-space optical communication links, and it lists out the requirements like power, aperture size, distance, and power density for 850 and 1550 nm wavelengths which are presented in Table 2.3. Higher classes of lasers are also used for FSO communication links for long distance communication or deep space missions. To ensure the safety of these systems, they are installed on higher platforms like rooftops or towers to prevent any kind of human injury. It is to be noted

that high-powered pulsed lasers are more dangerous than lower power continuous lasers. However, lower power laser beams can also be hazardous when given long-term exposure.

Table 2.2: Accessible emission limits for 850 and 1550 nm according to IEC standard

Laser classification	Average output optical power (mW)	
	850 nm	1550 nm
1	<0.22	<10
2	Used only for 400–700 nm and has same AEL as Class 1	
3R	0.22–2.2	10–50
3B	2.2–500	50–500
4	>500	>500

Table 2.3: Various requirements of Class 1 and 1M lasers for 850 and 1550 nm [16]

Classification	Power (mW)	Aperture size (mm)	Distance (m)	Power density (mW/cm2)
850 nm Wavelength				
Class 1	0.78	7	14	2.03
		50	2000	0.04
Class 1M	0.78	7	100	2.03
	500	7	14	1299.08
		50	2000	25.48
1550 nm Wavelength				
Class 1	10	7	14	26
		25	2000	2.04
Class 1M	10	3.5	100	103.99
	500	7	14	1299.88
		25	2000	101.91

Chapter 3

Experimental Setup and Link Budget Analysis

Chapter 3

Experimental Setup

The total experimental setup can be divided into two parts, this is shown in the chart below fig 3.1

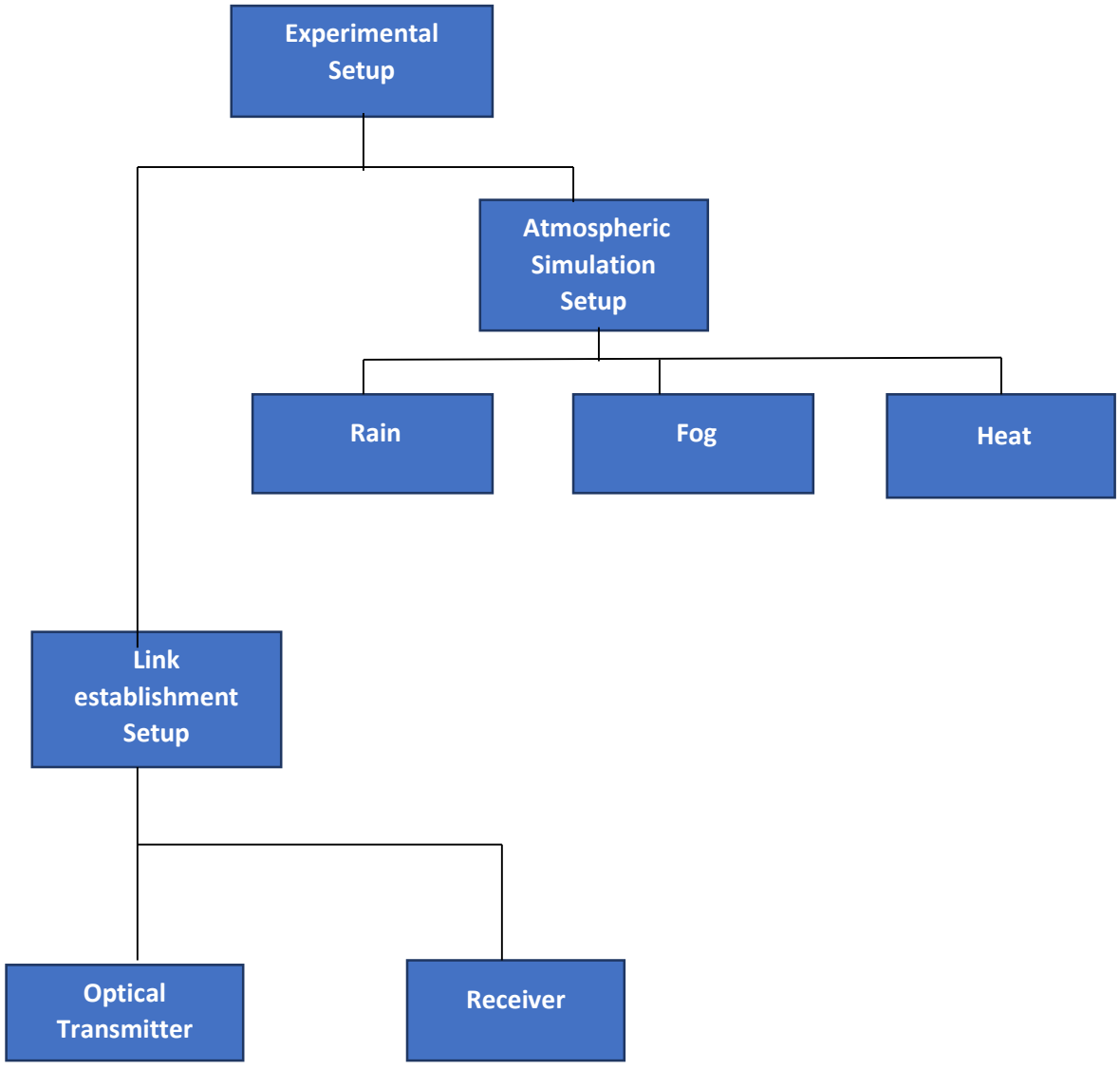

Fig 3.1: Schematic Diagram of the Setup

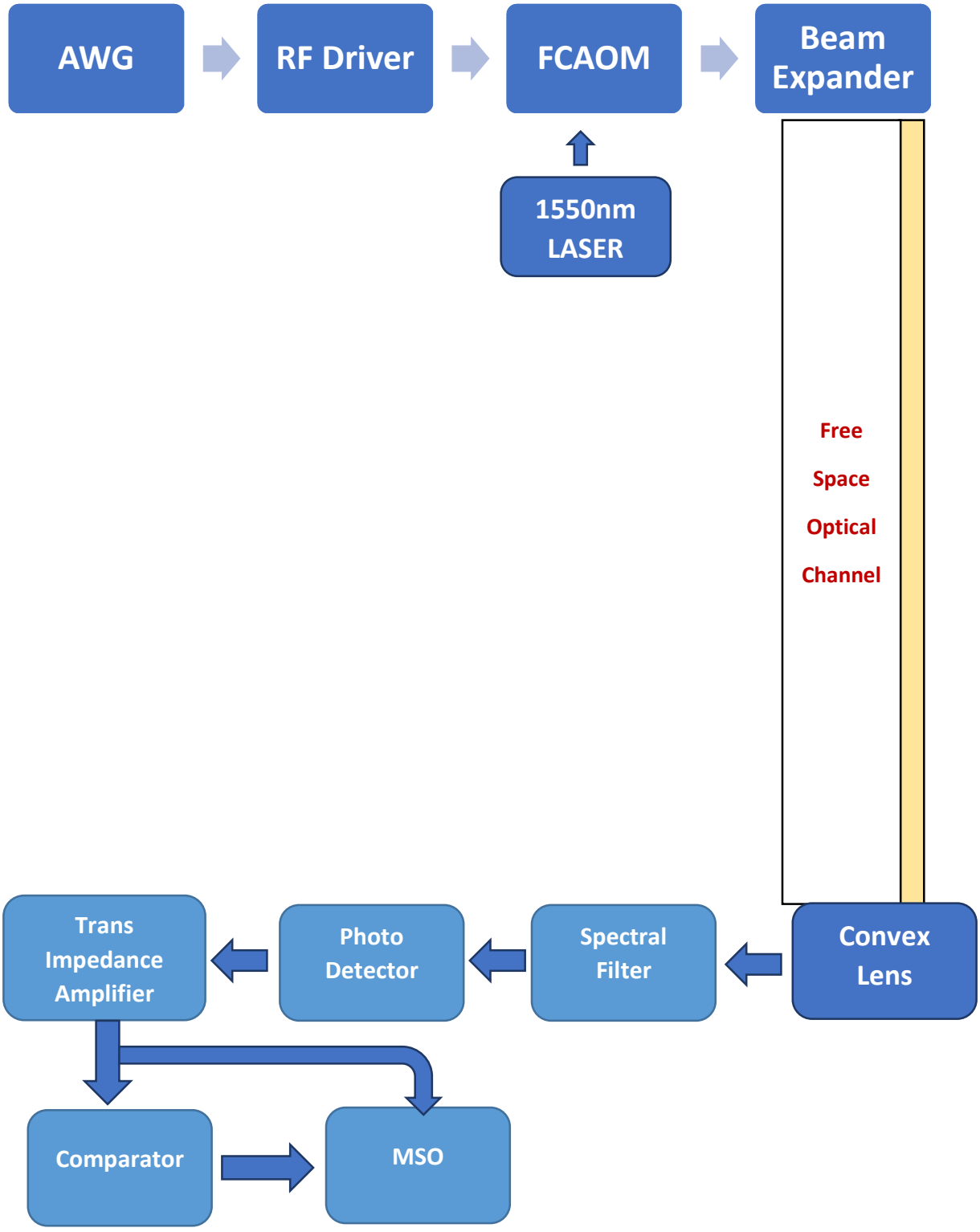

Fig 3.2: Figure of equipment Arrangements

3.1 Link Establishment Setup

3.1.1 Optical Transmitter

The optical transmitter including the choice of laser, concept of ATP system, and various types of modulation schemes and coding techniques used in FSO communication system are discussed in this section. Further, the details of communication and beacon detectors in FSO receiver are also discussed. The transmitter converts the source information into optical signals which are transmitted to the receiver through the atmosphere. The essential components of the transmitter are

(i) modulator

(ii) driver circuit for the optical source to stabilize the optical radiations against temperature fluctuations, and

(iii) collimator that collects, collimates, and direct the optical signals toward the receiver via atmospheric channel. The optical sources that are used for FSO transmission lie in the atmospheric transmission window that is ranging from 700 to 10,000 nm wavelength. The wavelength range from 780 to 1064 nm is most widely used as beacon operating wavelength. The 1550 nm wavelength is commonly used as data operating wavelength due to following reasons:

(i) Reduced background noise and Rayleigh scattering: The absorption coefficient of the Rayleigh scattering has functional dependence with the wavelength λ asλ^{-4}: Consequently, there is almost negligible attenuation at higher operating wavelengths as compared to those at the visible range.

(ii) High transmitter power: At 1550 nm a much higher power level (almost 50 times) than at lower wavelengths is available to overcome various losses due to attenuation.

(iii) Eye-safe wavelength: The maximum permissible exposure (MPE) for eye is much higher at 1550 nm wavelength than at 850 nm. This difference can be explained by the fact that at 850 nm, approximately 50 % of the signal can reach the retina whereas at 1550 nm, the signal is almost completely absorbed by cornea itself. And therefore, the signal received at the retina is negligibly small.

The component cost increases with the increase in the operating wavelength. For good optical transmitter, the choice of laser power and wavelength has to be made very carefully so that an appropriate optical power and transmit antenna gain can be achieved in order to form a closed loop communication link. However, this is not the only constraint for most laser sources. The selection of laser is influenced by several other factors including efficiency, operational lifetime, and achievable diffraction limited output power and weight. A good source will have narrow, stable spectral line width and nearly diffraction-limited single mode spatial profile. Some of the key requirements which affect the choice of the transmitter laser for FSO-based applications are given below:

(i) Pulse repetition frequency (PRF): The laser pulsing mechanism (e.g., Q-switching, cavity dumping) determines the PRF of the laser. Q-switched lasers using acousto-optic or electrooptic modulators have PRF less than 200 kHz. Cavity dumping lasers have PRF in the order of tens of megahertz. PRF up to several gigahertz can be achieved with the power amplified lasers used in conjunction with several stages of amplification.

(ii) Average output power: The laser should have sufficient average power for a reliable communication link with adequate link margin. For any good laser, it should provide pulse to pulse power stability and nearly constant average power over different data rates. The peak power of any laser is given by the product of energy per pulse and the pulse width. Solid-state lasers provide large peak power at low PRF. However, the maximum peak power is limited by the heat dissipation and laser safety norms.

(iii) Pulse width: Laser pulse width should be small to facilitate less background noise in narrow temporal slots.

(iv) Pulse extinction ratio: The ratio of laser power in on-mode to that of in off mode is called pulse extinction ratio. The extinction ratio should be as large as possible. If the laser emission is not switched to complete off-mode, it may degrade the extinction ratio resulting in a lower link margin. Solid-state lasers have modulation extinction ratio of 40 dB, whereas semiconductor lasers have relatively poor extinction ratio of about 10 dB. Fiber lasers and amplifiers have extinction ratios in the order of 30 dB.

(v) Output beam quality: The output of the laser should consist of single spatial mode or at least have single null in the center of far field pattern. To avoid undesired oscillations either within the laser or in the transmitted beam, feedback isolation of the laser from the back reflected beam is required.

(vi) Beam pointing stability: For FSO-based applications, the pointing accuracy on the order of micro-radian or better is desirable. Such an accuracy requires the pointing stability of the laser to be maintained by the use of optomechanical or spatial resonators within the laser.

(vii) Overall efficiency: In order to minimize the electrical power requirement, it is desirable to have highest possible overall efficiency.

(viii) Mass and size: For any space-based applications, the mass and size of all the components should be minimized to achieve low launch cost. It therefore necessitates the use of optomechanical designs of laser resonator.

(ix) Operational lifetime: The lifetime of the active laser components (e.g., diode laser, modulator and drivers, etc.) are expected to exceed the operational lifetime of the system. Redundancy of the active elements or block redundancy of the laser will help in extending the operational lifetime. It should be noted that the higher the pump power, the lower is the expected lifetime of the laser.

(x) Thermal control and management: An efficient thermal control is required so that the dissipated heat does not affect the optical alignment integrity of the system that would otherwise result in further loss.

Table 3.1 : Different optical source [26]

Wavelength(nm)	Type	Remark
~850-1064	Vertical cavity surface emitting LASER	• Cheap and readily available (CD lasers) • No active cooling • Lower power density • Reliable up to ~10Gbps

~1300/ ~1550	Fabry-perot distributed-feedback LASER	• Long life • Lower eye safety criteria • 50 times higher power density(100mW/cm^2) • Compatible with EDFAHigh speed, up to 40 Gbps • A slope efficiency of 0.03-0.2 W/A
~10,000	Quantum cascade laser	• Expensive and relative new • Very fast and highly sensitive • Better fog transmission characteristics • Components not readily available • No penetration through glass

A brief introduction of important components used in Transmitter Side and their functions

- **Arbitrary waveform generator:** It is a piece of electronic test equipment used to generate electrical waveforms. These waveforms can be either repetitive or single-shot (once only) in which case some kind of triggering source is required (internal or external). The resulting waveforms can be injected into a device under test and analysed as they progress through it, confirming the proper operation of the device or pinpointing a fault in it.

  Unlike function generators, AWGs can generate any arbitrarily defined waveshape as their output. The waveform is usually defined as a series of "waypoints" (specific voltage targets occurring at specific times along the waveform) and the AWG can either jump to those levels or use any of several methods to interpolate between those levels.
  Signal generated from AWG has been used as message signal in this experiment.

- **Radio Frequency (RF) Driver:** A RF driver produces a radio frequency signal which modulates with the message signal before transmission. This process is called modulation. The modulation techniques are discussed in details in

- **Fiber-coupled acousto-optic modulators (FCAOM):** offer a robust solution for amplitude modulation of fiber lasers, allowing direct control of the timing, intensity, and temporal shape of the laser output. According to the message signal the RF driver generates the RF signal which drives the FCAOM. FCAOM is an optical modulator which modulates the continuous optical beam to a pulsed optical beam according to the RF driver signal. The 1550 nm continuous laser beam is another input of FCAOM. The output of FCAOM is the modulated 1550 nm optical beam.

- **Beam Expander:** Before transmitting in air, a beam forming optic, namely beam expander is used to reduce the divergence angle of the laser, which will reduce the free space loss and the beam divergence loss of the system. In receiver side another beam forming optic, namely convex lens is used to increase the receiver aperture area; hence the beam divergence loss will be reduced. Then it passes through a 1550 nm spectral

filter, where the other optical wavelengths present in the sunlight will be suppressed and only 1550 nm modulated laser beam will be received by the 1550 nm photo-detector

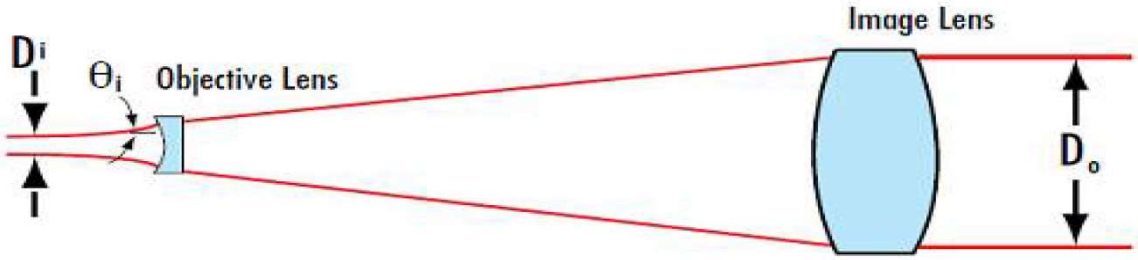

Fig 3.3: Beam expander

Table 3.2 : Specifications of the beam expander

SL no	Parameter	Specifications
1	Beam Expander Magnifying power	MP=10X
2	Entrance Aperture	4.5mm
3	Exit Aperture	45mm
4	Transmission	95%
5	Operating wavelength	1550nm

3.1.2 Optical Receiver

The receiver helps to recover the transmitted data after propagating through turbulent atmosphere. It consists of receiver telescope, filter, photo detector, signal processing unit, and demodulator. The receiver telescope comprises of lenses that focus the received optical signal onto the photo detector. The filter is used to reduce the amount of background noise. The noise sources present at the receiver include background, detector dark current, preamplifier, signal shot noise, and thermal noise. The photo detector converts the received optical signal into electrical signal which is passed on to the processing unit and then to the demodulator. In the

receiver, both PIN and APD can be used. In the FSO uplink, the received power level is quite low due to large free-space loss. At this power level, an APD receiver gives much better performance than the PIN receiver. The choice of optical receiver depends upon various fundamental issues and hardware parameters. Some of the important parameters are listed below:

(i) Modulation technique: The detection technique used at the receiver depends upon the modulation format. Not every detection technique is suited for every modulation format, e.g., direct detection receivers are insensitive to phase and polarization information.

(ii) Hardware availability, reliability, and cost: Different types of receiver have different hardware requirements which may or may not be readily available at reasonable cost. For example, high gain Si-APD works efficiently only at wavelength below 1000 nm. At higher wavelengths, other detectors like InGaAs/InGaAsP can be used depending upon the requirement.

(iii) Receiver sensitivity: This is a very important parameter in all optical communication system including FSO communication system. It is measured in terms of average received photons per bit and is given as

$$\eta_{av} = \frac{P_{av}}{h\nu R} \quad \text{.....(22)}$$

where hν is the photon energy at the transmit operating wavelength (λ=c/ν) and R the bit rate/data rate. The receiver sensitivity depends mainly on photon detection technique, modulation format, photodetector, and background noise. These are briefly described in later part.

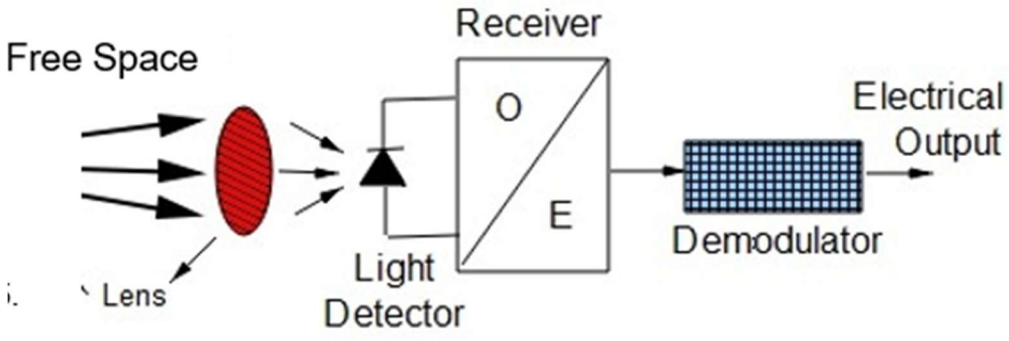

Fig 3.4 Schematic model of the receiver unit

A brief introduction of important components used in Receiver Side and their functions

- **Receiver Convex Lens:** The incoming optical radiation is collected by the receiver Lens and focused into the photo detector. A large receiver Lens aperture is desirable as it collects multiple uncorrelated radiations and focuses their average on photo detector. This is referred to as aperture averaging but a wide aperture also means more background radiation/ noise.

Table 3.3 : Specifications of the Receiver lens

Sl.No.	Parameter	Specification
1	Diameter	100 mm = $100X10^{3}$m
2	Focal length	150mm
3	Transmission	98%

Beam Divergence Loss: As the optical beam propagates through the atmosphere, it spreads out due to diffraction. It may result in a situation in which the receiver aperture is not able to collect a fraction of the transmitted beam and resulting in beam divergence loss as depicted in Fig. 3.4.

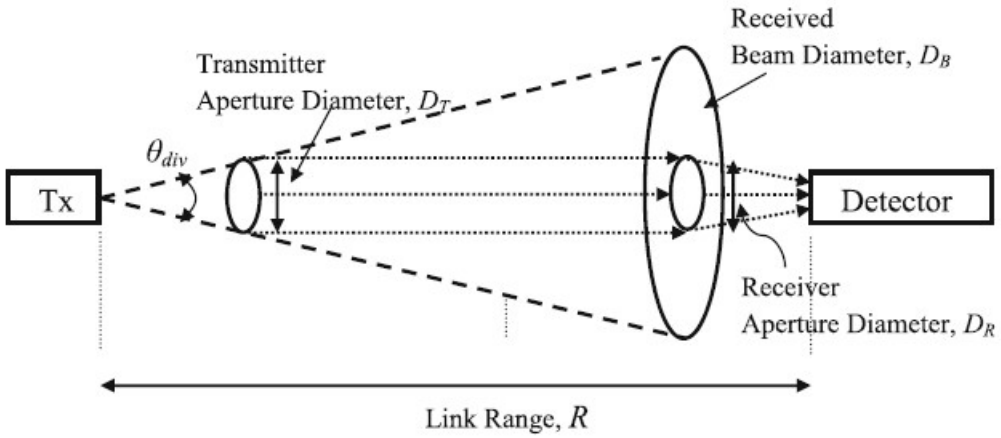

Fig.3.5. Transmitters Beam Divergence

Case 1: Diffraction Limited Condition:[28]

A typical FSO system transmits optical beam with narrow beam divergence at the transmitter. This beam spreads to roughly in larger diameters after propagating long distance. However, FSO receiver has narrow field of view (FOV), and it is not capable of collecting all the transmitted power resulting in the loss of energy as beam divergence loss where the receiver is capable of collecting only a small portion of the transmitted beam.[28]

The optical power collected by the receiver is given by

$$P_R = P_T.G_T.L_P.G_R \quad \text{.....(23)}$$

P_T= 1Watt = +30dBm ; D_T = 0.18mm & λ=1550nm

$$G_T = 10 \log (\pi D_T/\lambda)^2 \quad \text{.....(24)}$$

$$= 10 \log \{(3.14\times0.18X10^{-3})/ (1550\times10^{-9})\}^2 \text{ dB}$$

$$= 20 \log \{(314\times18\times10^2)/155\} \text{ dB} = \mathbf{51.237\ dB}$$

$$L_P = 10 \log[\lambda/4\pi R]^2 \quad \text{.....(25)}$$

$$= 10\log_{10}\{(1550\times10^{-9})/(4\times3.14\times1\times10^3)\}^2$$

$$= 10 \log (1.5\times 10^{-20}) = \mathbf{-198.18dB}$$

$$G_R = 10 \log [\pi D_R /\lambda]^2 \quad \text{.....(26)}$$

$$= 10\log_{10}\{(3.14\times100\times10^{-3})/ 1550\times10^{-9}) \}^2 \quad [D_R=100\text{mm}]$$

$$= 10 \log (3.14\times10^{+5}/155)^2 = 10 \log(314/155)^2 +100$$

$$= \mathbf{112.26dB}$$

Divergence loss= [+51.23 – 198.18 + 112.26] dB= **- 34.68 dB**

Case 2: Non- Diffraction Limited Condition:

In general, optical source with narrow beam divergence is preferable. But narrow beam divergence causes the link to fail if there is a slight misalignment between the transceivers. Therefore, an appropriate choice of beam divergence has to be made. in order to eliminate the need for active tracking and pointing system and, at the same time, reduce the beam divergence loss. Many times, beam expander is used to reduce the loss due to diffraction-limited beam divergence as beam divergence is inversely proportional to the transmitted aperture diameter.

2.1. Beam Expander:

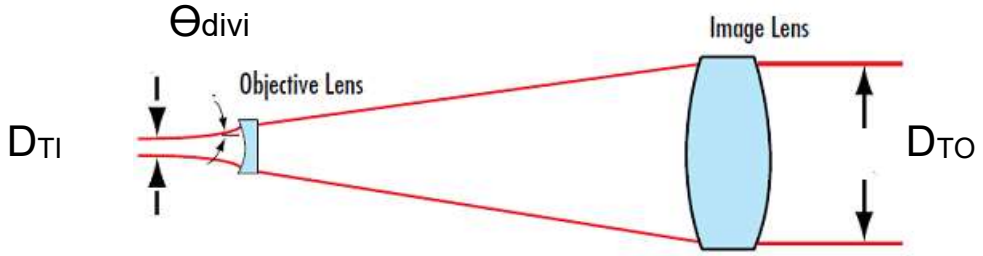

Fig.3.6. Beam Expander Diameter

Input Beam Divergence= Θdivi

Output Beam divergence= Θdivo

Input Beam Diameter=D_{TI}=1.8×10^{-3} m

Output Beam Diameter=D_{TO} (To be calculated)

The Magnifying Power MP= D_{TO}/ D_{TI} =10(given) =Θdivi / Θdivo

So, output Beam divergence Θdivo is decreases by 10 times.

Output Beam diameter D_{TO} =1.8×10^{-3} m × 10 = **18×10^{-3}m**

2.2 Effect of Beam Expander at Receiver:

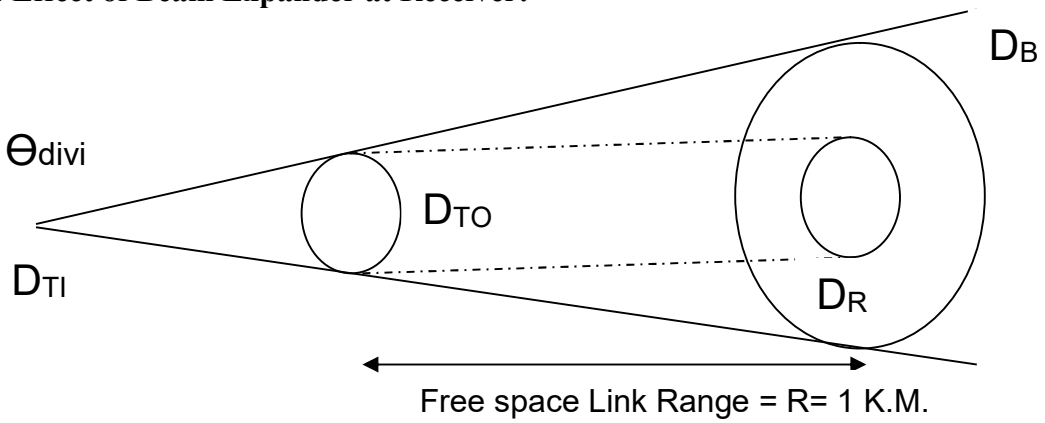

Fig.3.7. Receiver Beam Diameter

A Laser's input beam diameter and divergence can be used to calculate the output beam diameter at a specific link distance R.

Case 1: Without Beam Expander:

Beam Diameter at Receiver: $D_B = D_{TI} + R \tan(2\Theta divi)$ .....(27)

[Here factor 2 is required as Laser beam divergence is specified in terms of a half angle]

So Beam diameter at Receiver

$D_B = (0.18 \times 10^{-3}) + 1 \times 10^3 \tan(2 \times 1 \times 10^{-3})$

$= .18mm + 1 \times 10^3 \times 2 \times 10^{-3}$

$= .18mm + 2000\ mm = 2000.18\ mm$

$D_B =$ **2000.18 mm**

Case 2: With Beam Expander:

Now beam expander will increase the input beam and decrease the input divergence by the Magnifying power of 10& D_B become D_R[35].

$D_R = (MP \times D_{TI}) + R \tan(2\Theta divi/MP)$ .....(28)

$D_R = (MP \times D_{TI}) + R \tan(\Theta divo)$ .....(29)

Replace $(\Theta divi/MP) = \Theta divo$

Now FOR input Beam diameter=0.18mm= Θdivi

Input beam divergence= 1 mard

Link Range distance1= 1 Km

So, Output beam diameter at Receiver

$D_R = (10 \times 0.18 \times 10^{-3}) + 1 \times 10^3 \tan[(2 \times 1 \times 10^{-3})/10]$

$= 1.8 \times 10\text{-}3m + 1 \times 10^3 \times 2 \times 10^{-4}$

$= 1.8mm + 2 \times 10^{-1} = 201.8\ mm$

$D_R =$ **201.8 mm**

So, for non-diffraction-limited case, a source of divergence angle Θdivi and diameter D_{TI} will make the beam size of D_R for link distance equals to R. In this case, the fraction of received

power, P_R to the transmitted power, P_T can be calculated using the beam divergence or geometric loss which is in dB will be as follows [28]

Geometric loss $L_P = 20 \log [L_{DR}/ D_R]$ dB

Receiver lens diameter L_{DR}= 100 mm & D_R = **201.8 mm**

Geometric loss = 20 log [100/201.8]

= 20 log [0.49955]

L_P= **-6.028dB**

- **Optical Filter:** An optical filter is a device that selectively transmits light of different wavelengths according to operational bandwidth is used to reduce the background solar radiation.

Table 3.4: Specifications of Optical Filter

SL no	Parameter	Specifications
1	Centre Wavelength	1550nm±2.4nm
2	Bandwidth	12nm
3	Transmittance	50%
4	Diameter	25mm

- **Photo Detector:** An Indium Gallium Arsenide (InGaAs) Detector is used for detections of light signal with the following specification**.**

Table 3.5: Specifications of Photo Detector

SL No.	Parameter	Specification
1	Operational Laser Range	800mm –1700nm
2	Active Area	0.2 mm^2
3	Peak wavelength	1590 nm

4	Responsivity at peak	1.04 A/W
5	NEP	1.26×10^{-11} w√Hz
6	Bandwidth	150 MHz
7	Dark Current	Not available
8	Noise resistance	Not available

SNR of the Receiver:

In direct detection technique, the received optical signal is passed through optical band-pass filter to restrict the background radiation. It is then allowed to fall on the photo detector which produces the output electrical signal proportional to the instantaneous intensity of the received optical signal. It may be regarded as linear intensity to current convertor or quadratic (square law) converter of optical electric field to detector current. The signal-to-noise ratio (SNR) of direct detection receiver can be obtained by using noise models for a particular detector. With the received power at the receiver after link budget calculation and detector noise sources, the SNR expressions are obtained. The SNR for photo detector is given by[28]

$$\text{SNR} = \frac{(R_0 P_R)^2}{2qB(R_0 P_R + R_0 P_B + I_d) + \frac{4K_B TB}{R_L}} \quad \ldots\ldots\ldots\ldots\ldots\ldots\ldots\ldots\ldots (30)$$

P_R	Received power at receiver
R_0	Detector Responsivity
q	1.602×10^{-19}
B	Photodetector bandwidth
I_d	Dark Current
P_B	Background Solar Power
K_B	$1.38064852 \times 10^{-23}$
T	Temperature in Kelvin
R_L	Photo detector resistance

Quantum Efficiency:

The detector quantum efficiency η can be calculated by the following equation [28]

$R_0 = \eta q/h\nu$ …… (31)

$R_0 = 1.6 \times 10^{-9} \times \eta / 6.624 \times 10^{-34} \times 1.935 \times 1014 = 1.24\ \eta$

So, $\eta = 1.04/1.24 = .8387 = 83\ \%$

$\upsilon = C/\lambda = 3\times10^8/1550\times10^{-9} = 1.935\times10^{14}$

Noise in Photo-Detector:

(i)Shot Noise: Due to the statistical nature of photon to electron conversion and because the photons that arrive at the photodetector do so at random times described by a passion distribution. The spectral density of a shot noise is assumed to constant or white noise variance σ_{Sh}^2 given by as

$$\sigma_{Sh}^2 = 2\times qI_P\times B \quad \ldots\ldots\ldots\ldots\ldots\ldots\ldots\ldots\ldots\ldots\ldots\ldots(32)$$

(ii) Dark Current Noise- It is due to small reverse leakage current through device. Dark current noise variance is given by as

$$\sigma_{Dark}^2 = 2qBI_d \quad \ldots\ldots\ldots\ldots\ldots\ldots\ldots\ldots\ldots\ldots\ldots\ldots(33)$$

(iii) Thermal Noise: Noise variance in receiver due to shunt resistance, series resistance of photodetector & Load resistance R_L is given as

$$\sigma_{th}^2 = 4K_BT_eB/R_L \quad \ldots\ldots\ldots\ldots\ldots\ldots\ldots\ldots\ldots\ldots\ldots\ldots(34)$$

(iv) Solar Background Noise: it arises due to solar background power received P_{BG}. The background noise is a shot noise and its variance is given as

$$\sigma_{BG}^2 = 2qBI_B \quad \ldots\ldots\ldots\ldots\ldots\ldots\ldots\ldots\ldots\ldots\ldots\ldots(35)$$

$$I_B = R_0\times P_{BG} \quad \ldots\ldots\ldots\ldots\ldots\ldots\ldots\ldots\ldots\ldots\ldots\ldots(36)$$

The received power of solar radiation reflected from the background has influence on the photodiode signal to noise ratio. The level of received power depends on the day times season, geographic co-ordination, atmospheric condition etc.

The field of view (FOV) of the receiver is equal to the ratio of the detector size to the focal length.[30]

$$FOV = d/f = (d/D_R)F\# \quad \ldots\ldots\ldots\ldots\ldots\ldots\ldots\ldots\ldots\ldots\ldots\ldots(37)$$

Here, f= effective local length, D_R= receiver aperture,

F# is the f number, or ratio of focal length to diameter.

F#= 150/100=1.5

Receiver diameter= 0.5 mm

FOV= $(0.5\times10^{-3}\times\times1.5)/(100\times10^{-3})=0.75\times10^{-2}$ rad

The power of the receiver due to background can be calculated by[29]

$$P_B = N_B.T_R\,(\pi.D_R/2 \times FOV/2)^2\times B_{OPT} \quad \text{.....(38)}$$

[Where, N_B= irradiance, T_R = Receiver lens Transmittance=0.9, B_{OPT}= optical filter BW=12n]

For N_B= 100 watt/m^2/μm

P_{BG}= $100\times 0.9(22\times100\times10^{-3}\times0.75\times10^{-2}/7\times2\times2)^2\times0.012$ watt

= $(90\times0.012\times22\times22\times100\times100\times0.75\times0.75\times10^{-10}/7\times2\times2\times7\times2\times2)$ Watt

= $3750X10^{-10}$ Watt = 375 nw = -34 dBm

For N_B= 60watt/m2/μm

P_{BG} =225 nw = -36 dBm

The Solar background power P_{BG} is important when its value is equal to or less than the received signal power at photodetector.

The SNR of the photo detector cannot be calculated by using the classical formula as described above as the parameters such as photodectector shunt resistance, value of drain current is not known, and hence we may calculate the SNR from NEP of the photo detector.

After link budget analysis the received power at receiver is given as P_R= -27 dBm = 2 μWatt.

Noise Equivalent Power (NEP): Noise equivalent power is defined optical power that produces a signal (voltage/current) equal to the noise voltage or current of the photo detector. Lower NEP is the better to detect a weak signal. The Specific Detectivity (D) is derived from the NEP with relation to the active detector area A is given as

$$D = \left(\frac{\sqrt{A}}{NEP}\right)\left[\frac{cm\sqrt{Hz}}{W}\right] \quad \text{.....(39)}$$

Detectivity (D) = $(0.002\ cm^2)^{1/2}$ / 1.26×10^{-11}

= $0.04472/1.26\times10^{-11}$

= 0.35×10^{10}cm√Hz/W

High Values of detectivity means that detector is suitable for detecting weak signal in the presence of noise.

Minimum Detectable optical Power: This value represents the minimum detectable optical power without any additional output filtering assuming an SNR of 1.

P_{min} (detectable) = $1.26\times\times10^{-11}\times\sqrt{150\times10^{6}} = 15.43\times10^{-8}$

Photon per bit (N_P) at P_{min}:= $P_{min}/ (h\upsilon) \times R_b$ [31]

$N_P = 15.43\times10^{-8}/(6.624\times10^{-34}\times1.935\times10^{14}\times150\times10^{6})$

= 8025 photon/bit

Now, we can extract SNR from NEP of photo detector as [32]

$$SNR = \frac{P_R}{NEP\sqrt{\Delta f}} \qquad \text{……..(40)}$$

$$= \frac{2 \times 10^{-6}}{1.26 \times 10^{-11}\sqrt{150 \times 10^{-6}}}$$

$$= \frac{2 \times 10^{-6}}{1.26 \times 10^{-8} \times 12.24}$$

$$= 200/15.43 = 12.96$$

SNR (dB) = $10 \log_{10}(12.96) = 11.12$ dB

The Received power and corresponding SNR with available link margin is summarize in Table 3.6

Table 3.6: SNR at Receiver

Sl.No.	Received Power(P_R)	P_R (dBm)	SNR	SNR(dB)	Link Margin(dB)
1	2.0×10^{-6} W	-27	12.96	11.12	35
2	3.16×10^{-6} W	-25	20.47	13.11	33
3	3.98×10^{-6} W	-24	24.98	13.97	32
4	5.01×10^{-6} W	-23	32.46	15.12	31
5	6.31×10^{-6} W	-22	40.89	16.12	30
6	7.94×10^{-6} W	-21	51.45	17.12	29
7	10.0×10^{-6} W	-20	64.80	18.12	28
8	12.59×10^{-6} W	-19	81.59	19.12	27
9	15.85×10^{-6} W	-18	102.72	20.12	26
10	19.95×10^{-6} W	-17	129.29	21.12	25

SNR is often related to E_b/No as

$S/N = E_b/No + 10 \log (\text{data rate}/B.W)$ [33] ……(41)

$E_b/No = S/N + 10\log (BW/\text{data rate})$.

❖ **Trans impedance amplifier and Comparator circuit:**

The trans-impedance amplifier is used for amplify the captured photodetector signal and convert the photodetector current signal into voltage signal. The photodetector signal (PD IN) is fed to the inverter terminal of the U1A which is a high-speed op-amp. The value of R3 and C10 has been chosen according to the bandwidth requirement of the system. As the photodetector signal is fed to the inverting terminal of U1A, the signal is inverted. This inverted signal is not comparable with comparator unit, so, this signal is inverted in another stage (U1B), as a result this amplified signal is similar of photodetector signal (PD IN) which was not the

amplified signal. The second stage has been configured as a unity gain. This signal is fed to the high speed comparator (U2) non inverting side, and a minimum threshold value is set for the accurate operation of the comparator. Two voltage regulator has been used U3 and U4 for positive supply regulator and negative supply regulator respectively for proper functioning of the U1A, U1B, U2 respectively. Fig.3.8. shows Schematic layout of the trans-impedance amplifier and Fig.3.9. shows Trans-impedance and comparator unit.

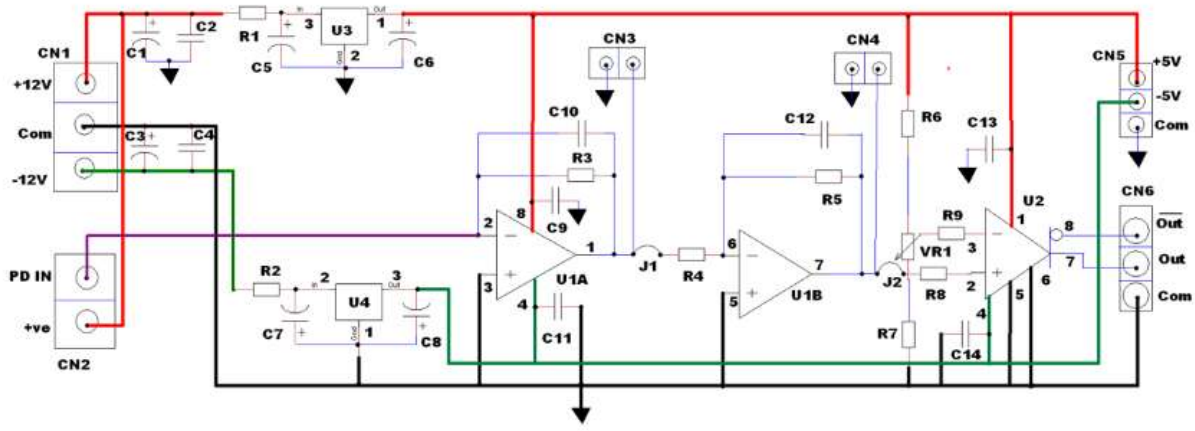

Fig.3.8. Circuit Diagram of the trans-impedance amplifier

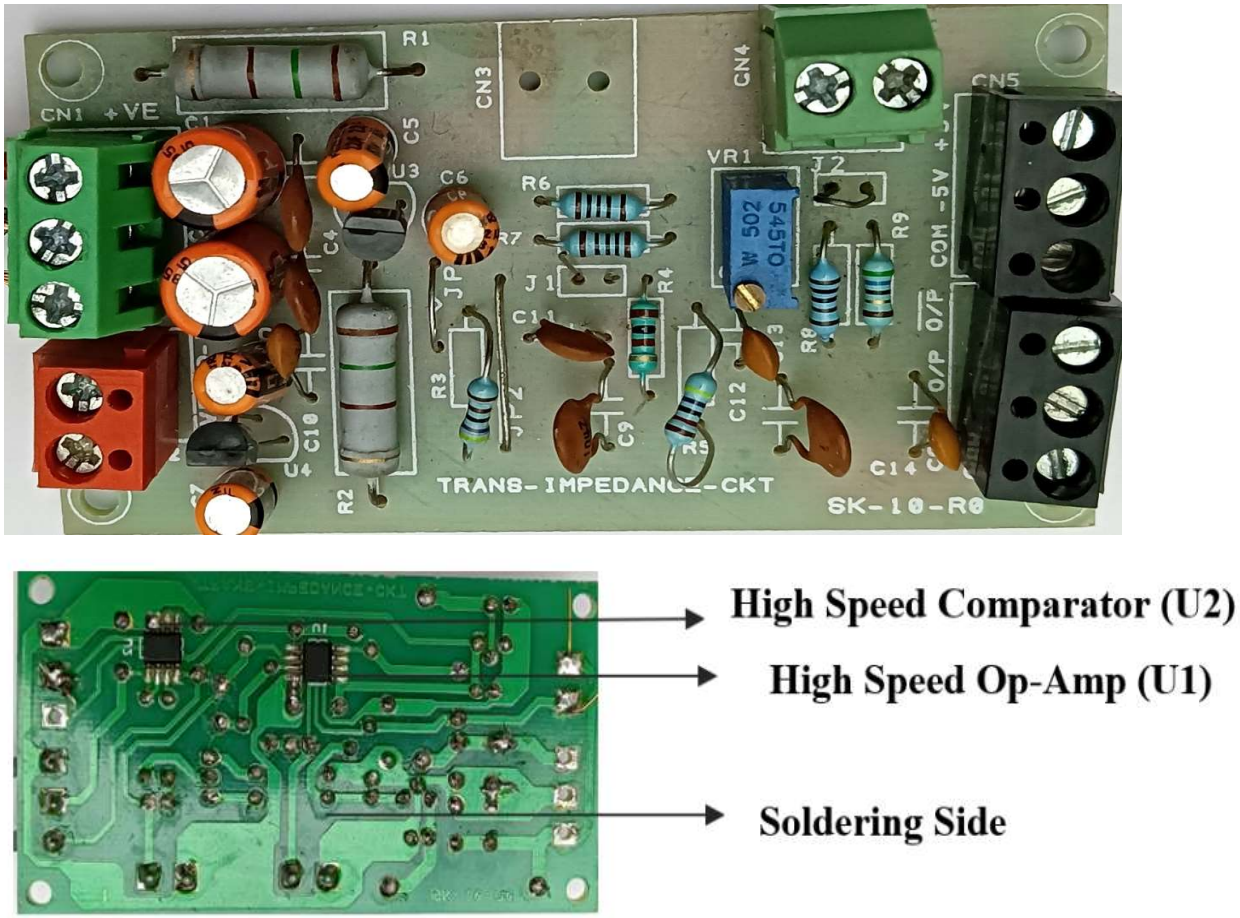

Fig.3.9. Trans-impedance and comparator unit

3.2 Atmospheric Simulation Setup

3.2.1: Rain Simulation setup

To simulate the rainy condition, we needed a system which acts like a water sprayer or sprinklers. The main concept of this simulation setup was that the water droplets from the sprayers or sprinklers were to be fall down directly on the FSO link. To achieve this simulation, water flowing pipes were tied with Thermo Mechanically Treated steel (TMT) based rigid structure which is shown in the fig. It was done to provide mechanical support to the pipes. The length of the structure was kept at 25ft. That means, the distance between sending side and the receiving side was kept at 25 ft. Nozzles, showers with various outlet diameter was fitted with the pipes. These were used as the sprinklers or sprayers. The whole system of pipes was connected with different valves and a motorized pump. This was done for controlling the speed

of the water droplets or simulated rain coming out from the nozzle inlet, shower. In this way different Rain rate was achieved. This simulated rain rate was measured by a rain gauge which was shown in the fig 3.10 , fig 3.11 and fig 3.12. Different rain rates were considered for the experiment.

Fig 3.10 . The rain simulation setup

Fig 3.11 The experiment is going on in the rain simulation setup

Fig 3.12: The rain gauge used for measuring rain rates for the experiment

3.2.2: Fog Simulation setup

To simulate foggy condition two main components were used.

(i) A totally closed wooden box structure:

The fog was to be created inside this box. The box was created almost leakproof so that fog does not come out of the box during experiment. But also had some small windows to clear out all the fog quickly after the experiment was over and also for the purpose of cleaning inside the box. for had been made. The length of the box was m. Schematic diagram of the box is given in the fig 3.13 and the actual figures of the box is given in the fig and fig .3.14

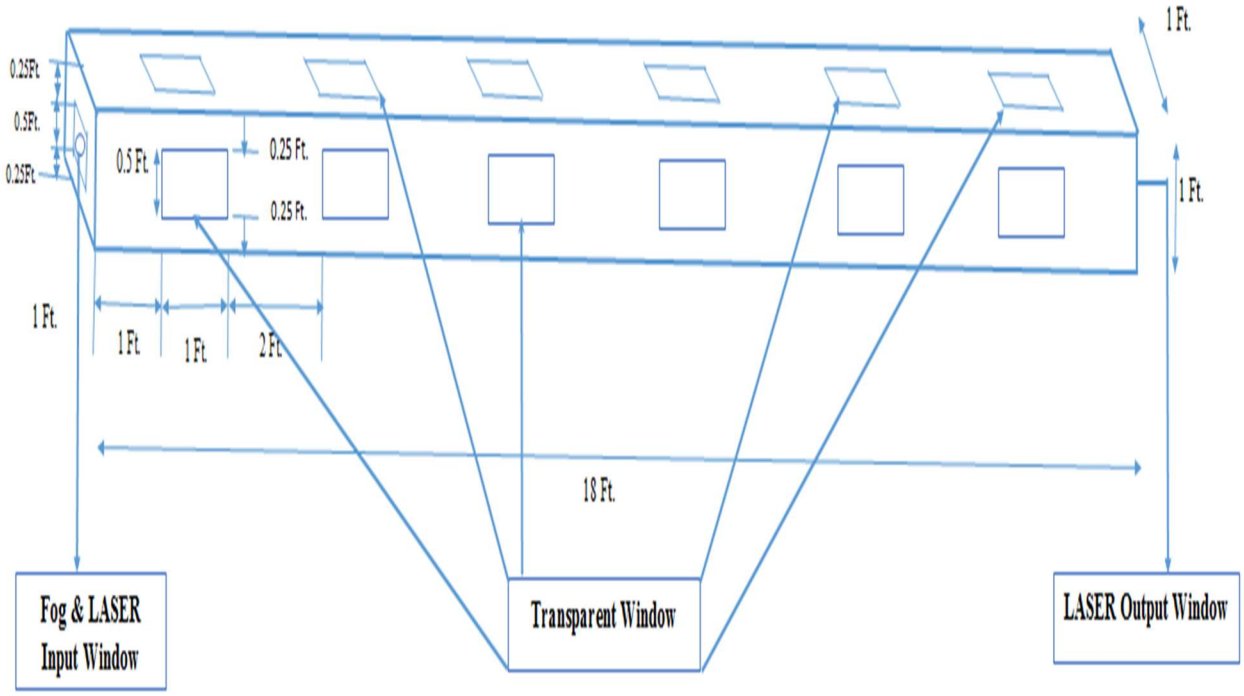

Fig 3.13 : Schematic diagram of the fog simulation box/chamber

Fig 3.14: Actual figure of the artificial fog simulation box/chamber

Fig 3.15: Inside view of the artificial fog simulation box/chamber

(ii) Artificial Fog Creation System:

Fog is a visible aerosol consisting of tiny water droplets or ice crystals suspended in the air at or near the Earth's surface.

Ultrasonic nebulizers work on the principle that high frequency sound waves can break up water into aerosol particles. This form of nebulizer is powered by electricity and uses the piezoelectric principle. This principle is described as the ability of a substance to change shape when a charge is applied to it.

This is how ultrasonic nebulizer was used to produce artificial fog. The artificial fog produced by the ultrasonic nebulizer was fed to the wooden chamber to make a simulated artificial foggy atmospheric condition. This is shown in the fig 3.15 , fig 3.16. The ultrasonic nebulizers also had controller to control the amount of simulated fog to be produced. This is how various artificial foggy atmospheric conditions like lite, medium, dense fog was created by using the controller.

Fig 3.15 : Artificial fog simulation setup with ultrasonic nebulizers

Fig 3.16 : Artificial fog inside the wooden box/chamber

3.2.3: Heat Simulation setup

To simulate heated condition, some current carrying copper coils were used. The were put inside the same previous wooden box used for artificial foggy conditions. Three different coils with the power rating of 1500W each were used. The end terminals of each of the coils were connected with separate AC Voltage source and a separate variac. The variacs were used to control the voltage across the coils or current in the coils. Due to flow of the current, heat was produced in the coils as per the Joule's law. This heat generation by the coil was used to create warm or hot atmospheric condition. The amount of heat produced in the coil is proportional to the square of the current flowing in the coil. The coils were put on some ceramic pots so that the heated coils do not touch the surface of the wooden box (fig 3.17). It also gives the rigid support to the heated coil as they got expanded from their initial conditions due to heat. Digital thermometers were used to monitor the ambient temperature inside the wooden box. The whole setup is shown in the fig 3.18 and fig 3.19.

Two separate coil systems were put at the two ends inside the wooden box. The separated systems were connected with two separated variacs and AC power sources. This is how the temperature difference between the two ends of the wooden box was easily made by varying the the current in the coil using two different variac. This temperature difference between two ends inside the wooden box resulted the variation in refracting index of the air inside the box along vertical direction. Due to this effect scintillation of the beam was achieved.

Fig 3.17: Coils are put on the ceramic pots

Fig 3.18: Setup for the heated condition

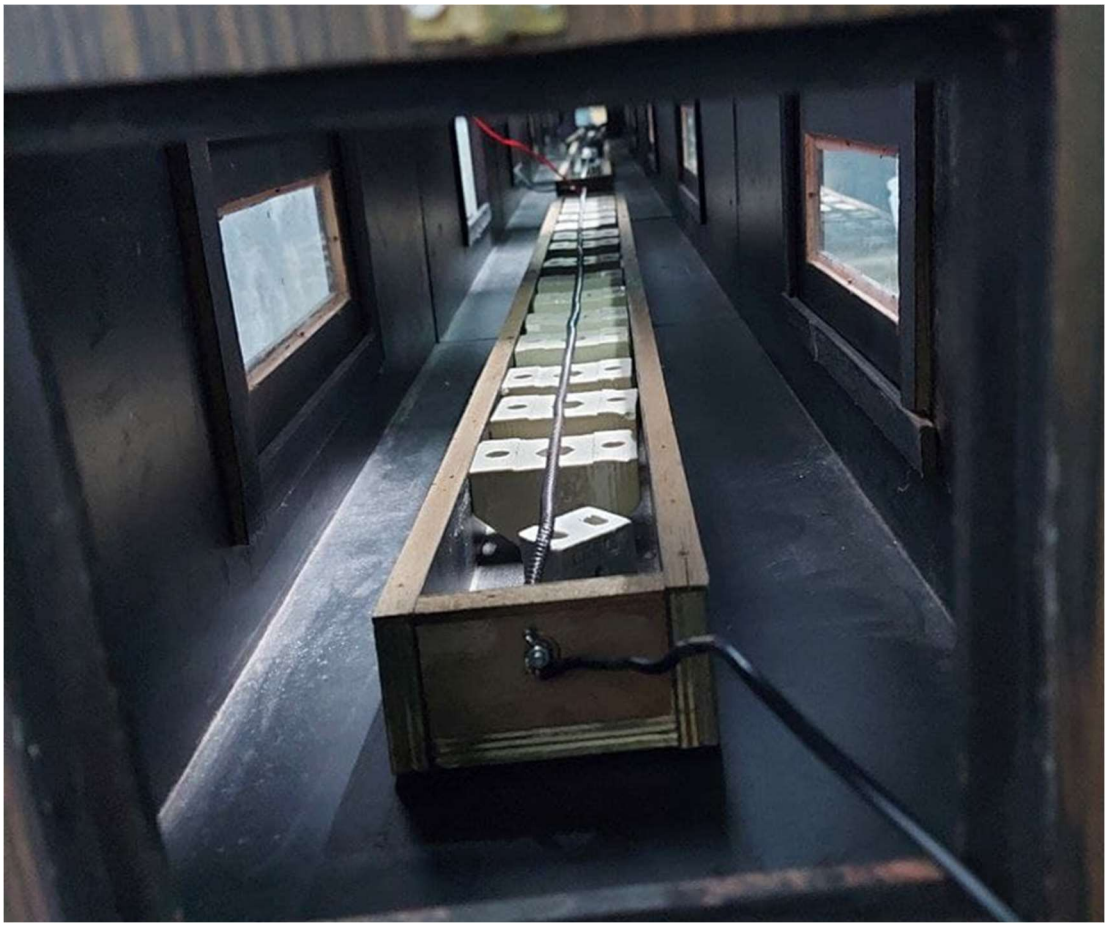

Fig 3.19: Inside the wooden box

3.3 Modulation Technique and BER

There are different types of modulation schemes which are suitable for Free Space Optics (FSO) communication systems, among which On-Off Keying (OOK), and frequency Shift Keying modulation schemes are used.

OOK modulation:

It is the dominant modulation scheme employed in commercial terrestrial FSO communication systems. This is primarily due to its simplicity and resilience to the innate nonlinearities of the laser and the external modulator. OOK can use either Non Return-to-Zero (NRZ) or Return-to-Zero (RZ) pulse formats. In NRZ-OOK, an optical pulse of peak power "αePT" represents a digital symbol "0" while the transmission of an optical pulse of peak power "PT " represents a digital symbol "1". The optical source extinction ratio "αe" has the range $0 \leq \alpha e < 1$. The finite duration of the optical pulse is the same as the symbol duration "T.[34]

If OOK modulation is used then **B= f_b =B.W= data rate & S/N = E_b/No**

The probability of error for NRZ-OOK-coded optical data, detected with a photodiode, can be expressed as a function of the Signal-to-Noise Ratio (SNR) as in

$$BER_{NRZ-O} = \left(\frac{1}{2}\right) erfc\left(\left(\frac{1}{2\sqrt{2}}\right)\sqrt{SNR}\right) \quad \text{.....(42)}$$

In RZ-OOK, the required SNR is equal to half "-3dB" of the required SNR of the regular NRZ-OOK to achieve the same BER performance, with the expense of doubling the bandwidth, and the BER for RZ-OOK can be expressed as a function of Signal-to-Noise Ratio (SNR) as follows:

$$BER_{RZ-OOK} = \left(\frac{1}{2}\right) erfc\left(\left(\frac{1}{2}\right)\sqrt{SNR}\right)$$

With RZ-OOK, the pulse duration is lower than the bit duration, giving an improvement in power efficiency over NRZ-OOK at the expense of an increased bandwidth requirement.

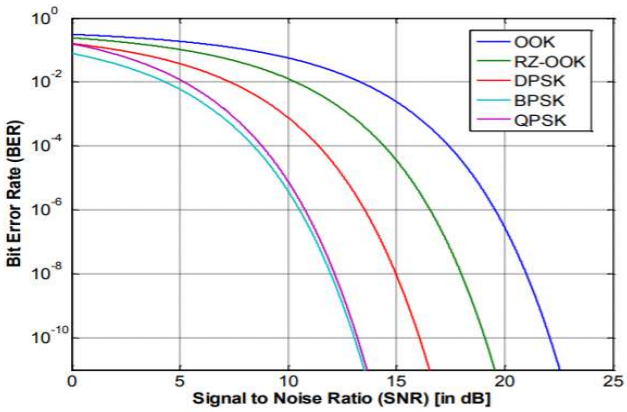

Fig 3.20.:. BER and required SNR & E_b/No

For SNR of 20.12 dB at receiver the corresponding BER for NRZ-OOK modulation can be calculated as

$BER_{NRZ-OOK}$ = ½ erfc (1/2√2×√102.72)

= ½ erfc (3.583)

= 2.019322×10^{-7}

For SNR of 17.12 dB at receiver the corresponding BER for RZ-OOK modulation can be calculated as

$BER_{NRZ-OOK}$ =

= ½ erfc (3.586)

= 1.9748×10^{-7}

Hence to achieve same BER for RZ-OOK 3 dB less power is required.

3.4 Link Budget Calciulation

Link Power Budget: The link budget, overall calculation of the link performance of laser communication system is given in Table 5) The link analysis is performed for a ground –to ground range of 1Km with 1Watt transmitter laser operating at wavelength 1550 nm at the data rate of 150MHz/sec(10MHz usable) using a detector as a receiver.

Table 3.7: Link Power Analysis

Sl.No.	Parameter	Value	Power(dBm)
1	Tx output power	1 watt	+ 30 dBm
2.	Tx implementation optical Loss	-5 dB	+25 dBm
3.	Space loss	-6 dB	+19 dBm
4.	Atmospheric Loss in Clear visibility& without turbulence	-2 dB	+17 dBm
5.	Rx implementation optical Loss	-5 dB	+12 dBm
6.	Receiver sensitivity for 12 dB SNR	-27 dBm	--
Obtained Link Margin		**39dB**	
Link Margin for Atmospheric Turbulence/ Scintillation		**4 dB**	
Available Link Margin for adverse Atmospheric condition: Fog/Rain/Snow		**35 dB/25dB**	

Link Margin Budget [36]: The link margin matrix for different combination of adverse Atmospheric condition such as Fog/Rain/Snow & its combination is summarized in Table 3.8

Table 3.8: Link Margin Matrix

Sl.No.	Atmospheric Condition	Value	Req. Margin
1	Foggy condition	Visibility : 300m	35 dB
2.	Rainy Condition	Rain rate: 100mm/hr	24 dB

3.	Snowy Condition	Snowfall Rate :20mm/hr	34 dB
4.	Fog & Rain Combination 1	Visibility : 500m Rain rate: 50mm/hr	20 dB+15dB = 35 dB
5	Fog & Rain Combination 2	Visibility : 1Km Rain rate: 100mm/hr	10dB+24 dB = 34 dB
8.	Fog & snow Combination 1	Visibility :500m Snow rate:5mm/hr	20 dB+13dB = 33 dB
9.	Fog & snow Combination 2	Visibility :1 Km Snow rate:10mm/hr	10 dB+21dB = 31 dB

The presence of matter in the atmospheric such as gases, aerosols, fog, rain, snow, cloud, dust and haze along the propagation path decreases the availability and reliability of FSO link. To get 99.9 % link availability in these conditions there are a link margin for these in link budget design as calculated in the link budget analysis. These atmospheric losses can be mitigated either by increasing the transmitter power or by decreasing the data rate to maintain the same acceptance E_b/N_o at the receiver. Initially design a system for clear weather with minimum atmospheric attenuation for clear visibility and keep maximum atmospheric attenuation as link margin for the system.

Calculated maximum Link Margin to mitigate adverse atmospheric condition.

(i) For Fog-Maximum Link Margin of **35 dB** (calculated)

The FSO system may not work less than visibility of 300m.

(ii) For Rain- Maximum Link Margin **25 dB** (calculated)

The FSO system may work for rain rate up to 100mm/hr

(iii) For Snow- Maximum Link Margin **35 dB** (calculated)

The FSO system may not work more than wet snow rate of 20 mm/hr.

The T_X will operate at minimum required power under clear atmospheric condition, as the Fog/Rain/Snow will come into effect and using sensor data at T_X/R_X will feedback to increase the T_X Power as per Fog/Rain/Snow rate.

Chapter 4

Experimental Results

Chapter 4

Experimental Results

4.1 Rainy condition simulation

Initially, the minimum optical power, required for pulsing has been set to establish the communication link for a bit error rate of 10^{-11}. The link range is considered 25 m. In fig 4.1, the first window indicates the eye diagram of the received photodetector signal and second window indicates the comparator signal's eye diagram at clear weather condition.

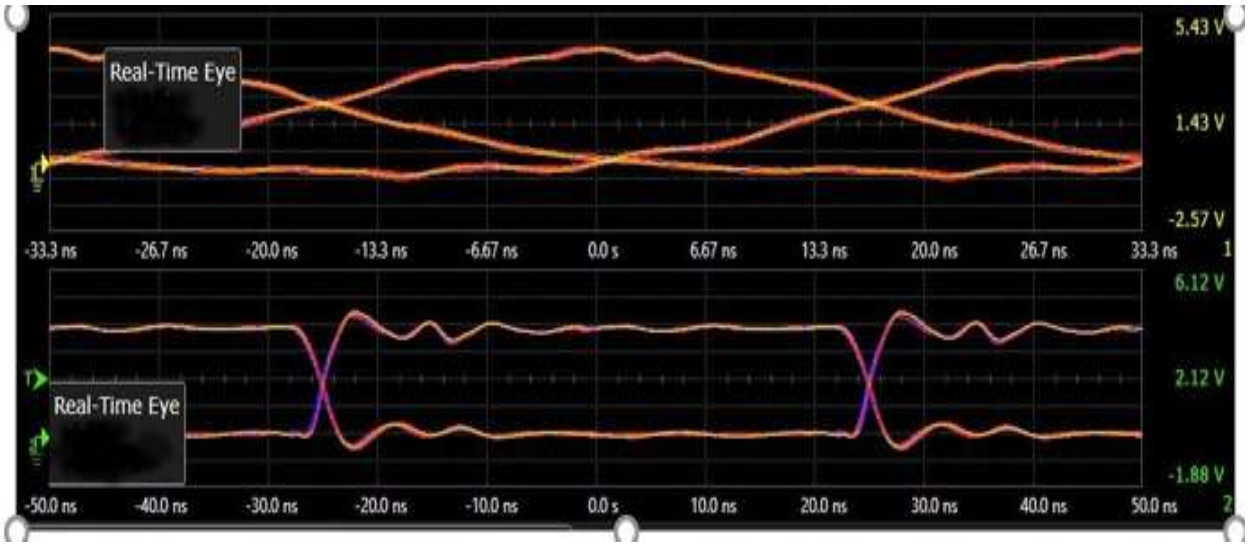

Fig. 4.1: 10 MHz signal and corresponding eye diagram at the receiver side

Artificially, different rain rates are created, the rain rates are 6 mm/hr, 24 mm/hr, 50 mm/hr, 85 mm/hr, 116 mm/hr respectively. The artificial rain simulation arrangement is describing in the previous section. In shows the optical power attenuation at a rai rate of 6 mm/hr and corresponding eye diagram of the received signal depicts in The upper trace of the indicates the photodetector signal eye diagram and lower trance of the Fig.ure shows the comparator output's eye diagram. As the rain rate is increased, the optical power attenuation also increased which are depicted in Fig. 4.2, 4.4, 4.6, 4.8, 4.10 for rain rate of 6 mm/hr, 24 mm/hr, 50 mm/hr, 85 mm/hr and 116 mm/hr respectively. The eye diagram is an intuitive graphical representation of optical

communication signal. The quality of the signal (the amount of inter symbol interference) can be judged from the appearance of the eye. As the rain rate has been increased from the 6 mm/hr to 115 mm/hr the eye height is also decreased gradually. The eye diagram of the different rain rates is depicted in 4.3, 4.5, 4.7, 4.9, 4.11 for different rain rates respectively. The optical power and corresponding optical signal data has been taken for 1-minute time duration.

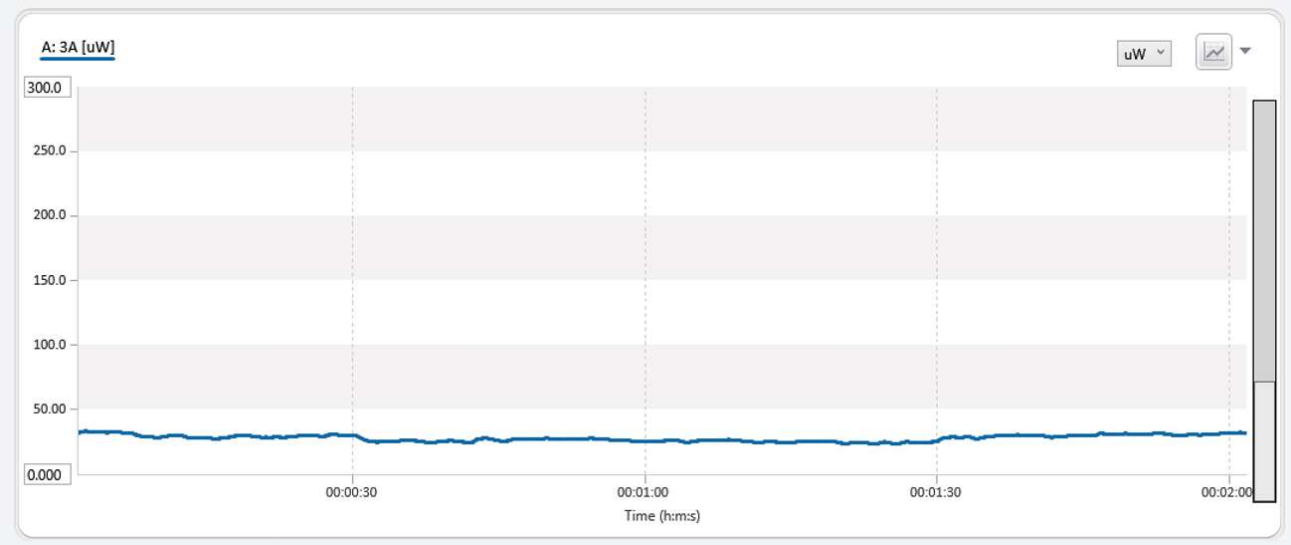

Fig. 4.2: Optical power attenuation at a rain rate of 6 mm/hr

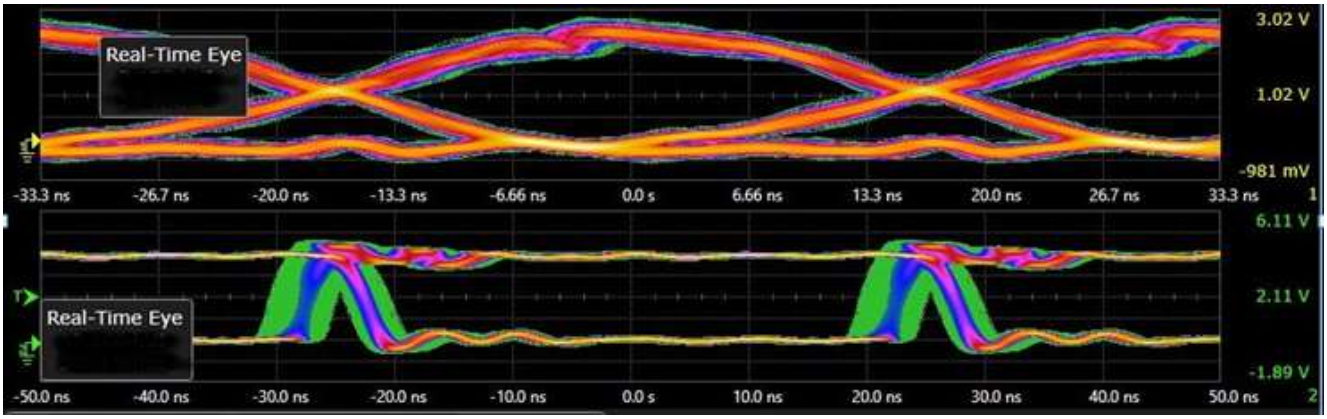

Fig.4.3: Eye diagram photodetector signal & comparator signal at a rain rate of 6 mm/hr

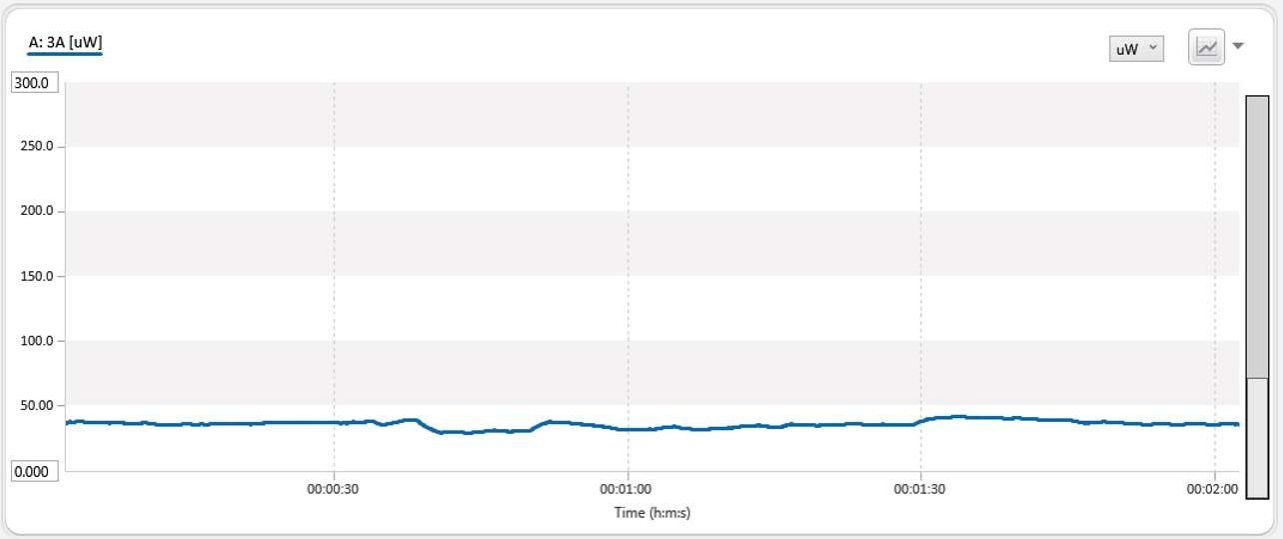

Fig. 4.4: Optical power attenuation at a rain rate of 24 mm/hr

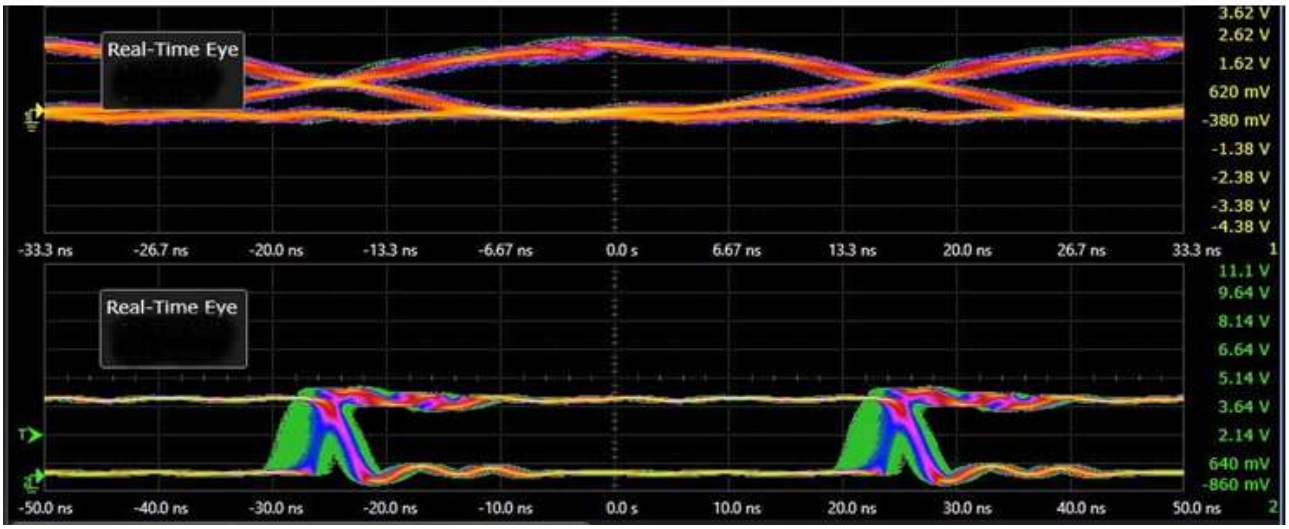

Fig. 4.5: Eye diagram of photodetector signal & comparator signal at a rain rate of 24 mm/hr

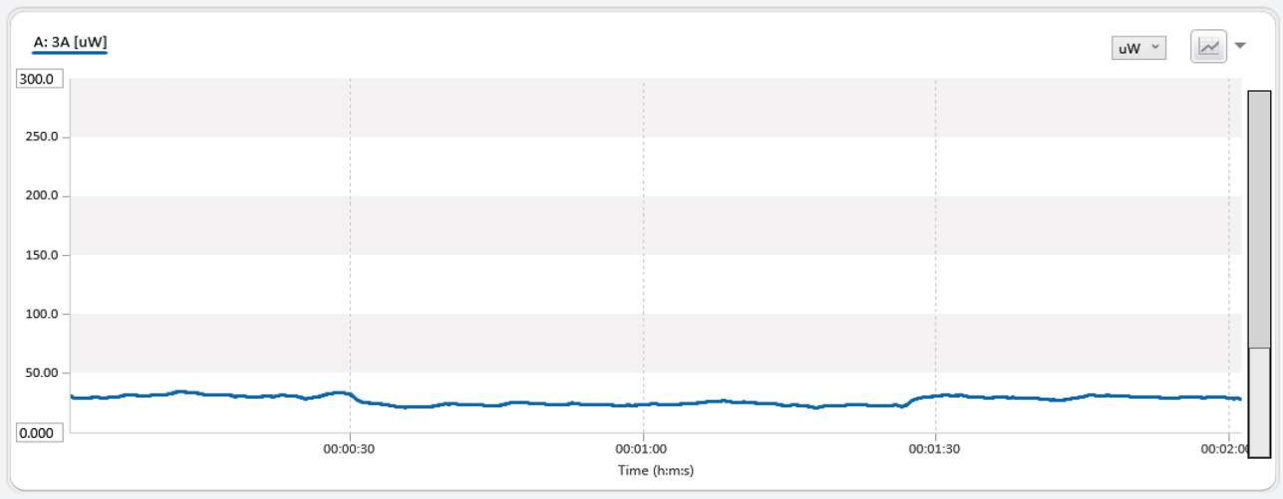

Fig. 4.6: Optical power attenuation at a rain rate of 50 mm/hr

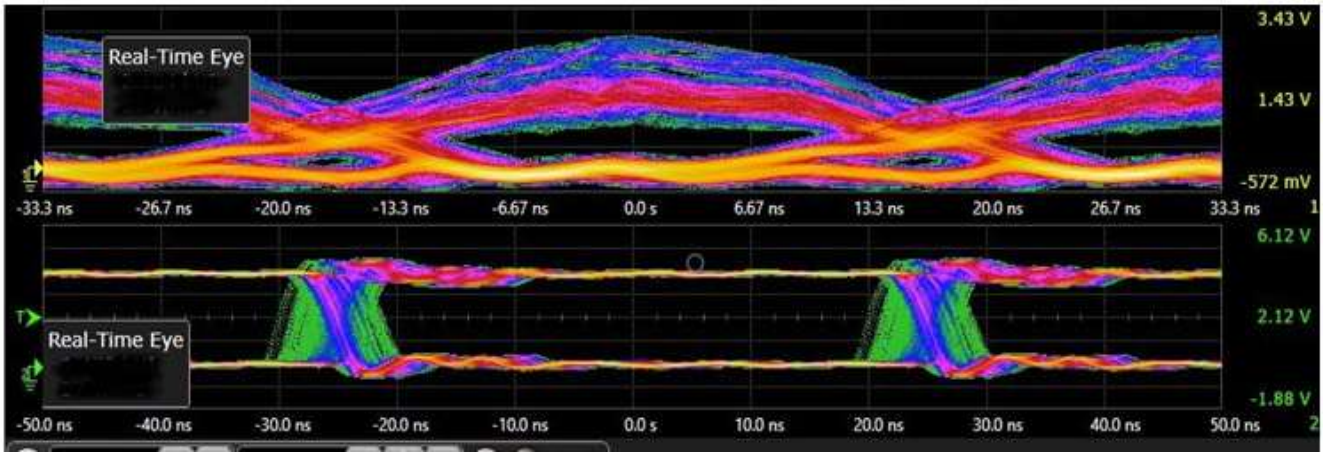

Fig. 4.7: Eye diagram of photodetector signal & comparator signal at a rain rate of 50 mm/hr

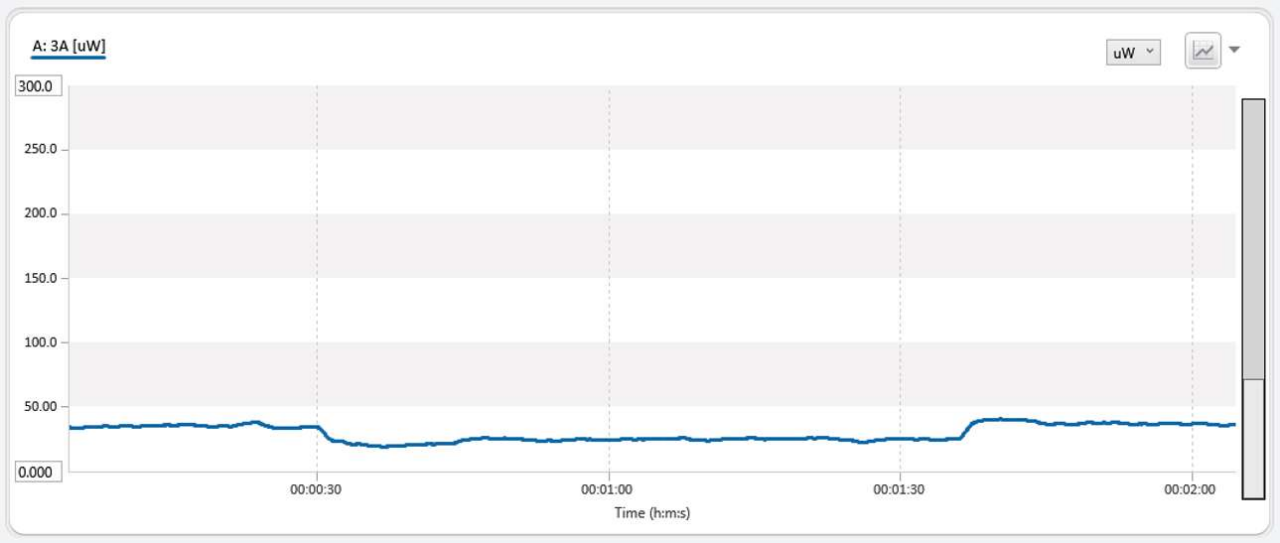

Fig. 4.8: Optical power attenuation at a rain rate of 85 mm/hr

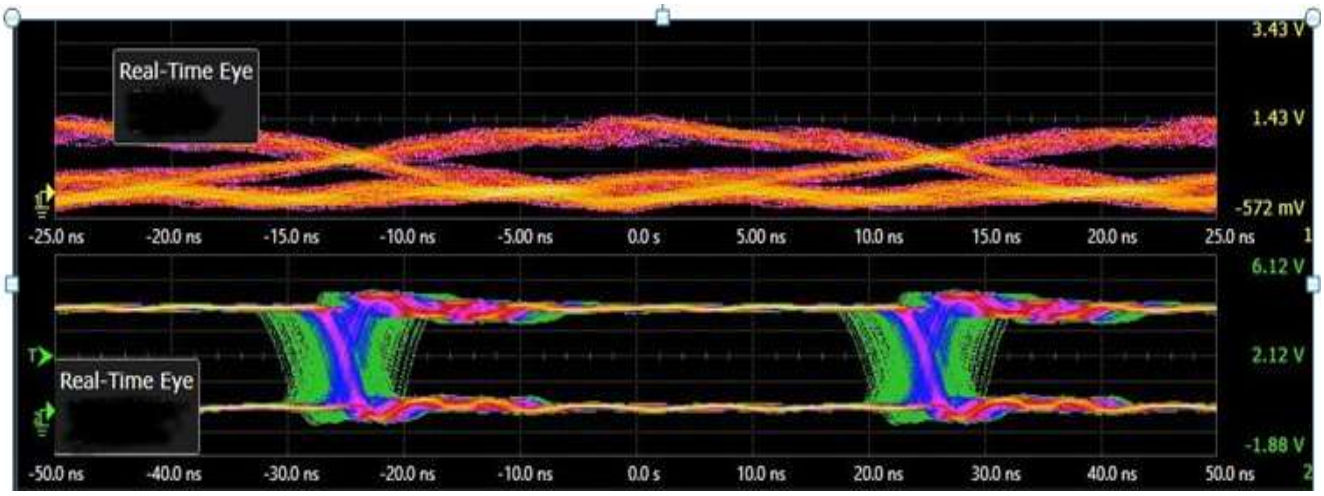

Fig. 4.9: Eye diagram of photodetector signal & comparator signal at a rain rate of 85 mm/hr

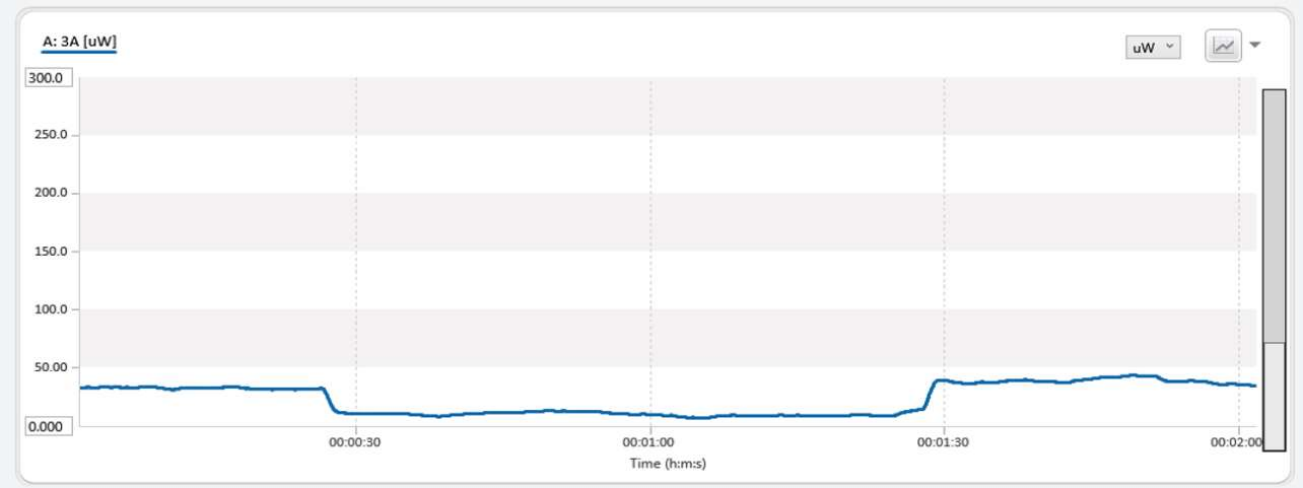

Fig. 4.10: Optical power attenuation at a rain rate of 116 mm/hr

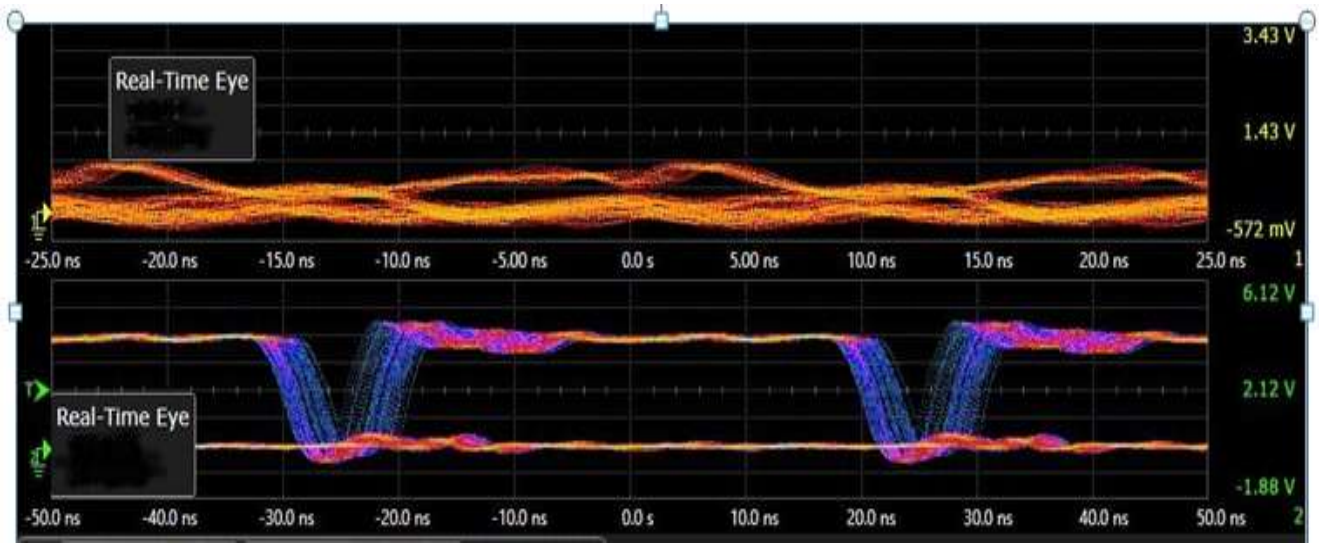

Fig. 4.11: Eye diagram of photodetector signal & comparator signal at a rain rate of 116 mm/hr

The measured optical power attenuation has been depicted for different rain rates are given in Fig. 4.12. The measured bit error rate has been depicted for different rain rates at a link range of 20m has been shown in fig 4.13

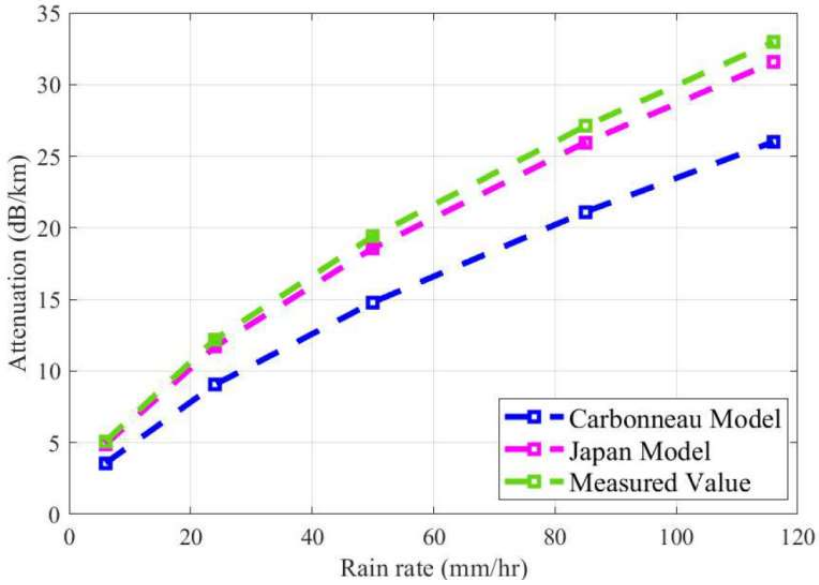

.

Fig. 4.12: Optical power attenuation at different rain rate

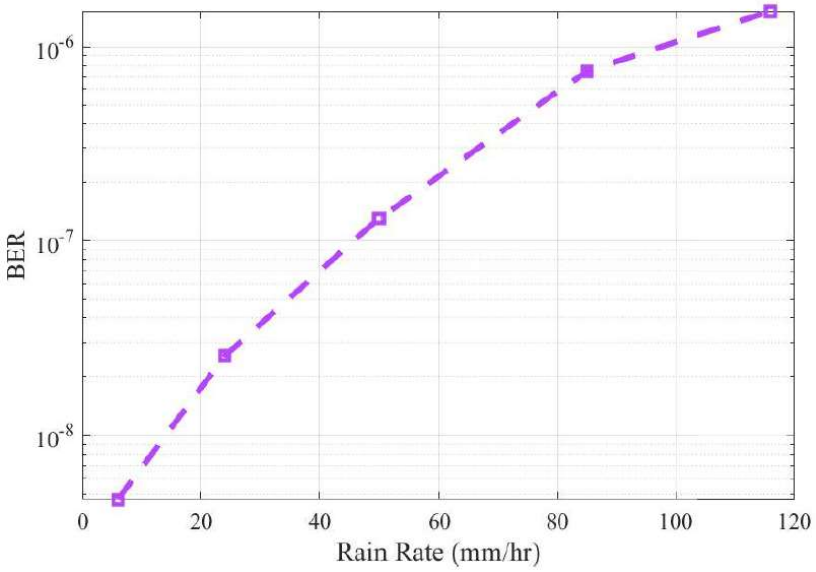

Fig. 4.13: BER varies with different rain rates

4.2 Foggy condition Simulation

Fog is another important natural element which is attenuate the laser beam in free space, very severely. Fig. 4.14 indicates that the optical power is attenuated in different visibility conditions with respect to time.

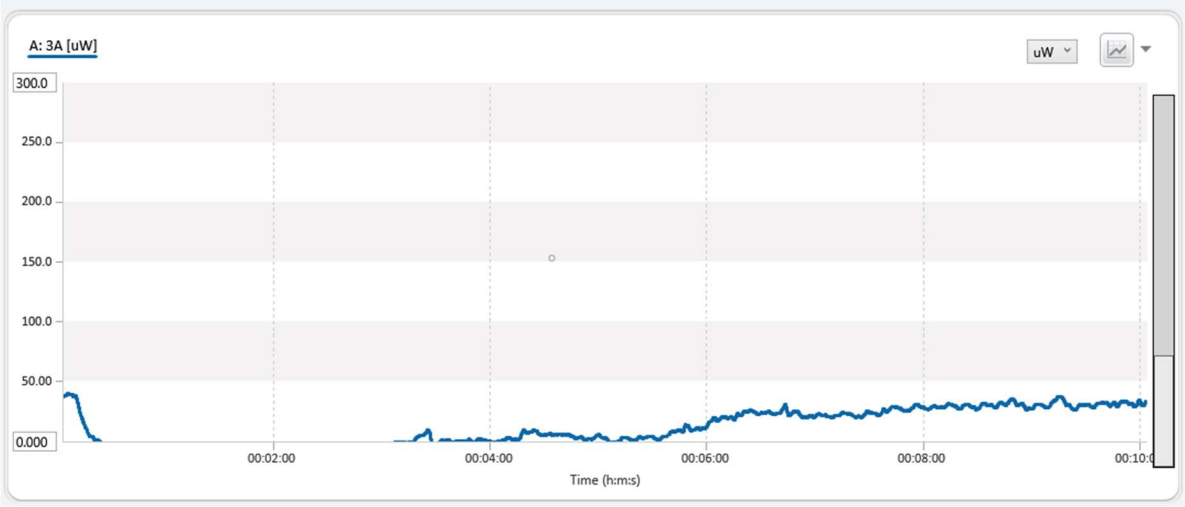

Fig. 4.14: Optical power attenuation at different visibility with respect to time

From the Fig. 4.14, the Visibility range has been found with respect to time which is depicted in Fig. 4.15.

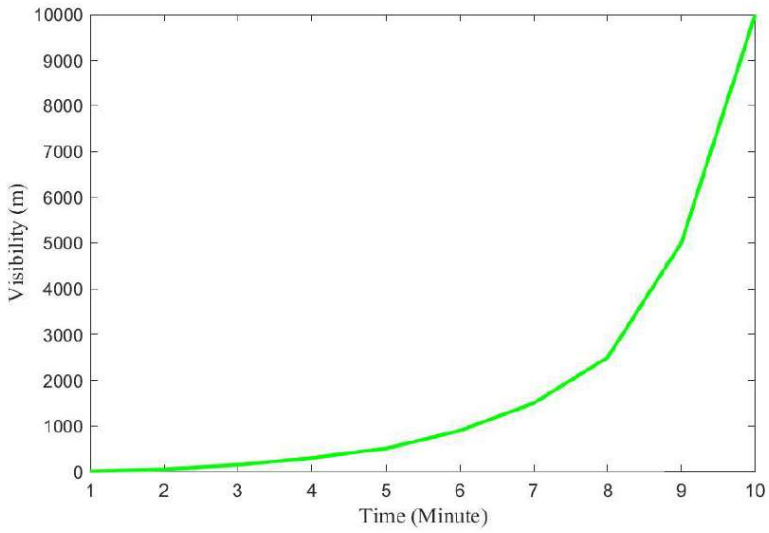

Fig. 4.15: Visibility vs time plot

Similarly, the attenuation (dB/km) can be predicted from Fig. 4.15 at different visibility conditions which are depicted in Fig. 4.16.

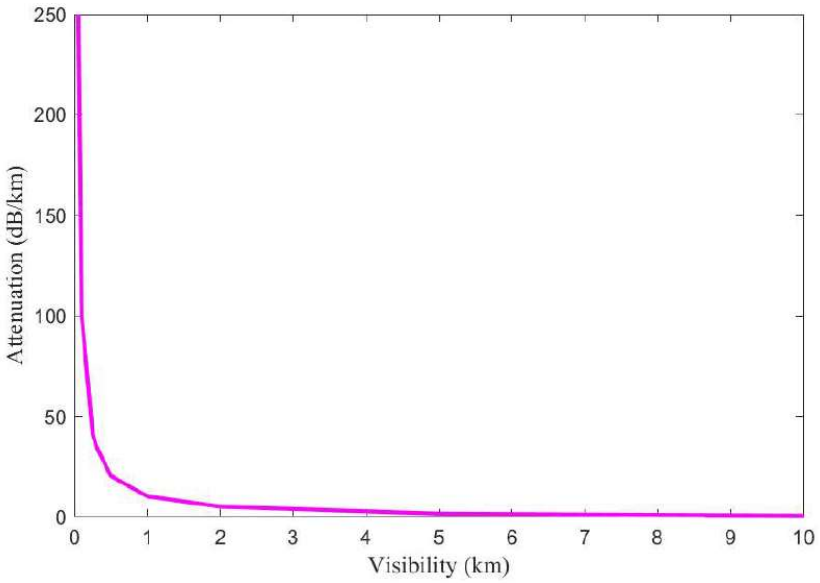

Fig. 4.16: Visibility vs optical attenuation (dB/km)

Fig. 4.17 shows the eye diagram of the 10 MHz signals at the visibility of 300 m. Similarly, Fig. 4.18, 4.19, 4.20 shows the eye diagram of the 10 MHz signals at the visibility of 510 m, 930 m, 1500 m respectively.

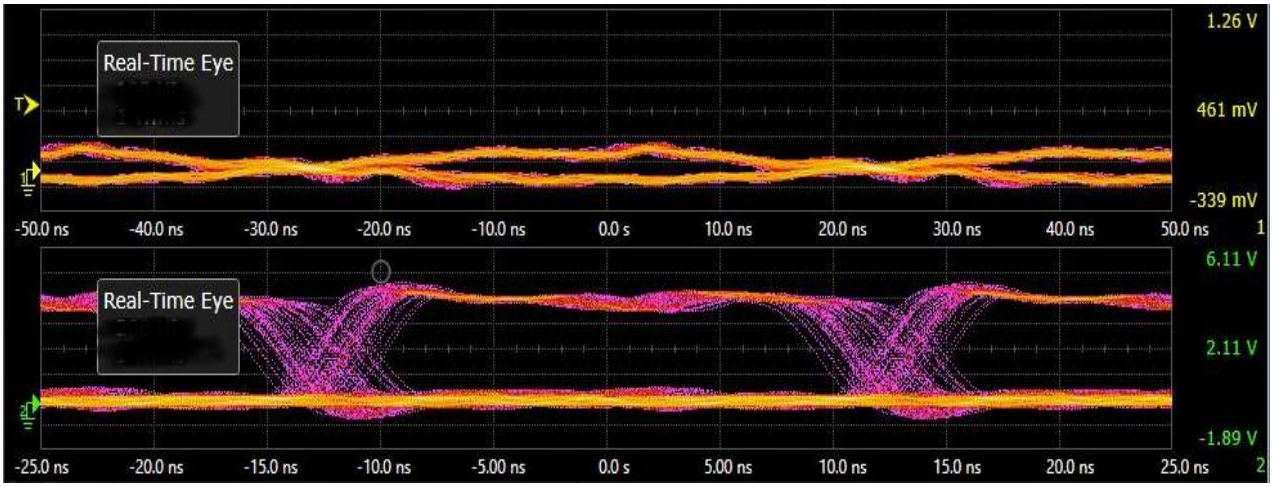

Fig.4.17: Eye diagram of the 10 MHz signals at the visibility of 300 m

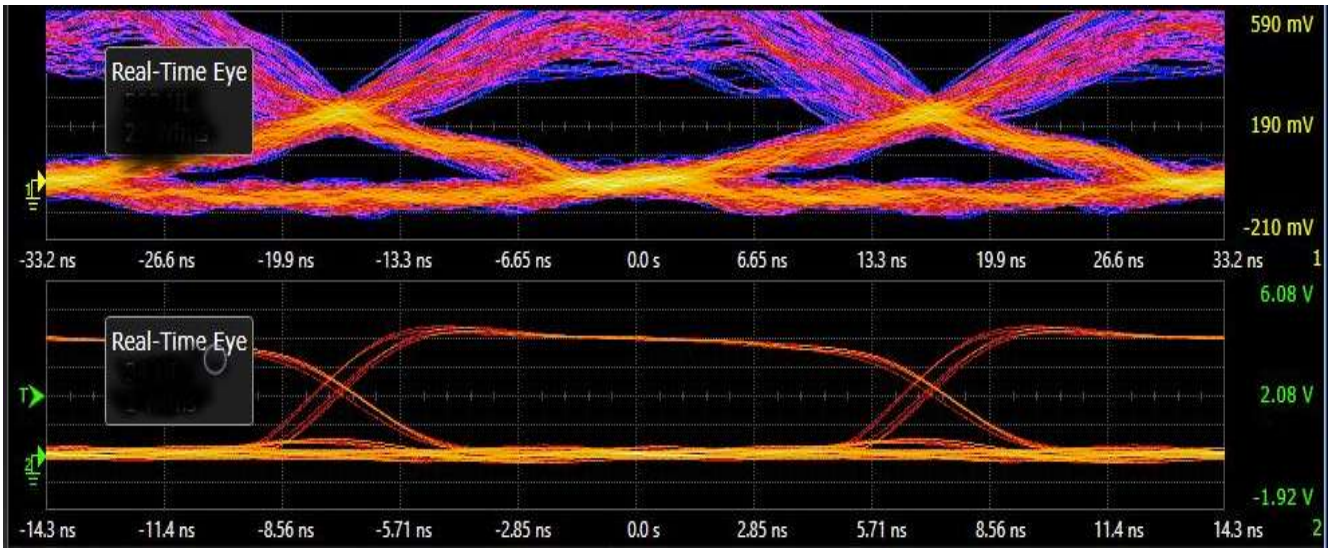

Fig.4.18. Eye diagram of the 10 MHz signals at the visibility of 510 m

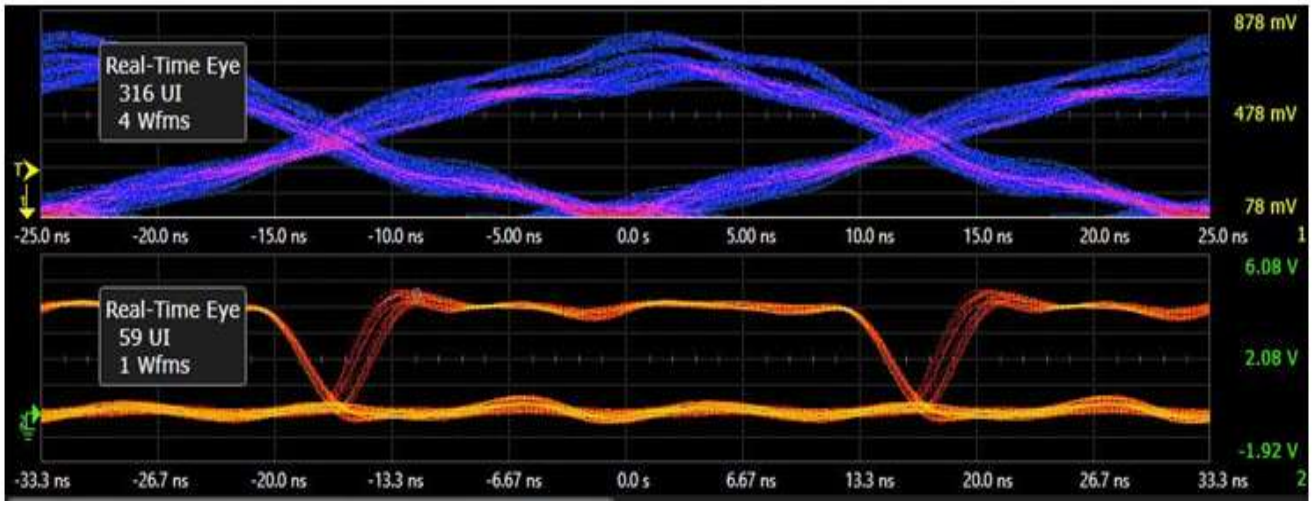

Fig.4.19. Eye diagram of the 10 MHz signals at the visibility of 930 m

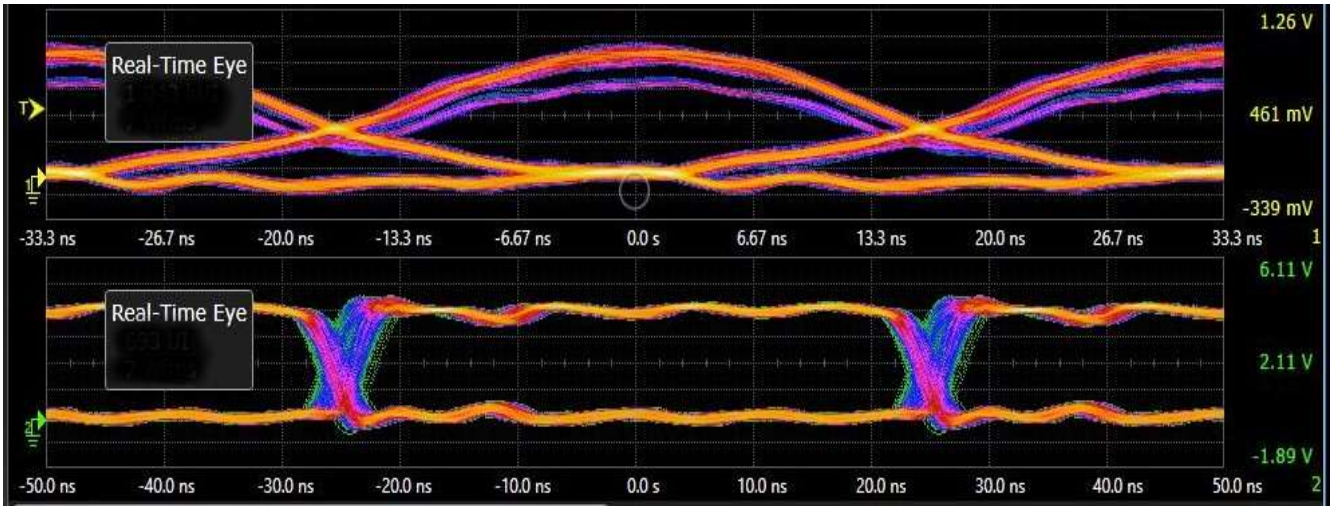

Fig.4.20: Eye diagram of the 10 MHz signals at the visibility of 1500 m

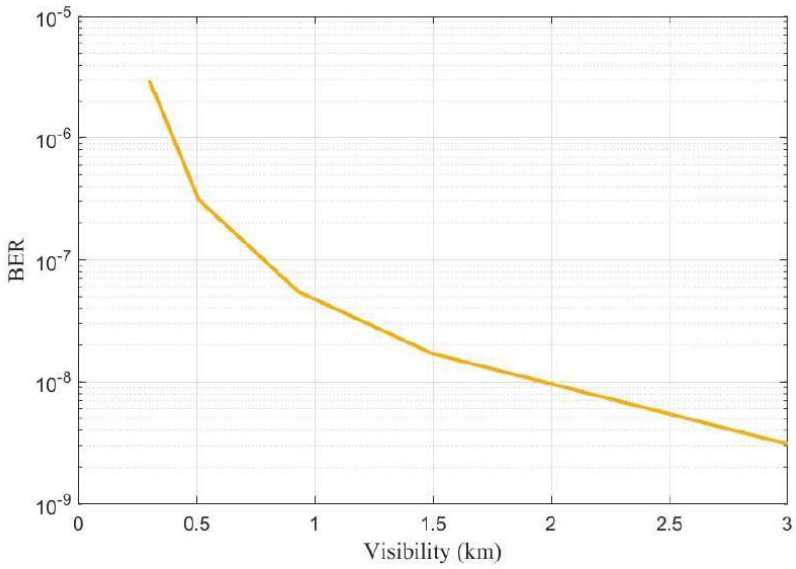

Fig. 4.21: Visibility vs BER plot

From Fig. 4.21, it has been shown that, when the visibility is increased from dense fog to light fog, the BER decreased.

4.3 Temperature simulation

The performance of free space optical (FSO) communication is affected by various phenomena such as absorption, scattering, and turbulence. For FSO link, the major factors that degrade the performance are "turbulence-induced scintillation and beam wander effect." The effect of scintillation causes fluctuations in the received irradiance and the beam wander effect leads to the displacement of the beam centroid significantly. The experimental results show that variance of beam wander displacement increases linearly with the temperature gradient which can result in serious impairment of FSO link.

A very useful parameter that describes the strength of the turbulence is called refractive index structure parameter and is given as in equation 43 [68]

$$C_n^2 = [79 \times 10^{-6} \frac{P}{T^2}]^2 C_T^2 \quad \ldots\ldots\ldots\ldots\ldots\ldots\ldots\ldots\ldots\ldots\ldots\ldots\ldots (43)$$

where and are the pressure (in mbar) and temperature of the atmosphere (in Kelvin), C_T^2 is the temperature structure parameter, C_T^2 can be written as by equation 44.

$$C_T^2 = \Delta T^2 r^{-1/3} \quad \ldots\ldots\ldots\ldots\ldots\ldots\ldots\ldots\ldots\ldots\ldots\ldots\ldots\ldots\ldots\ldots (44)$$

ΔT= T_1-T_2 and T_1 and T_2 are the temperatures of two arbitrary points separated by distance r

Optical power attenuation (dB) due to scintillation for a particular link distance can be predicted by the equation 45 [69][70].

$$\alpha_{Scin} = 2\sqrt{23.17 \times \left(\frac{2\pi}{\lambda} \times 10^9\right)^{\frac{7}{6}} C_n^2 \times L^{\frac{11}{6}}} \quad \ldots\ldots\ldots\ldots\ldots\ldots\ldots\ldots\ldots (45)$$

Where C_n^2 = refractive index parameter structure ($m^{-2/3}$), λ = Wavelength of the coherent optical source (nm), L = Terrestrial FSO link range (m).

Table 13. C_n^2values for different temperature differences

Sl No.	Temperature Difference (In Kelvin)	Refractive index structure parameter ((C_n^2) in $m^{-2/3}$
1.	15	5.6×10^{-11}
2.	1.5	5.6×10^{-13}
3.	0.1	2.7×10^{-15}

Table 13 shows the C_n^2values for different temperature differences.

Fig.4.22 & 4.23 shows that optical power fluctuation for the C_n^2 = 10^{-15} $m^{-2/3}$& 10 MHz signal eye diagram for the C_n^2 = 10^{-15} $m^{-2/3}$ respectively.

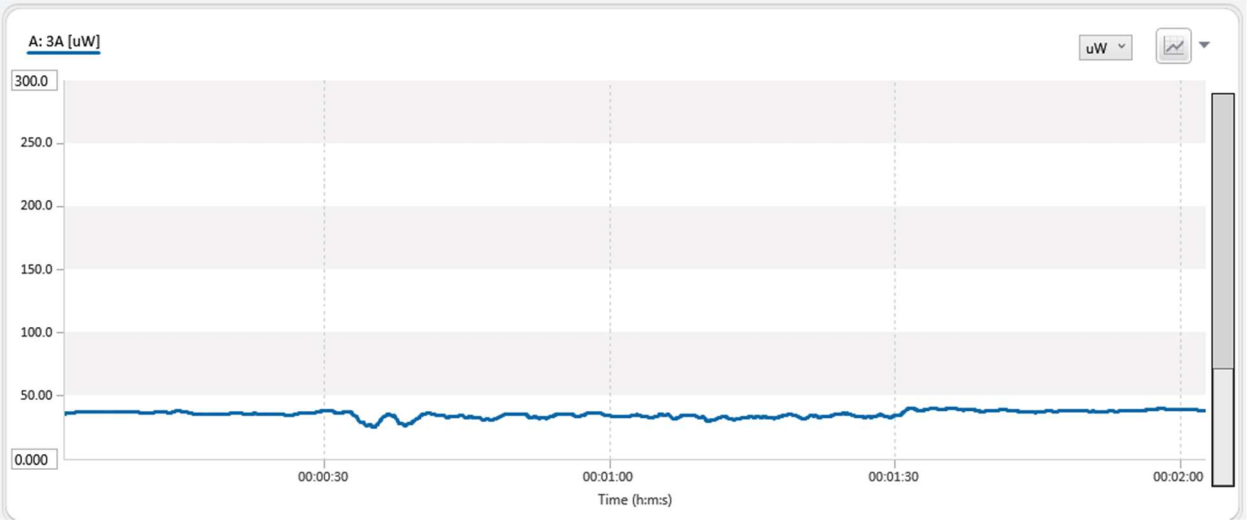

Fig. 4.22. Optical power fluctuation for the C_n^2 = 10^{-15} $m^{-2/3}$

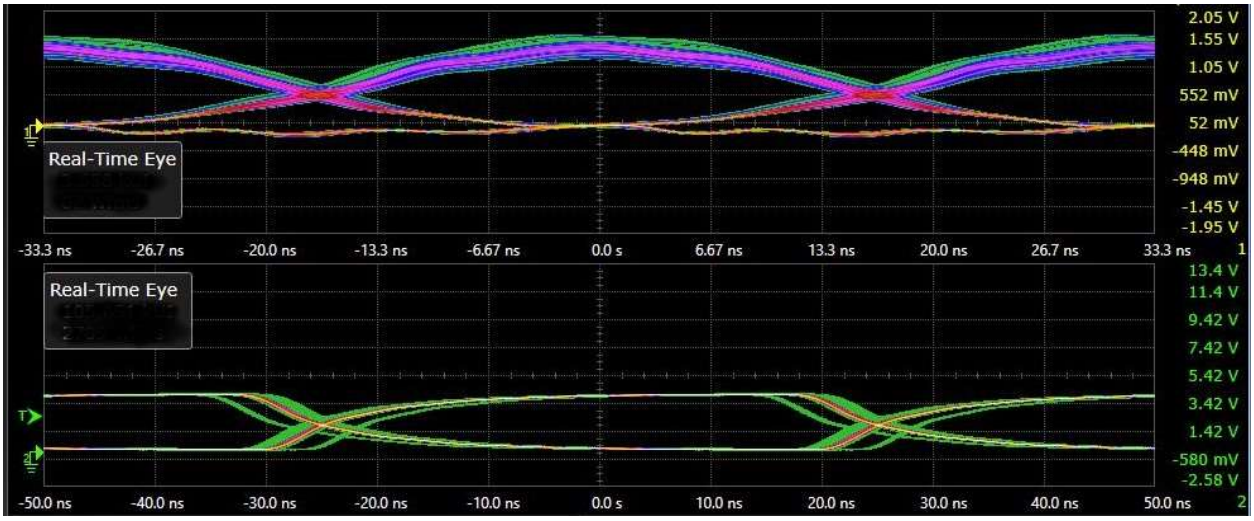

Fig. 4.23. 10 MHz signal eye diagram for the C_n^2 = 10^{-15} $m^{-2/3}$

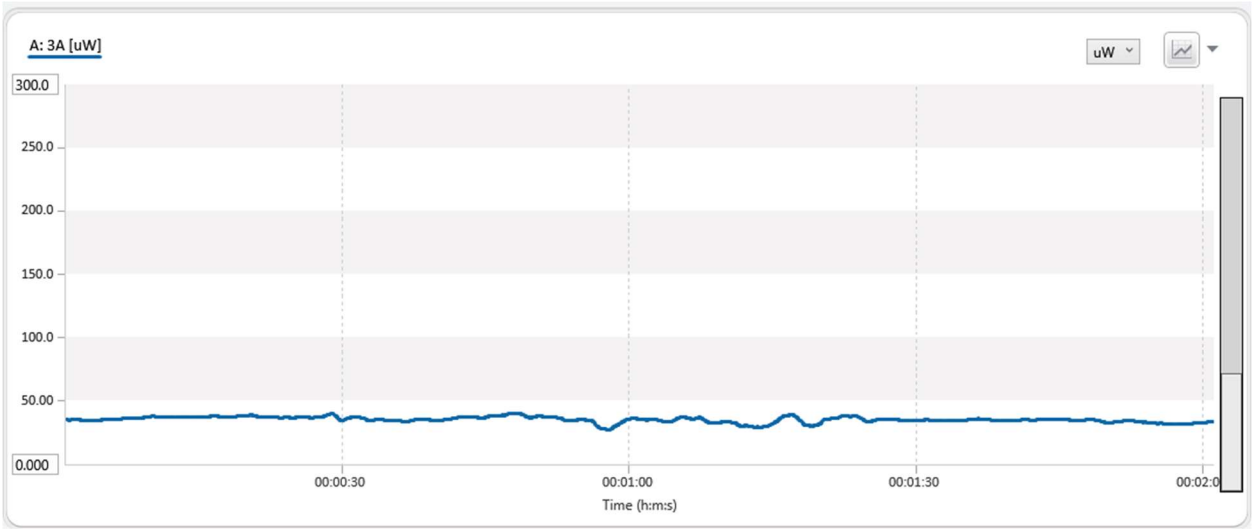

Fig. 4.24.Optical power fluctuation for the C_n^2 = 10^{-13} $m^{-2/3}$

Similarly, Fig. 4.24 & 4.25 shows the optical power fluctuation for the for the C_n^2 = 10^{-13} $m^{-2/3}$and 10 MHz signal eye diagram for the C_n^2 = 10^{-13} $m^{-2/3}$ respectively.

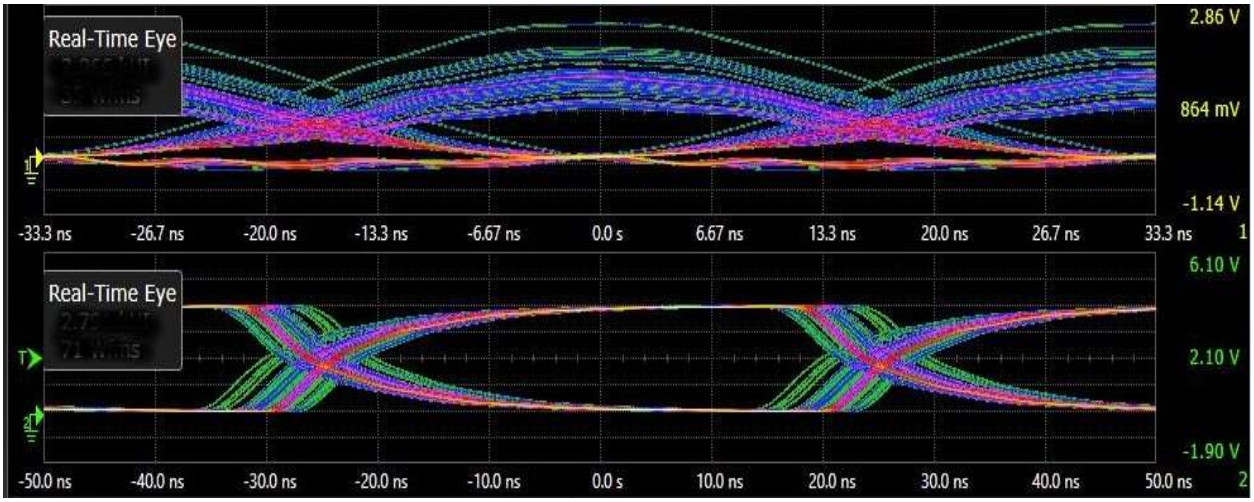

Fig. 4.25: 10 MHz signal eye diagram for the $C_n^2 = 10^{-13}$ m$^{-2/3}$

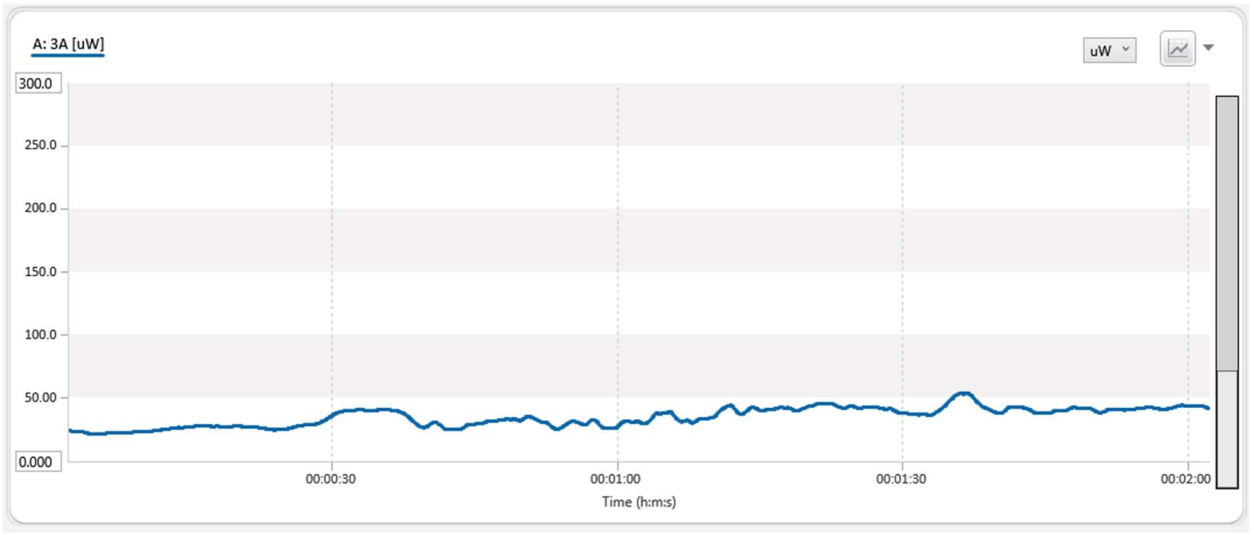

Fig.4.26: Optical power fluctuation for the $C_n^2 = 10^{-11}$ m$^{-2/3}$

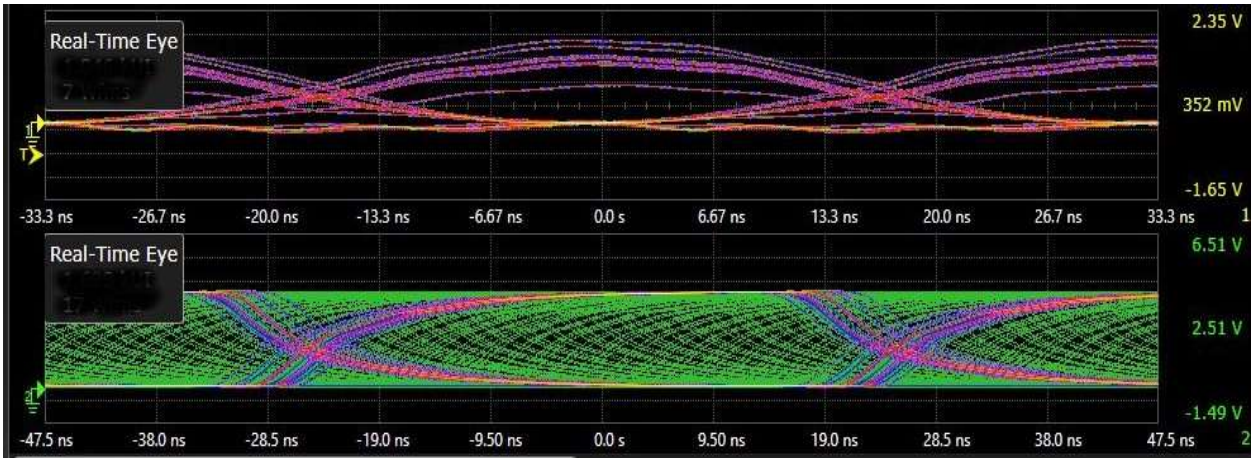

Fig.4.27: 10 MHz signal eye diagram for the C_n^2 = 10^{-11} $m^{-2/3}$

Fig.4.26 & 4.27 show the Optical power fluctuation for the C_n^2 = 10^{-11} $m^{-2/3}$ and 10 MHz signal eye diagram for the C_n^2 = 10^{-11} $m^{-2/3}$.

Fig.4.28 and 4.29 show the optical power attenuation due to different scintillation ranges and the BER range for a link distance of 20 m. From the above Fig.4.29, it has been shown that BER is increased as the value of scintillation index structure parameter is increased.

The value of refractive index parameter structure (C_n^2= 10^{-11}) means that very high turbulence which is got from the simulation result. In Indian atmospheric condition situation, this type of turbulence is occurred very rarely.

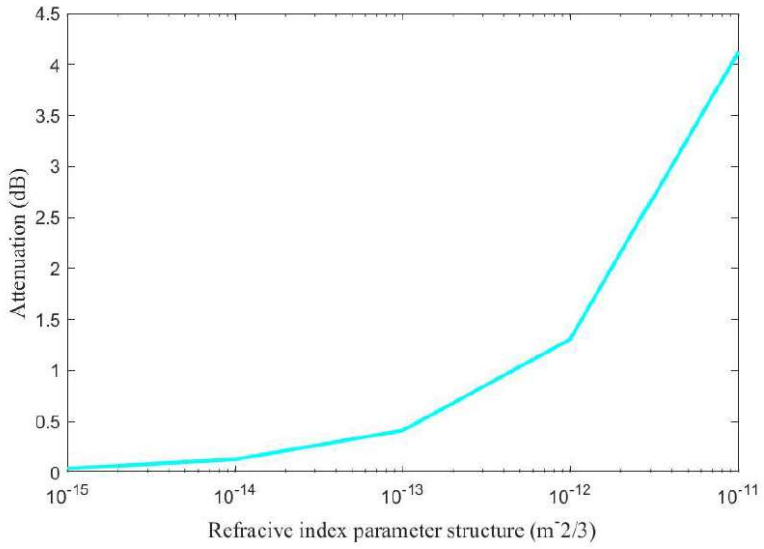

Fig.4.28 : Optical power attenuation due to different refractive index parameter structure

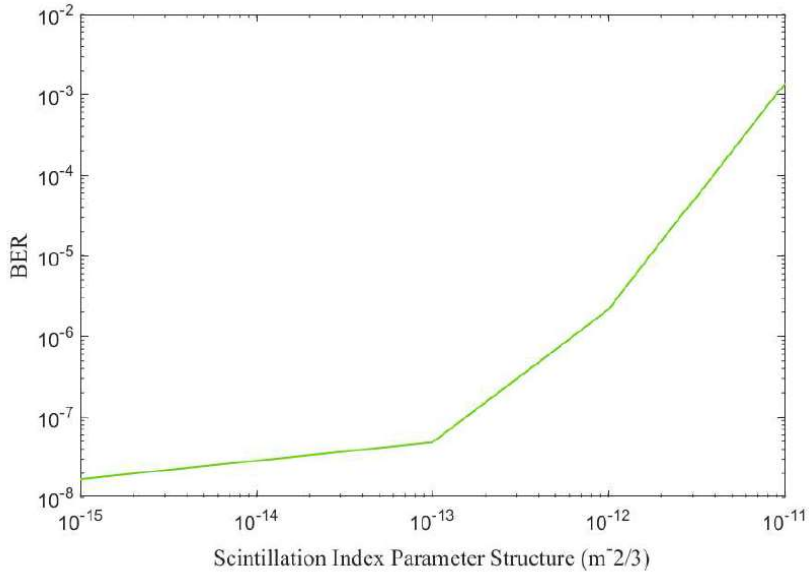

Fig.4.29:. BER due to different refractive index parameter structure

Chapter 5

Conclusion and Future Scope

Chapter 5

Conclusion and Future Scope

Optical communication in free space is a newer technology that has many benefits. Due to its advantages over RF communication, such as its high bandwidth, high data rate, and unlicensed spectrum, FSO is a viable alternative. Even though FSO has benefits, its flaws must be resolved in order to fully get benefited from FSO communication. In FSO, turbulence, absorption, and scattering are the main obstacles. This paper focuses on the weather effect as the most important parameter affecting the performance of FSO links , those are heat, rain and fog.

In this experiment, 10 MHz communication channel has been established using 1550 nm laser source in laboratory and it is tested at a distance of 25 m in laboratory environment. OOK modulation has been used. Fog Chamber for artificial foggy environment, proper heating arrangement for warm weather condition and artificial rain setup for rainy atmosphere has been done separately for proper laboratory simulation. Link budget analysis also has been done successfully. Collected data from this experiment has been used for producing graphs those has been shown in chapter 4.

From Chapter 4 it can be easily shown that the LASER link gets most affected by the warm weather followed by foggy and rainy weather respectively. That means attenuation of the receiving power of the 1550nm LASER is maximum for heated condition and minimum for rainy condition.

For future scope, these experiments may be done in Single Input Multiple Output (SIMO) arrangement to get more received power and less BER. Aperture averaging i.e, varying the diameter of the receiver can be done to avoid scintillation especially for heated condition. Different modulation techniques may be used to study different results. This experiment can be also performed with increased bandwidth for less attenuation and high data speed. Effect of snow could not be performed due to lack of infrastructure. That may be performed according to the availability of proper infrastructure.

FSO is considered as alternative choice that can be employed as a reliable solution to broadband short distance applications. FSO system can be used as an alternative of conventional Fiber optics communication. Also as network-centric warfare becomes a cornerstone of military

operations, data flow will continue to increase. Networking technologies have provided enhanced interoperability, but the need for increased raw link capacity will continue, potentially beyond many RF systems that are used today and in the near future. Optical communications can provide a mechanism for increased capacity, and some of the most critical challenges have been described along with mitigation approaches. These challenges span the protocol stack and, through methodical research and development, this powerful capability can be delivered to the battlefield.

REFERENCES

References

[1] J. Li, J.Q. Liu, D.P. Taylor, Optical communication using subcarrier PSK intensity modulation through atmospheric turbulence channels. IEEE Trans. Commun. 55(8), 1598–1606 (2007)

[2] J.H. Franz, V.K. Jain, Optical Communications: Components and Systems (Narosa Publishing House, Boca Raton, 2000)

[3] H. Hemmati, Deep Space Optical Communications (John Wiley & Sons, Hoboken, 2006)

[4] A. Jurado-Navas, J.M. Garrido-Balsells, J. Francisco Paris, M. Castillo-Vázquez, A. PuertaNotario, Impact of pointing errors on the performance of generalized atmospheric optical channels. Opt. Exp. 20(11), 12550–12562 (2012)

[5] Weblink: http://www.cie.co.at/, 28 Feb 2012

[6] O. Bader, C. Lui, Laser safety and the eye: hidden hazards and practical pearls. Technical report: American Academy of Dermatology, Lion Laser Skin Center, Vancouver and University of British Columbia, Vancouver, B.C., 1996

[7] Andrews L (2004) Atmospheric optics, SPIE Optical Engineering Press

[8] Andrews L, Phillips R, Hopen C (2001) Laser beam scintillation with applications, SPIE Optical Engineering Press

[9] Gagliardi R, Karp S (1995) Optical communications. Wiley, New York

[10] Gappmair W (2011) Further results on the capacity of free-space optical channel sin turbulent atmosphere, IET Commun, 5(9), 1262–1267

[11] Lee IE, Ghassemlooy Z, Ng WP, Khalighi MA (2013) Joint optimization of a partially coherent Gaussian beam for free-space optical communication over turbulent channels with pointing errors. Opt Lett 38(3):350–352

[12] FSO History and Technology. http://www.laseroptronics.com/index.cfm/id/57–66.htm

[13] Vigneshwaran S, Muthumani I, Raja AS (Feb. 2013) Investigations on free space optics communication system. In: IEEE International Conference on Information and Embedded System (ICICES), Chennai, India, 819–824

[14] Weblink: http://www.chem.wwu.edu/dept/dept/tutorial/

[15] Safety of laser products-part 12: safety of free space optical communication systems used for transmission of information. Technical report: IEC 60825-12, 2004

[16] Weblink: http://web.mst.edu/~mobildat/Free%20Space%20Optics/

[17] R.K. Long, Atmospheric attenuation of ruby lasers. Proc. IEEE 51(5), 859–860 (1963)

[18] R.M. Langer, Effects of atmospheric water vapour on near infrared transmission at sea level, in Report on Signals Corps Contract DA-36-039-SC-723351 (J.R.M. Bege Co., Arlington, 1957)

[19] A.S. Jursa, Handbook of Geophysics and the Space Environment (Scientific Editor, Air Force Geophysics Laboratory, Washington, DC, 1985)

[20] H. Willebrand, B.S. Ghuman, Free Space Optics: Enabling Optical Connectivity in Today's Networks (SAMS publishing, Indianapolis, 2002)

[21] M. Rouissat, A.R. Borsali, M.E. Chiak-Bled, Free space optical channel characterization and modeling with focus on algeria weather conditions. Int. J. Comput. Netw. Inf. Secur. 3, 17–23 (2012)

[22] H.C. Van de Hulst, Light Scattering by Small Particles (Dover publications, Inc., New York, 1981)

[23] P. Kruse, L. McGlauchlin, R. McQuistan, Elements of Infrared Technology: Generation, Transmission and Detection (Wiley, New York, 1962)

[24] I.I. Kim, B. McArthur, E. Korevaar, Comparison of laser beam propagation at 785 nm and 1550 nm in fog and haze for optical wireless communications. Proc. SPIE 4214, 26–37 (2001)

[25] M.A. Naboulsi, H. Sizun, F. de Fornel, Fog attenuation prediction for optical and infrared waves. J. SPIE Opt. Eng. 43, 319–329 (2004)

[26] Ghassemlooy, Z. and Popoola, W.O. , "Terrestrial Free-Space Optical Communications", Optical communications research group, NCR Lab, Northumbria University, Newcastle upon Tyne, UK.

[27] Free-Space Laser Communication-Principles and advances" – Arun k. Majumder,Jennifer C.Rickcin , Springer Plublication

[28] Free Space optical communication". Hemani Kaushal, V.K.Jain and Subrat Kar. Springrr

[29] Optical communication Systems" Narottam Das , Intechweb.org

[30] Terrestrial Free-space Optical Communications" Chassemlooy,Z. and Popoola W.O.,Optical Communication Research Group NCR Northumbria university, UK

[31] Optical Communication Receiver Design" Stephen B. Alexander Ciena Corporation

[32] White paper "Noise Equivalent Power" ThorLabs

[33] Link Performance Analysis of a Ship-to-Ship Laser Communication System " Ang Toon Yiam Ronny.

[34] Taissir Youssef Elganimi "Performance Comparison between OOK, PPM and PAM Modulation Schemes for Free Space Optical (FSO) Communication Systems: Analytical Study" International Journal of Computer Applications (0975 – 8887) Volume 79 – No 11, October 2013

[35] Laser Beam Expander" Laser Optical Resource guide, Edmund Optics

[36] Free-Space Laser Communication-Principles and advances" – Arun k. Majumder,Jennifer C.Rickcin , Springer Plublication.

[37] Wang, B.; Wu, C. Safety informatics as a new, promising and sustainable area of safety science in the information age. J. Clean. Prod. 2020, 252, 119852

[38] Information Age. Available online: https://www.information-age.com

[39] A. A. Huurdeman, The Worldwide History of Telecommunications, Wiley Interscience, 2003

[40] G. J. Holzmann and B. Pehrson, The Early History of Data Networks (Perspectives), Wiley, 1994.

[41] D. J.C. Phillipson, "Alexander Graham Bell," The Canadian Encyclopedia, http://www.thecanadianencyclopedia.com/articles/alexander graham-bell

[42] J. Hecht, "Laser evolution," SPIE Professional Magazine, http://spie.org/x34446.xml.

[43] F. E. Goodwin, "A review of operational laser communication systems," Proceedings of the IEEE, vol. 58, no. 10, pp. 1746–1752, Oct. 1970.

[44] D. L. Begley, "Free-space laser communications: a historical perspective," Annual Meeting of the IEEE, Lasers and Electro-Optics Society (LEOS), vol. 2, pp. 391–392, Nov. 2002, Glasgow, Scotland

[45] W. S. Rabinovich, C. I. Moore, H. R. Burris, J. L. Murphy, M. R. Suite, R. Mahon, M. S. Ferraro, P. G. Goetz, L. M. Thomas, C. Font, G. C. Gilbreath, B. Xu, S. Binari, K. Hacker, S. Reese, W. T. Freeman, S. Frawley, E. Saint-Georges, S. Uecke, and J. Sender, "Free space optical communications research at the US naval research laboratory," Proceedings of SPIE, Free-Space Laser Communication Technologies XXII, vol. 757, Feb. 2010, San Francisco, CA.

[46] Infrared Data Association (IrDA), http://www.irda.org/.

[47] "Visible light communication (VLC) - a potential solution to the global wireless spectrum shortage," GBI Research, 2011, http://www.gbiresearch.com/Report.aspx?ID=Visible-LightCommunication-(VLC)-A-Potential-Solution-to-the-Global-Wireless Spectrum-Shortage&ReportType=Industry Report.

[48] "Global visible light communication (VLC)/Li-Fi technology free space optics (FSO) market (2013-2018)," MarketsandMarkets,2013 http://www.marketsandmarkets.com/PressReleases/visible-lightcommunication.asp

[49] D. Killingern, "Free space optics for laser communication through the air," Optics and Photonics News, vol. 13, no. 10, pp. 36–42, Oct. 2002.

Appendix

Appendix A

Instruments Used in the experiment

1) 33600A Series Trueform Waveform Generators (AWG)

Fig.5.1. Front view of AWG

Features of 33600A Series Trueform Waveform Generators (AWG)

100 MHz PULSE	High-bandwidth pulse, 100 MHz, DDS pulse limited to 50 MHz Set leading and trailing edge times independently
PRBS Patterns	Provides standard PRBS patterns, PN3 through PN32 Select PN type, set bit rate, set edge times
2-Channel Coupling	Dual-channel coupling, frequency and amplitude, and tracking Set start phase for each channel, phase shift between channels
Combining Signals	Sum two signals together, frequency and amplitude independent 2-tone (4-tone on 2-ch), square-sine, noise on pulse, and others
Trueform Arbs	Create up to 4 million samples standard, 64 million optional Connect arb segments together, with up to 512 segments
Low Voltage Settings	Lower voltage range at 1 mVpp, DDS is only 10 mVpp Set high and low voltage limits to prevent overload on DUT
Band-Limited Noise	Adjust bandwidth to concentrate the energy of the noise Noise source goes to full 120 MHz bandwidth

2) D C Power Supply – GPD 4303S

Fig.5.2: Front view of DC Power Supply

Features of D C Power Supply – GPD 4303S

- 2,3,and 4 Independent Isolated Output
- Digital Panel Control (Rotary Encoder Switch, Rubber Key With Indicator)
- User-Friendly Operation, Coarse / Fine Volume Control
- 4 Sets Save / Recall
- PC Software & USB Driver
- The tracking series and parallel mode can be selected with a single touch
- Indicators embedded in the keys provide an instant view of the power supply status; the Key Lock feature prevents improper operation
- Smart cooling fan control offers a well-balanced cooling mechanism, ensuring quiet operation

3) Fiber-coupled acousto-optic modulators (FCAOM)

Fig 5.3: Picture of FCACOM

4) Radio Frequency(RF) driver

Fig 5.4: Picture of RF Driver

Working Voltage: 90-240V

Maximum power: 35W

5) Connet 1550nm Class IV Fiber Optics LASER Module

Part no: VFLS-1550-M-MP-1-1-SF **Serial no:** 202010055

Operating Voltage: 12V DC **Operating Current:** 2A **Power output:** 1 Watt

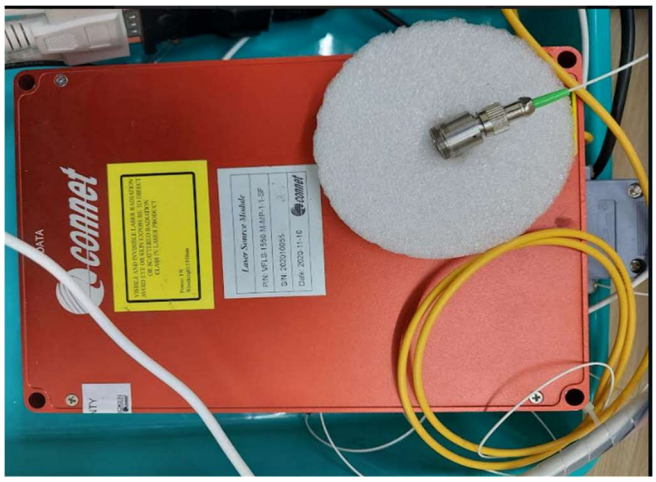

Fig 5.5: Picture of the LASER module

6) Keysight Infiniium S-Series Mixed Signal Oscilloscope – MSOS054A

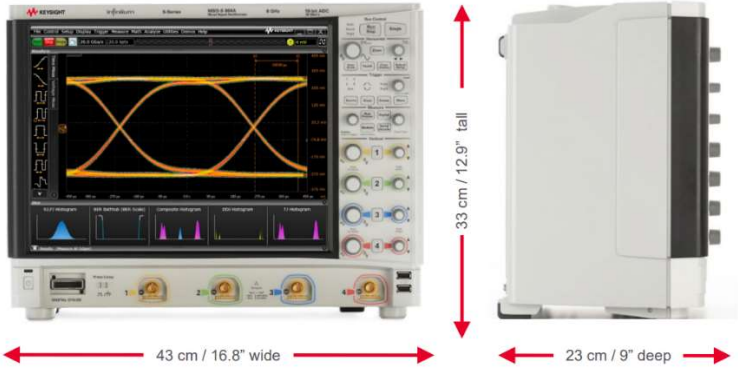

Fig.5.6: Front and Side view of MSO

Specification of Keysight Infiniium S-Series Mixed Signal Oscilloscope – MSOS054A

Bandwidth	500 MHz – 8 GHz
Optimized for	Signal integrity
Max memory (2 ch)	820 Mpts

ADC Bits	10
Inputs	50 Ω, 1 MΩ
Operating System	Windows 10
Hard drive	256 GB Removable SSD
Motherboard	Quad core i5, 8 GB RAM
Data offload	USB 3.0, 1000BASE-T LAN

Features of Keysight Infiniium S-Series Mixed Signal Oscilloscope – MSOS054A

Bandwidth (-3 dB)	50 Ω - 500 MHz
	1 MΩ - 500 MHz
Vertical Resolution	10 bits, up to 16 bits with high-resolution mode
Typical rise/fall time	10/90% - 860 ps
	20/80% - 620 ps
Input Impedance	50 Ω ± 3.5% (typically +1% at 25 °C)
Input Sensitivity	1 MΩ: 1 mV/div to 5 V/div
Input Coupling	50 Ω : DC
Bandwidth Limit Filters	Digital: 18.3 MHz up to scope bandwidth, in increments of 100 kHz (under 1 GHz) or 10 MHz (1 GHz and above). Filter options: Brick Wall, 4th Order Bessel, or Bandpass
Channel-to-channel Isolation	100 MHz to 1 GHz: 40 dB
DC gain accuracy	± 2% full scale (± 1% typical)
Max input voltage	1 MΩ: 30 V_{RMS} or ± 40 V_{MAX} (DC+V_{PEAK}). Probing technology allows for testing of higher voltages; the included N2873A 10:1 probe supports 300 V_{RMS} or ± 400 V_{MAX} (DC+V_{PEAK}).
Offset range	1 MΩ
Offset accuracy	≤ 2 V: ± 0.1 div ± 2 mV ± 1%
Dynamic range	+4 divisions from centre screen
DC voltage measurement accuracy	Dual cursor: ± [(DC gain accuracy) + (resolution)]
	Single cursor: ± [(DC gain accuracy) + (offset accuracy) + (resolution/2)]

7) Ophir Vega Laser Power Meter & Sensor

Fig.4. Front and back view of laser power meter

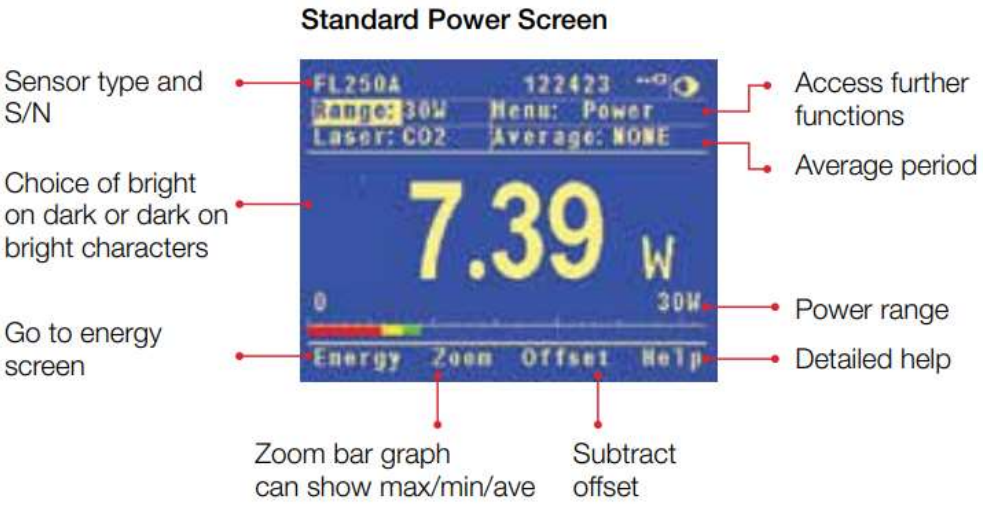

Fig.5.7: Display screen of the laser power meter

Specifications of Ophir Vega Laser Power Meter

Power Meter Features	Brilliant color TFT 320 x 240 pixel graphics LCD. Large 16mm digits. High resolution analog needle also can be chosen. Many screen features including power with multicolor bar graph, energy, average, exposure, frequency, graphs, scaling, special units, and more. Complete on line context sensitive help screens.
Outputs	USB, RS232 and user selectable 1, 2, 5 and 10 Volt full scale analog output.

Screen Refresh	15 times/sec
Case	Molded high impact plastic with optimized angle two level kickstand. Rubberized sides for easy grip and protection against damage.
Size	Folds to a compact 210mm L x 109mm W x 36mm H
Battery	Rechargeable NiMH batteries with typically 18 hours between charges. The charger can be ordered from your local distributor. The charger also functions as an AC adapter.
Data Handling	Data can be viewed on board or transmitted to pc: On Board: Non-volatile storage of up to 250,000 data points in up to 10 files. Max onboard data logging rate 4000 points/s and Max data logging rate to the PC 2000 points/s.
Sensor Features	Works with Thermopile, Beam Track, Pyroelectric (PE-C series) and Photodiode sensors.
Program Features	Preferred start up configuration can be set by user. User can recalibrate power, energy, response time and zero offset.
Compliance	CE, UKCA, China RoHS

Fig.5.8: 3A-P-THz High Sensitivity Thermal Sensors

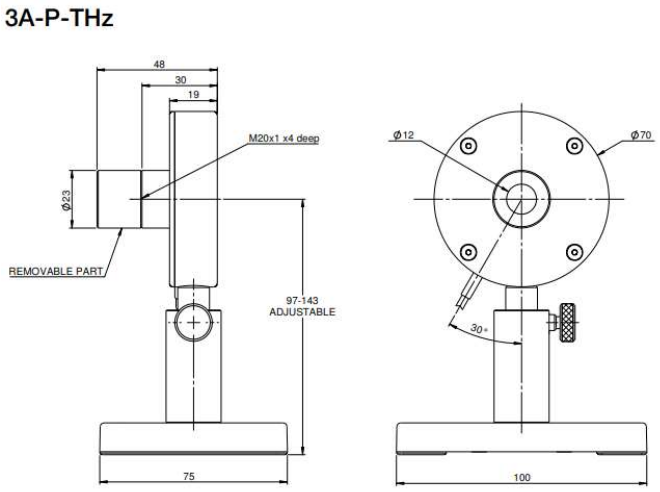

Fig.5.9: Schematic diagram of 3A-P-THz High Sensitivity Thermal Sensors

Specifications of 3A-P-THz High Sensitivity Thermal Sensors

Absorber Type	P type
Spectral Range µm	0.1THz - 30THz
Aperture mm	Ø12mm
Maximum Beam Divergence	NA
Power Mode	
Power Range	15µW - 3W
Power Scales	3W to 300µW
Power Noise Level	4µW
Thermal Drift (30min)	5 - 30µW
Maximum Average Power Density kW/cm2	0.05
Response Time with Meter (0-95%) typ. s	2.5
Calibration Uncertainty ±%	1.9
Power Accuracy ±%	8
Linearity with Power ±%	1
Energy Mode	
Energy Range	20µJ - 2J

Energy Scales	2J to 200µJ
Minimum Energy	20µJ
Maximum Energy Density J/cm2	
<100ns	1
0.5ms	1
2ms	1
10ms	1
Cooling	Convection
Weight kg	0.2
Fiber Adapters Available	ST, FC, SMA, SC
Compliance	CE, UKCA, China RoHS

8) UltraSonic Nebulizer WH2000

.

Fig.5.10: Front view of UtraSonic Nebulizer WH-2000

Fig.5.11: Top view of UtraSonic Nebulizer WH-2000

Specification of UtraSonic Nebulizer WH-2000

Particlediamer	1-5 um and with 1 year manufacturer Warranty
Max nebulizing rate	> 2ml /min
Medicine cup capacity	50 ml
Setting of Nebulization time	Continuously or from 0 to 60 min for time setting
Product size (mm)	250 x150 x 225mm Suggested Application : Clinical, Nursing Home, Home Care

9) Digital Thermometer TP-101

Fig.12: TP101 digital thermometer

Specifications of TP101 digital thermometer

Measuring Temperature Range: -50-300 degree (-58-572 Fahrenheit)

Fit for your kitchen, laboratory, factory or BBQ

Stainless Steel Temperature Probe

Accurate temperature display

Low battery sensation and display

Measures in Fahrenheit or Celsius

Memorizes the last measuring data

Weight: 48g

10) Variac

Fig.13: Variac

Specifications of Variac

Power	2 Amp- 300 Amp
Phase	Three Phase
Voltage	0 - 230 Volts

Usage/Application	Testing Purpose
Cooling Type	Dry Type/Air Cooled, Oil Cooled
Ambient Temperature	45 Degree Celsius Above Ambient
Input Voltage	230 Volts
Frequency	50 Hz
Output Voltage	0-270 Volts/ 0-300 Volts
Winding	Copper
Usage	Industry, Laboratory

11) Fluke 115 True RMS Multimeter

Fig.14: Fluke 115 True RMS Multimeter

Specifications of Fluke 115 True RMS Multimeter

Maximum voltage (between any terminal and earth ground)	600 V rms
Safety	IEC 61010-1, Pollution Degree 2 IEC 61010-2-033 CAT III 600 V, 10 A EMC IEC 61326-1: Portable
Fuse for A input	11 A, 1000 V, IR 17 kA (Fluke PN 803293)

Display	Digital: 6,000 counts, updates 4/sec; Bar Graph: 33 segments, updates 32/sec
Temperature	
Operating	-10 °C to +50 °C
Storage	-40 °C to +60 °C
Humidity	0 % to 90 % to 35 °C; 75 % to 40 °C; 45 % to 50 °C
Temperature coefficient	0.1 x (specified accuracy/°C) (< 18 °C or > 28 °C)
Operating altitude	2,000 meters
Battery	9 Volt Alkaline (IEC 6LR61)
Battery life	400 hours typical, without backlight
Certifications	CE, CSA, RCM
IP rating (dust and water protection)	IP42

Appendix B

Bill of material of Trans-impedance amplifier & comparator circuit

Sl. No.	Item	Legend	Part No./ Value	Quantity	Remarks
1.	Voltage Feedback Amplifier	U1A, U1B	AD8039	1	SOIC Package
2.	Ultra-fast low-power precision comparators	U2	TL3016	1	SOIC Package
3.	Voltage Regulator	U3	L78L05ACZ	1	TO92 Package
4.	Voltage Regulator	U4	L79L05ACZ	1	TO92 Package
5.	Resistor	R1	150E/2W	1	-
6.	Resistor	R2	150E/2W	1	-
7.	Resistor	R3	2.7 kΩ/0.25 W	1	-
8.	Resistor	R4	2.7 kΩ/0.25 W	1	-
9.	Resistor	R5	2.7kΩ/0.25 W	1	-

10.	Resistor	R6	100 Ω/0.25 W	1	-
11.	Resistor	R7	100 Ω/0.25 W	1	-
12.	Resistor	R8	1 kΩ/0.25 W	1	-
13.	Resistor	R9	56E/0.25 W	1	-
15.	Variable Resistor	VR1		1	3296 Multi turn
16.	Capacitor	C1,C3	100µF/40 V	2	Electrolytic Capacitor (Radial)
17.	Capacitor	C2,C4,C9,C11,C13,C14	0.1µF	6	Ceramic Disk Capacitor
18.	Capacitor	C10, C12	2.2 pF	2	Ceramic Disk Capacitor
19.	Capacitor	C5,C6,C7,C8	2.2 µF/35 V	4	Tantalum Capacitor
20.	Jumper	J1,J2	-	2	-
21.	Connector	CN1,CN5,CN6	PBT3	3	-
22.	Connector	CN2,CN3,CN4	PBT2	3	-

AD8039 Voltage Feedback Amplifier

ANALOG DEVICES

Low Power 350 MHz Voltage Feedback Amplifiers

AD8038/AD8039

FEATURES
Low Power
1 mA Supply Current/Amp
High Speed
350 MHz, –3 dB Bandwidth (G = +1)
425 V/µs Slew Rate
Low Cost
Low Noise
8 nV/√Hz @ 100 kHz
600 fA/√Hz @ 100 kHz
Low Input Bias Current: 750 nA Max
Low Distortion
–90 dB SFDR @ 1 MHz
–65 dB SFDR @ 5 MHz
Wide Supply Range: 3 V to 12 V
Small Packaging: SOT23-8, SC70-5, and SOIC-8

APPLICATIONS
Battery-Powered Instrumentation
Filters
A/D Driver
Level Shifting
Buffering
High Density PC Boards
Photo Multiplier

CONNECTION DIAGRAMS

SOIC-8 (R)

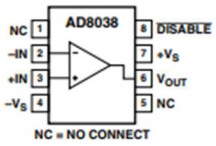

NC = NO CONNECT

SC70-5 (KS)

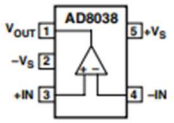

SOIC-8 (R) and SOT23-8 (RT)*

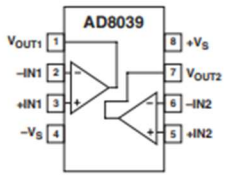

TL3016 Ultra-fast low-power precision comparator

TL3016, TL3016Y
ULTRA-FAST LOW-POWER
PRECISION COMPARATORS
SLCS130D – MARCH 1997 – REVISED MARCH 2000

- Ultrafast Operation . . . 7.6 ns (Typ)
- Low Positive Supply Current 10.6 mA (Typ)
- Operates From a Single 5-V Supply or From a Split ±5-V Supply
- Complementary Outputs
- Low Offset Voltage
- No Minimum Slew Rate Requirement
- Output Latch Capability
- Functional Replacement to the LT1016

D AND PW PACKAGE
(TOP VIEW)

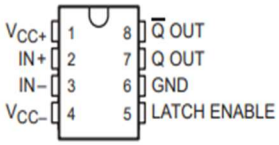

symbol (each comparator)

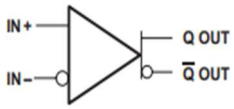

L78L05ACZ Voltage Regulator

L78L00 SERIES

POSITIVE VOLTAGE REGULATORS

- OUTPUT CURRENT UP TO 100 mA
- OUTPUT VOLTAGES OF 3.3; 5; 6; 8; 9; 10; 12; 15; 18; 20; 24V
- THERMAL OVERLOAD PROTECTION
- SHORT CIRCUIT PROTECTION
- NO EXTERNAL COMPONENTS ARE REQUIRED
- AVAILABLE IN EITHER ±5% (AC) OR ±10% (C) SELECTION

TO-92

SCHEMATIC DIAGRAM

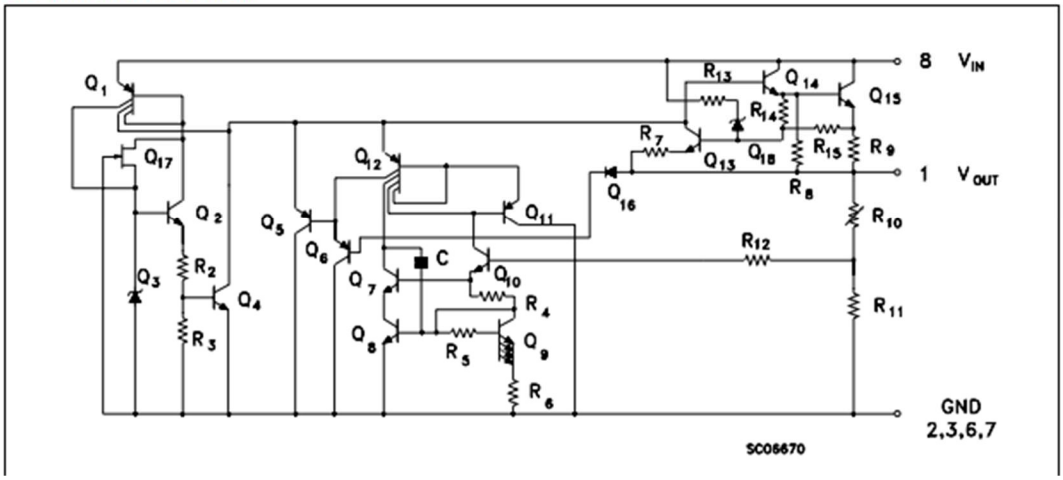

CONNECTION DIAGRAM (top view)